WHITE MATTER DAMAGE AFTER ACUTE BRAIN INJURY

Eileen McCracken B.Sc. (Hons)

A Thesis submitted for the degree of Doctor of Philosophy
to the Faculty of Medicine, University of Glasgow.

Wellcome Surgical Institute and Hugh Fraser Neuroscience Laboratories
University of Glasgow
Garscube Estate, Bearsden Road, Glasgow. G61 1QH.

ProQuest LLC.
789 East Eisenhower Parkway
P.O. Box 1346
Ann Arbor, MI 48106 – 1346

CONTENTS

LIST OF TABLES

LIST OF FIGURES

DECLARATION

I declare that this thesis comprises my own original work and has not been accepted in any previous application for a degree. The work, of which it is a record, has been carried out by myself, except as where acknowledged and indicated in the thesis. All sources of information have been specifically referenced.

Eileen McCracken

ACKNOWLEDGEMENTS

As I near completion of this thesis I would like to take the time to thank a number of people for their assistance and kindness. First and foremost, my sincerest gratitude goes to my supervisor Dr. Deborah Dewar for her constant support throughout the past three years. I would also like to extend my thanks to Professor James McCulloch and Dr. Karen Horsburgh for their intellectual and experimental advice.

During my Ph.D I was fortunate enough to have the opportunity to work in SmithKline Beecham through my industrial supervisor Dr. Jackie Hunter. I would like to thank her and the neurobehavioural research group for making me feel welcome during my time there and funding a research trip to an international conference. Thank you for providing large quantities of SBAbS2.

Further thanks to my collaborators Professor David Graham at the Southern General Hospital for supplying human post-mortem tissue and his expertise in this field. I would also like to thank Dr. Valerio Valeriani for providing rat tissue for one of the studies. I must also acknowledge the technical assistance of the staff of the Wellcome Surgical Institute and my fellow Ph.D students for their co-operation during periods of intense stress, which was almost every week!

A special thank you to my parents for their loving and financial support, without whom I would not be here today. Finally, I would like to thank Derek, who probably deserves a degree for keeping us both sane especially over the last five months, I hope that one day I can repay both him and my parents for everything. I dedicate this thesis to you.

SUMMARY

White matter damage induced by multiple pathogenic mechanisms following acute brain injury was investigated in this thesis. White matter tissue from human head-injured patients, experimental animal models of oxidative stress and lipid peroxidation, an *in vitro* model of lipid peroxidation and an *in vivo* model of focal cerebral ischaemia were used to determine cytoskeletal changes in white matter. These models were also used to determine if there were interactions between primary pathogenic mediators and secondary mechanisms.

Cytoskeletal breakdown in the corpus callosum of head-injured patients and alterations in calpain activity

Cytoskeletal proteins are essential for the structural integrity and function of axons. In this study, the levels of cytoskeletal proteins were measured by Western blotting in the corpus callosum tissue from human post-mortem head-injured and control patients. There were significant reductions in the levels of neurofilament protein subunits in the corpus callosum of head-injured patients compared to controls. In contrast, there was no change in the level of β-tubulin or the microtubule associated protein, tau detected by Western blotting between the head-injured and control patients. The accumulation of β-amyloid precursor protein (β-APP) in head-injured patients detected by immunohistochemistry within myelinated axons suggests that cessation of axonal transport had occurred in these patients. Increased protein levels of calpain mediated-spectrin breakdown products were detected in the corpus callosum of head-injured patients compared to controls. Calpain-mediated spectrin breakdown products were also identified within myelinated axons in sections processed for immunohistochemistry. This immunostaining correlated with the pattern of axonal pathology detected by β-APP accumulation. The data suggests that calpain-mediated proteolysis has a direct role in axonal damage after human head injury.

White matter damage following systemic injection of the mitochondrial inhibitor, 3-nitropropionic acid in the rat

An experimental animal model of oxidative stress was induced by systemic injection of 3-nitropropionic acid (3-NPA). Animals received an intraperitoneal injection of 10, 15,

20 or 30 mg/kg 3-NPA or vehicle and were killed 24 hours later. 3-NPA produced a concentration dependent increase in axonal pathology within the striatum reflected by the amount of β-APP and SNAP-25 accumulation. Axonal damage was anatomically coincident with the neuronal lesion. There was no neuronal or axonal damage in the subcortical white matter or cerebral cortex in any of the animals treated with 3-NPA. Manganese superoxide dismutase immunoreactivity was present in the vehicle and all 3-NPA treated groups. The amount of Mn-SOD cellular staining was concentration dependently increased within the striatum supporting a role for oxidative stress in the mechanism of 3-NPA toxicity. In contrast to the association observed between β-APP accumulation and calpain-mediated spectrin breakdown products in head injured patients, the presence of calpain-mediated breakdown products was not associated with accumulation of β-APP in this experimental animal model. However, calpain immunopositive oligodendrocyte-like cells along the subcortical white matter were increased in a concentration dependent manner by 3-NPA. Therefore in this experimental model, mitochondrial inhibition may lead to the initiation of oxidative stress and calpain activation, which could mediate cytoskeletal breakdown in axons and oligodendrocytes suggesting an interaction between at least two pathogenic mechanisms.

The lipid peroxidation by-product, 4-hydroxynonenal is toxic to axons and oligodendrocytes *in vivo* and *in vitro*

Effects of 4-hydroxynonenal *in vivo:* The cytotoxic lipid peroxidation by-product 4-hydroxynonenal (4-HNE), was stereotaxically injected into rats which were sacrificed 24 hours later. 4-HNE produced widespread axonal pathology in the subcortical white matter demonstrated by conventional histology and accumulation of β-APP. Damaged axons detected by accumulation of β-APP were observed transversing medially and laterally away from the injection site following intracerebral injection of 4-HNE. In contrast, in the control animals axonal damage was restricted to an area surrounding the injection site. This pattern of pathology did not appear to be mediated by endogenous 4-HNE or calpain activation. The lack of evidence of 4-HNE-Michael adducts and calpain-mediated spectrin breakdown products after intracerebral injection of 4-HNE

suggests that 4-HNE might induce other secondary pathogenic mechanisms that could account for the axonal pathology observed distant from the injection site.

Effects of 4-HNE *in vitro:* Oligodendrocyte cultures were incubated with different concentrations of 4-HNE over a period of 1, 2 or 4 hours. Exogenous 4-HNE produced time dependent and concentration dependent increase in oligodendrocyte cell death in culture. After 4 hours the highest concentration of 4-HNE (50μM), produced 100% oligodendrocyte cell death. The antibody to the cytoskeletal protein spectrin, detected morphological changes in oligodendrocytes where the perikarya had become shrunken and processes fragmented at 10 and 50μM 4-HNE compared to the vehicle or 1μM 4-HNE. The results from these studies show that exogenous 4-HNE causes changes in cytoskeletal proteins in axons and oligodendrocytes.

Production of endogenous 4-HNE in a model of permanent focal cerebral ischaemia: Conventional histology demonstrated a characteristic ischaemic lesion following 24 hours of permanent focal cerebral ischaemia in the rat. β-APP accumulation within myelinated axons was widespread within the ischaemic lesion. 4-HNE-Michael adducts were present in neuronal perikarya, axons and glial cells within the infarcted region. The distribution of 4-HNE-Michael adducts in axons paralleled β-APP accumulation observed in adjacent sections. In the cerebral cortex 4-HNE-Michael adducts marked a boundary between ischaemic and normal tissue. This data supports a role for endogenous 4-HNE after acute brain injury.

Collectively the data has demonstrated that myelinated axons and oligodendrocytes are vulnerable to pathogenic mechanisms following acute brain injury. The diversity of toxic mediators that contribute to both neuronal and axonal damage highlights the complexity of the pathophysiology after acute brain injury. However, multiple sites of action could provide targets for pharmacological manipulation.

ABBREVIATIONS

AMPA	α-amino-3-hydroxy-5-methyl-4-isoxazolepropionic
ATP	Adenosine triphosphate
β-APP	β- Amyloid precursor protein
aCSF	Artificial cerebrospinal fluid
BBB	Blood brain barrier
CNS	Central nervous system
DAI	Diffuse axonal injury
DMEM	Dulbecco's modified eagles medium
GFAP	Glial fibrillary acidic protein
GSH	Glutathione
GPx	Glutathione peroxidase
4-HNE	4-hydroxynonenal
H & E	Haematoxylin and eosin
HBSS	Hanks balanced salt solution
LDH	Lactate dehydrogenase
MDA	Malondialdehyde
Mn-SOD	Manganese superoxide dismutase
MLP	Membrane lipid peroxidation
MTs	Microtubules
MCA	Middle cerebral artery
MTT	3-(4,5-dimethylthiazol-2-yl)-2,5-diphenyltetrazolium bromide
NMDA	N-methyl-D-aspartate
NF	Neurofilament
NO	Nitric oxide
3-NPA	3-nitropropionic acid
RNS	Reactive nitrogen species
ROS	Reactive oxygen species
SDS-PAGE	Sodium Dodecyl Sulphate Polyacrylamide Gel Electrophoresis

SOD	Superoxide Dismutase
PLP	Phospholipid protein
PDGF	Platelet Derived Growth Factor
PUFAs	Polyunsaturated Fatty Acids
TBI	Traumatic Brain Injury
XDH	Xanthine dehydrogenase

CHAPTER I
INTRODUCTION

1.1. CENTRAL NERVOUS SYSTEM

Central nervous system (CNS) neurons can be either excitatory or inhibitory, and modulate motor, sensory or secretory functions. The neuron appears in a variety of shapes and sizes throughout the CNS consisting of four parts: cell body (soma or perikaryon); numerous apical dendrites; a long myelinated fibre tract (referred to as the axon) and a fibre terminal or synapse (Figure 1.1). Neuronal perikarya are rich in organelles, which function to maintain the neuron. Intercommunication between neurons occurs via chemical or electrical synapses. Axons are components of white matter and it is their myelin sheath that gives it the distinguishable white colour. Although the neuronal perikaryon and synapse are important in neuronal function and if damaged have deleterious consequences for brain function, they are mainly located within grey matter. As the focus of this thesis is mechanisms of white matter damage only the cytoarchitecture and function of the axon will be discussed in this introduction.

1.1.1 Myelinated axons in the central nervous system

A single axon extends away from the cell body and is frequently enwrapped in a myelin sheath by oligodendrocytes (see 1.1.2.1). Myelin covers axons in segments (internodes) interrupted by nodes of Ranvier. Nodes of Ranvier are regions of bare axolemma where ionic exchange takes place. This unique structural arrangement is the basis for saltatory conduction and allows the axon to function in an energy-efficient manner (Salzer, 1997). The speed of the conduction is proportional to the thickness of the axon and its myelin sheath. Axons function to transport electrical impulses from the soma to the effector cell. Essential proteins are also transported either anterograde (soma to terminal) or retrograde (terminal to soma) by either slow (1-3mm/day) or fast (400mm/day) axonal transport.

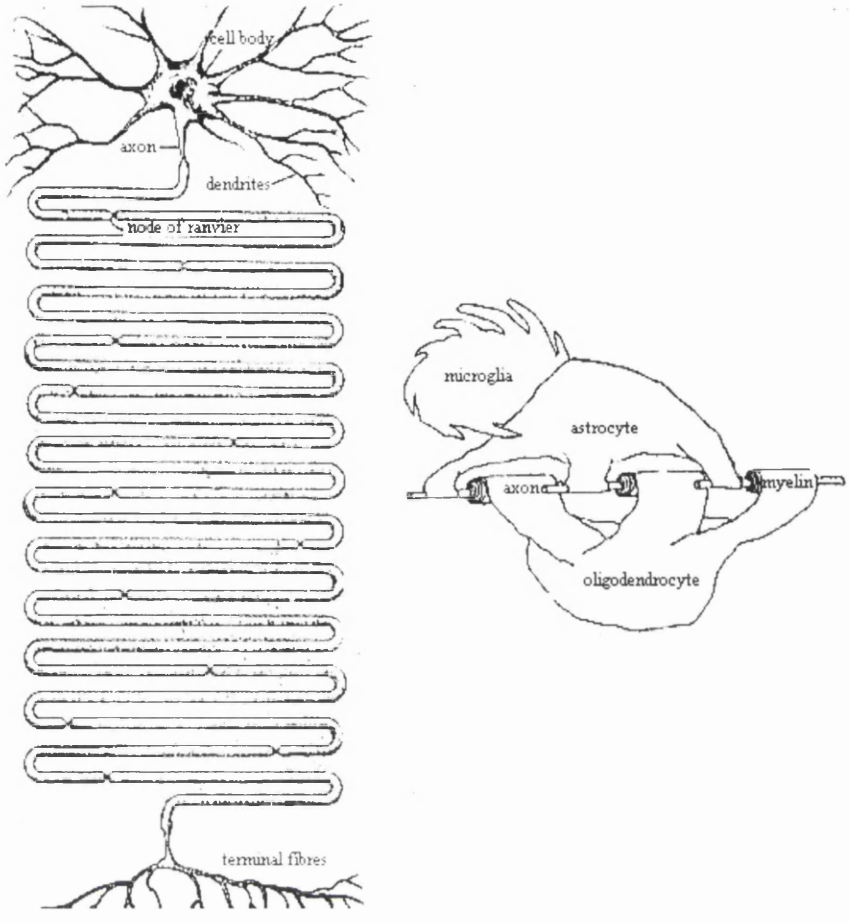

(Modified from Kandel & Schwartz 1985 and Compston 1993)

Figure 1.1 Central nervous system neuron and surrounding neuroglia cells.

CNS neurons are made of a *cell body* that is metabolically active and contains the genetic make-up necessary for protein synthesis. *Dendrites* receive signals from other neurons. An *axon* transmits electrical impulses and transports proteins anterograde and retrograde along the axon. The *presynaptic terminal* releases electrical or chemical signals into the extracellular space. Only about 10% of the cells in the CNS are neurons and are surrounded by non-excitable cells, known as neuroglia. Neuroglia cells have an important relationship with neurons helping to maintain and support the function of the neuron. *Astrocytes* function to repair neurons, *oligodendrocytes* are responsible for myelination of the axon and *microglia* are macrophage precursors activated after an inflammatory response.

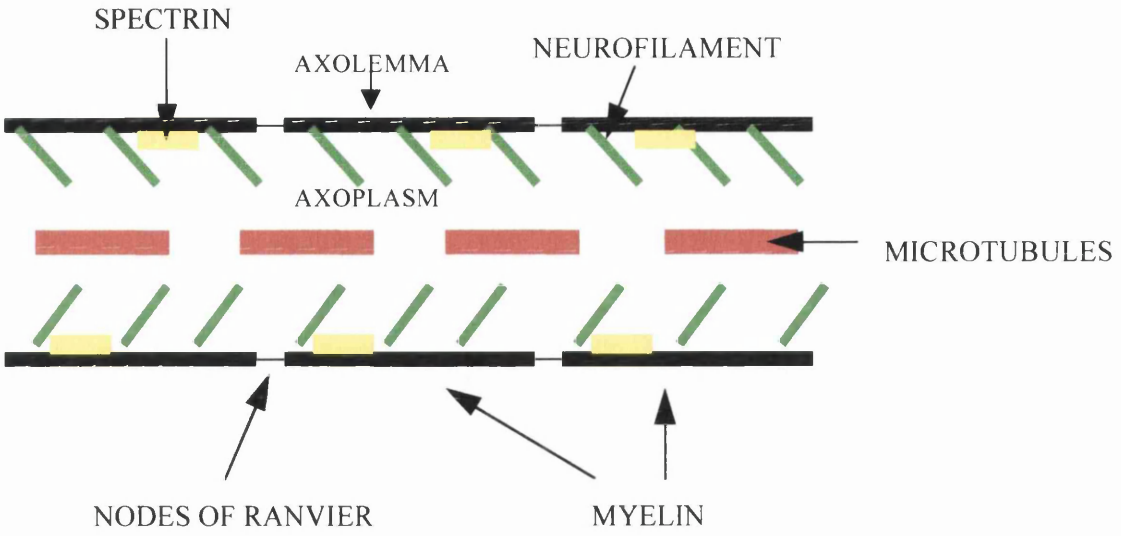

Figure 1.2 Axonal structure

The unique cytoarchitecture of the axon consists of microtubules, neurofilaments and membrane bound proteins that provide structural stability and allow the transportation of organelles anterograde or retrograde along the axon.

In the axon, there are two specialised regions, the axoplasm and the axolemma. Crosslinkage of neurofilaments and microtubules form a cytoskeletal core deep in the axoplasm. Adjacent to this region lies the membrane bound network of actin binding proteins. Microtubules are composed of α- or β-tubulin subunits that assemble and disassemble providing a dynamic rather than a static framework (Mitchison and Kirschener 1984). Tubulin polymers form rows of protofilaments where the β-tubulin of one dimer is joined to the α-tubulin of the next dimer. Microtubule motility is mediated by two families of proteins: kinesin, involved in fast anterograde transport and dyneins, which play a role in slow retrograde transport. Microtubule associated proteins (MAPs), help to maintain the dynamic structure and stability of microtubules. MAP1A, MAP1B and tau are abundant in the axon their function being to bind and stabilise microtubules (Binder et al., 1985). Neurofilaments are highly abundant in mature axons and are part of the interfilament family. The primary type of neurofilament is formed from subunit polypeptides collectively called neurofilament triplet proteins. The molecular weight of neurofilament subunits has been estimated by gel electrophoresis to be 200kDa = NF-H,

neurofilament subunits has been estimated by gel electrophoresis to be 200kDa = NF-H, 150kDa =NF-M and 68kDa = NF-L. NF-L is an assembly protein in the axonal core whereas NF-M and NF-H triplet proteins are crosslinking proteins. NF-M and NF-H are heavily phosphorylated and thought to have an important role in regulating polymerisation of other interfilaments (Sternberger and Sternberger 1983). It has also been proposed that neurofilaments are directly involved in the modulation of the axonal calibre. Spectrin is an actin binding protein associated with the cytoplasmic surface of the plasma membrane. Spectrin is expressed in both neurons and glia cells either as α- or β-spectrin. α-Spectrin in axons is sometimes referred to as fodrin. Spectrin bestows mechanical stability on the membrane and links transmembrane proteins to the cytoskeleton (Goodman and Zagon 1986). Following acute brain injury, there may be a decline in cytoskeletal integrity and thus disruption of axonal transport leading to degeneration.

1.1.2 Neuroglia cells

During the last century Virchow (Virchow 1846) recognised a non-nervous interstitial substance that separated fibrous nervous tissue from blood vessels and referred to it as the neuroglia cells "nerveglue". It was not until the beginning of this century that the neuroglia cells were distinguished and separated. (Cajal 1913; 1916). This classification was further verified by the introduction of metallic impregnation and light microscopy. Basic dye stains of nuclei distinguished different types of neuroglia cells: astrocytes and oligodendrocytes, collectively known as macroglia and microglia. More recently ependymal cells have been identified. There are two types of astrocytes, fibrous and protoplasmic. The functions of astrocytes include the storage of glycogen for periods of decreased aerobic respiration and regulation of ionic and osmotic homeostasis. These cells bridge between the vascular system, neurons and themselves and detect perturbations in the microenvironment. Microglia act as macrophage precursors and become activated after an inflammatory response. Infiltrating blood borne macrophages in concert with the resident microglia undergo morphologic and functional changes which then migrate to the site of injury where they become fully activated. Ependymal cells are of cilia type structure lining the ventricle and spinal cord. Their exact function

is unknown as yet. The introduction to this thesis will now focus on the importance of oligodendrocytes.

1.1.2.1 Oligodendrocytes

Oligodendrocytes were first described by Robertson (Robertson 1899) and several decades later, classified by a detailed histological description by Del Rio Hortega (1921, 1928) who categorised two types of oligodendrocytes according to their position within the central nervous system. Oligodendrocytes that are located mainly within white matter, in rows between myelinated fibre tracts, are interfascicular and thought to be involved in myelination. The other, perineuronal satellite cells, usually appear in association with neurons in grey matter and may regulate the local environment for growth and maintenance of axons (Ludwin, 1997). Oligodendrocytes are derived in the subventricular zone from the neuroectoderm in the late gestational period and migrate into the CNS (Goldman, 1992, Levison et al., 1993). The cell migrates, proliferates and differentiates into a mature, multi-process cell, with a small dark soma, approximately 10-20μm in diameter, (Wood and Bunge 1984; Wood and Bunge 1986;) and is more chromophillic compared to astrocytes. Oligodendrocytes are the myelin forming cells in the CNS and are viewed as the structural elements that provide the electrical insulation of axons (Bunge 1962; Bunge et al, 1968). One oligodendrocyte can ensheath up to 50-60 axons (Ludwin, 1997).

1.1.2.2 Migration, proliferation and differentiation

Oligodendrocytes are derived from mitotic bipolar precursor cells, known as the O-2A progenitor. O-2A progenitor cells were first found in cultures of the developing optic nerve (Raff, 1989) and other regions of the CNS (Levi et al., 1986; Ingraham and McCarthy 1989; Miller et al 1989; Goldman, 1992). Aspects of oligodendrocytes have determined by the use of *in vitro* systems. O-2A cells migrate, proliferate and differentiate in to either oligodendrocytes or type 2 astrocytes, depending on the local microenvironment (Levison and Goldman 1993; Miller et al., 1989). However, there is still some controversy as to whether type 2 astrocytes exist *in vivo* (Espiniosa et al., 1993; Williams and Price 1992; Williams et al., 1995). Migration of O-2A progenitors *in vitro* resembles migration of progenitors into white and grey matter *in vivo* (Goldman, 1992). Similarities in the proliferation of oligodendrocytes have been

demonstrated between the *in vivo* and *in vitro* situation. Mitogenic factors, such as, platelet derived growth factor (PDGF) and basic fibroblast growth factor (bFGF) regulate the proliferation of O-2A progenitors *in vivo*. Continuous cell division occurs in serum free cortical glia cultures and optic nerve preparations in a similar time frame to cell proliferation *in vivo* suggesting that the same growth factors might be responsible for proliferation (Raff, 1992). Other growth factors are also thought to be involved in the development of O-2A progenitors into post-mitotic multipolar process bearing oligodendrocytes (Komoly 1992). What regulates these growth factors is still unclear, although adjacent type-1 astrocytes secreting PDGF *in vivo* and *in vitro*, or electrical signals from axons have been suggested to control oligodendrocyte development (Barres and Raff 1993).

1.2 CLINICAL CONDITIONS OF ACUTE BRAIN INJURY

1.2.1 Stroke

Stroke is the third leading cause of death in the United Kingdom. Approximately, 500,000 patients (Forbes 1993) are admitted to hospital per annum and approximately 80% of these patients either die or are left disabled (Bamford et al., 1988). The prevalence of stroke means that 1/5 of acute national health service beds and a quarter of long term beds in the UK are occupied by these patients. There are two types of stroke, ischaemic and haemorrhagic. Ischaemic stroke can be further subdivided into thrombotic and embolic. Haemorrhagic stroke can also be divided into intracranial or subarachnoid haemorrhage.

1.2.2 Head injury

Head injury is the leading cause of death from accidents in young adults. Many patients who sustain a traumatic brain injury are adolescents or young adults who require care by their family for a long time. One family in every 300 has a member with such a disability emphasising the social and economic problems associated with this type of injury. There are two main types of traumatic brain injury: missile and non-missile (blunt) head injury. Missile head injury results from moving or fallen objects impacting on the brain. Types of missile brain damage are classified as depressed, penetrating or

perforating and each type depends on the mass, shape and velocity of the missile. Blunt (non-missile) head injury is the more common type of head injury in patients admitted to hospital. Over a 15 year period a comprehensive study of 635 fatal head injured patients was conducted at the Institute of Neurological Sciences, Glasgow and these injuries resulted from road traffic accidents (53%); falls (35%); assaults (5%) and others (7%) (Adams and Graham 1996).

1.3 BRAIN PATHOLOGY AFTER ACUTE BRAIN INJURY

1.3.1 Ischaemic stroke

Ischaemic stroke is the most common form of stroke. Cerebral ischaemia occurs when there is a reduction in blood flow to a region of the brain from a major artery. Cerebral arteries can be occluded by either the build up of a thrombus or due to the presence of an embolus lodged in the artery. Reduction of blood flow reduces the delivery of oxygen and consequent energy failure, leads to cell death. Morphological changes observed after ischaemia within grey matter comprise necrotic neurons that are recognisable by their intensely eosinophilic cytoplasm and their poorly stained nucleus with haematoxylin. It was previously believed that white matter pathology was secondary to neuronal necrosis (Marcoux et al., 1982). It could be that methods used previously to determine grey matter damage are not suitable for assessment of white matter pathology after cerebral ischaemia. Grey and white matter differ in many respects from one another in terms of their blood supply, rates of glucose utilisation, and ionic composition (Hansen 1985; Stys et al., 1990; Ransom et al., 1990; Pantoni and Garcia 1997; Kumura et al., 1996; Kuroiwa et al., 1998). However, although they differ in their cellular and elemental composition it might be that certain neuropathogenic factors leading to damage are similar in both grey and white matter. Although there is an overwhelming body of evidence for perikaryal damage in grey matter following cerebral ischaemia there is little evidence of white matter damage in the literature. There is however, some experimental evidence suggesting that following focal cerebral ischaemia in the rat that axons (Yam et al., 1998b) and oligodendrocytes (Pantoni et al., 1996) are vulnerable within 1 hour post injury.

1.3.2 Head injury

Brain damage resulting from blunt head injury can arise from a variety of processes depending on the severity of the injury. Certain types of brain damage cannot be determined using neuroradiological equipment and need to be examined post-mortem either macroscopically or with the aid of a light or electron microscope. Striking differences in the macroscopic changes are observed between mild, moderate and severe head injury. There is increasing awareness that what separates mild, moderate and severe head injury is not so much the nature of the lesion but its amount and distribution, microscopically. Pathology after blunt head injury is either classified as focal and diffuse (Table 1.1) or primary and secondary (Table 1.2).

The introduction of this thesis is interested in white matter damage following acute brain injury and therefore I will focus on the characteristics of axonal injury after head injury.

Table 1.1
Focal and Diffuse pathology

FOCAL	DIFFUSE
Scalp lesions	Diffuse axonal injury
Skull fractures	Ischaemic brain damage
Contusions & lacerations	Brain swelling
Intracranial haemorrhages	Diffuse vascular injury
Secondary damage due to raised ICP	Infection

Table 1.2
Primary and Secondary pathology

PRIMARY	SECONDARY
Scalp lesions	Intracranial haemorrhages
Skull fractures	Ischaemic brain damage
Contusions & lacerations	Brain swelling
Diffuse axonal injury	Secondary damage due to raised ICP
Diffuse vascular injury	Infection

1.3.2.1 Diffuse axonal injury

Diffuse axonal injury (DAI) is considered to be one of the most important types of pathology in patients who sustain a blunt head injury. Diffuse axonal injury is a

common cause of coma in the absence of any intracranial mass lesion (Graham et al., 1995; Graham and Gennarelli 1997). In patients who died some time after the initial head injury and remained in a vegetative or severely disabled state (McLellan et al., 1986), DAI was the major type of pathology at post-mortem (Graham and Gennarelli 1997). DAI has previously been described as diffuse degeneration to white matter (Strich 1956); shearing injury (Peerless et al., 1967); diffuse white matter shearing (Zimmerman et al., 1978); diffuse damage of impact type (Adams et al., 1977) or inner cerebral trauma (Grcevic 1982) however the term now universally used is "diffuse axonal injury" (Adams et al., 1982; Gennarelli et al., 1982).

1.3.3 Assessment of axonal injury

The levels of DAI pathology in human head injury was originally graded using silver impregnation (Adams et al., 1982; Adams et al., 1989) In grade I DAI, there is histological evidence of axonal injury in the white matter of the parasagittial white matter, corpus callosum and brain stem with the absence of focal lesions. In grade II DAI, there is widespread axonal injury and also a focal lesion in the corpus callosum. In grade III DAI, there is in addition to the diffuse axonal pathology observed in grades I & II macroscopical evidence of focal lesions in one or both the dorso-lateral quadrants of the rostral brain stem (Adams et al., 1989). Patients with a longer survival time displayed a different pattern of pathology, with the appearance of reactive astrocytes, gliosed lesion within which are haemosiderin-containing macrophages (Adams and Graham 1989). Some lesions in the corpus callosum and brainstem can be seen macroscopically, but the axonal damage can only be recognised microscopically (Adams and Graham 1989).

Silver impregnation techniques can only detect axonal damage if the patient survived for 15 hours or longer after the injury (Adams et al., 1982). However, in the last 10 years a new more sensitive technique has been introduced for detecting axonal injury using an antibody to beta amyloid precursor protein (β-APP). β-APP, is a transmembrane bound protein that is carried along the axon by fast anterograde axonal transport (Koo et al., 1990) and will accumulate in disrupted axons. Adjacent sections from a group of head-injured patients were stained for either silver impregnation or β-

APP immunohistochemistry. Silver staining revealed that only 30% of the cases had evidence of axonal injury while β-APP immunohistochemistry revealed that 90% of the head-injured cases had axonal injury. Therefore this demonstrated approximately a 60% difference in the amount of axonal injury observed in the head-injured cases between the two stains (Figure 1.3) (Gentleman et al., 1995). The use of β-APP immunohistochemistry is a more sensitive marker than silver staining and has made the identification of earlier and more subtle changes in axonal injury possible. The late introduction of sensitive markers of white matter damage, such as β-APP, may have contributed to the underestimated importance of white matter damage following acute brain injury.

Evidence of axonal injury in a group of head-injured patients can be detected at 2-3 hours survival using β-APP immunohistochemistry (Sherriff et al., 1994; McKenzie et al., 1996). The amount and distribution of axonal bulbs increased with survival time with increased β-APP accumulation being present in patients surviving for as long as 99 days (Blumbergs et al., 1994). β-APP immunostaining has not only been valuable in assessing axonal injury after head injury but has also been demonstrated at the margin of an ischaemic lesion in the human brain (Oghami et al., 1992; Suenaga et al., 1994; Jendroska et al., 1997). Others have reported β-APP accumulation after focal cerebral ischaemia in cat (Yam et al., 1999), rat (Yam et al., 1997; Yam et al., 1998a) and a rat model of thromboembolic stroke (Dietrich et al., 1998). Irreversible axonal damage was once thought to occur solely at the moment of injury and there was a general consensus that axons were primarily vulnerable to mechanical loading (Povlishock and Christman 1995; Gennarelli 1996). However, it is now recognised that although a proportion of axons may become severed at the time of injury, so called primary axotomy, many axons undergo secondary or delayed axotomy (Graham and Gennarelli 1997; Maxwell et al., 1997). The processes leading to secondary axotomy, during which axons undergo a sequence of reactive changes which precedes physical disconnection, is thought to occur over a period of 12 hours or longer in humans (Gentleman et al., 1993; Grady et al., 1993; Blumbergs et al, 1994; Blumbergs et al., 1995; Christman et al., 1994).
Another important type of pathology after head injury is ischaemic brain damage. Ischaemic damage to axons may also be an important pathological consequence after head injury. Approximately 90% of head-injured patients have microscopic evidence of

ischaemic damage post-mortem (Graham et al., 1978). Although the precise biological mechanisms underlying the processes of secondary axotomy are unknown at present, it is hypothesised that secondary ischaemic brain damage, excitotoxicity (via non-NMDA receptors), an increase in intracellular calcium and oxidative stress may all play an interactive role in the breakdown of the axonal cytoskeleton. It is during this period of secondary axotomy that recovery might be possible if the damage is reversible.

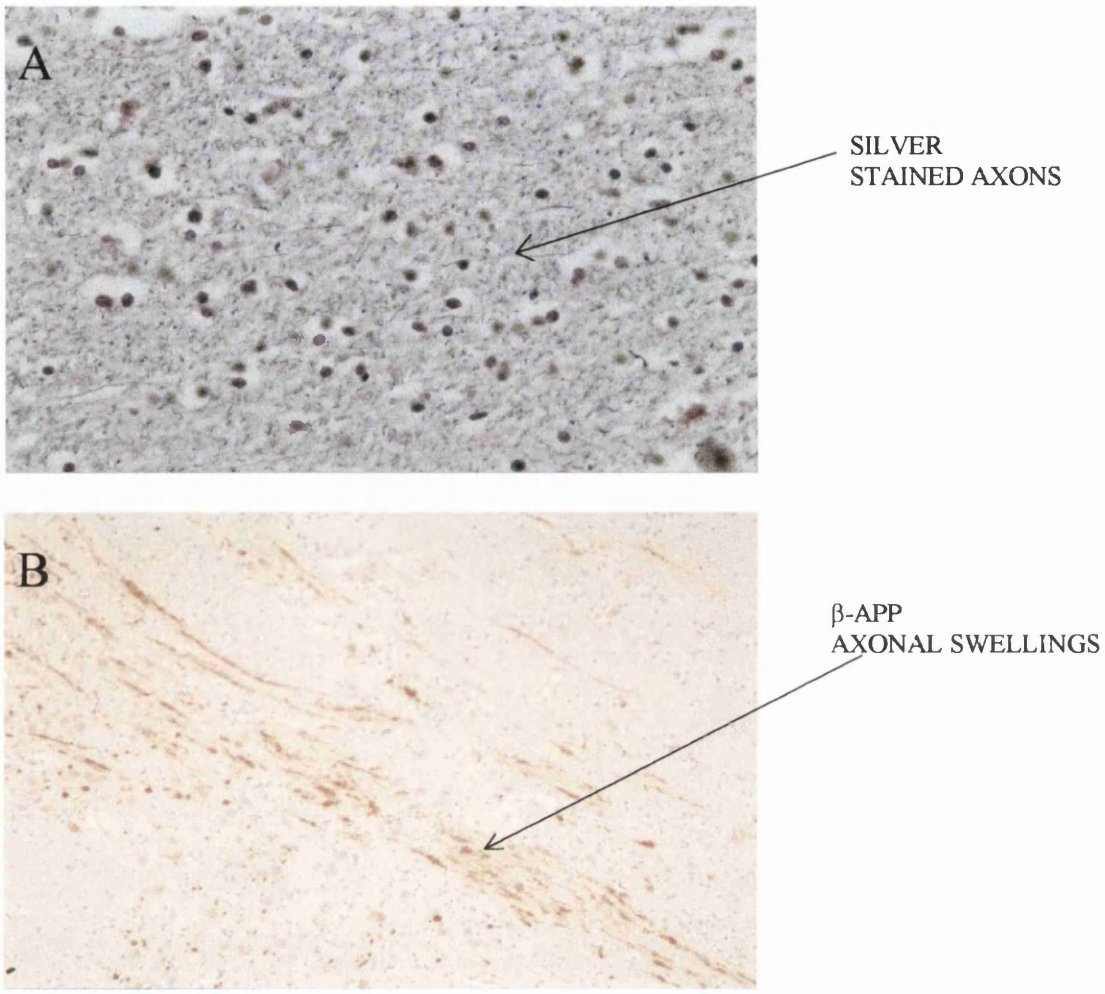

Figure 1.3 Comparison of silver staining and β-amyloid precursor protein accumulation as a marker of axonal injury

Adjacent sections from a head-injured patient (5 hours survival) were stained for both A) silver and B) β-APP. Silver impregnation did not reveal any morphological changes in myelinated axons. However, adjacent sections stained with β-APP illustrated diffuse β-APP immunoreactive axonal swellings and bulbs. This clearly demonstrates that β-APP is a more sensitive marker of axonal injury than the classically used silver impregnation technique.

1.4 ANIMAL MODELS OF ACUTE BRAIN INJURY

Animal models have been developed over the years in a quest to try and mimic specific features of the clinical situation after acute brain injury. The use of animal models allows metabolic, neurochemical and behavioural changes to be detected and pathogenic mechanisms to be elucidated. The use of animal models allows physiological status, age and sex matching to be tightly controlled which contrasts with the complex pathophysiology observed in humans after acute brain injury. Different types of models have been developed to try and cover the clinical spectrum of human brain pathology. Models not only provide information about primary damage but also give us an insight into the mechanisms of secondary damage.

A variety of animal models of stroke have been developed over the years comprising the pathology of either focal and global ischaemia. Focal models of ischaemia can be induced either permanently or transiently. The most commonly used model of permanent focal cerebral ischaemia is the occlusion of the middle cerebral artery (MCA). Occlusion of the MCA can be achieved by either electrocoagulation of the artery itself (Tamura et al., 1981) or advancement of an intraluminal thread via the carotid artery to the origin of the MCA (Longa et al., 1989). Transient cerebral ischaemia can be induced either by topical application of the vasoconstrictor peptide, endothelin 1 (Macrae et al., 1993; Dawson et al., 1993) or placement and withdrawal of an intraluminal thread (Longa et al., 1989) and such models have been developed to investigate the effects of reperfusion mimicking the clinical situation where blood flow has been restored.

In relation to head injury, a variety of different traumatic brain injury models (TBI) are used to mimic different types of injury including: cortical impact model (Dixon et al.,1991), fluid percussion model (Lindgren and Rinder 1966; Sullivan et al., 1976), stretch model of axonal injury (Gennarelli et al., 1989; Maxwell et al., 1991) and a model of subdural haematoma (Miller et al., 1990; Bullock et al., 1991). (For more detail about trauma models see review Povlishock et al., 1994 and Maxwell et al., 1997).

1.5 PATHOGENIC MECHANISMS OF DAMAGE

There are multiple mechanisms proposed to be responsible for the pathophysiology observed in white matter following acute brain injury. The mechanisms described in detail below are applicable to both ischaemic stroke and secondary factors involved after a head injury.

1.5.1 Calcium

Calcium homeostasis is an important factor in the pathogenesis of cell death following acute brain injury. Rapid elevation of intracellular calcium $(Ca^{2+})i$ can occur due to both mechanical injury (Shapria et al., 1989; Fineman et al., 1993) and cerebral ischaemia (Choi 1988; Siesjo and Bengtsson, 1989). The intracellular concentration of Ca^{2+} during physiological conditions is less than 0.1μM, that is several orders of magnitude less than the concentration in the extracellular milieu. Therefore, movement of calcium is tightly controlled by a number of ionic transporters and exchangers. Under pathological conditions, loss of control by these systems leads to derangements of the calcium gradient. (Figure 1.4). Lack of adenosine triphosphate (ATP) as a consequence of ischaemia contributes to the failure of key enzymes responsible for the uptake/exclusion of the Ca^{2+} ion.

An isolated optic nerve preparation has been developed to investigate ionic changes in axons and glia after anoxia without the complicating influence of neuronal synapses (Hildebrand and Waxman 1984). Following a 60 minute anoxic period accumulation of K^+ ions in the axoplasm leads to rapid membrane depolarisation (Ransom and Philbin 1992; Fern et al., 1994; Leppanen and Stys 1997). The unique architecture of the axon, with high densities of Na^+ channels present at the nodes of Ranvier, ~1000μm^2 (Waxman 1995) means that slight perturbations in the axolemmal permeability will then cause even larger ionic imbalances to occur. The concept that axonal damage is a consequence of Ca^{2+} overload has been studied using this optic nerve preparation (Stys et al., 1990; Waxman et al., 1993). There are conflicting views as to whether Ca^{2+} directly induces axonal damage or indirectly as a result of other ionic changes. Almost ten years ago addition of voltage operated calcium channel (VOCC) blockers did not prevent irreversible injury suggesting that Ca^{2+} entered the axoplasm via a different

route. However, upon re-examination of these VOCC blockers protective effects were reported (Fern 1995). There are still discrepancies in this theory since VOCC blockers also inhibit release of Ca^{2+} from intercellular stores (Genazzani et al., 1996) and from electrophysiology studies there is no convincing evidence that VOCCs are present on axons (Stys 1998). There is another proposal that Ca^{2+} overload occurs downstream as a consequence of other ionic changes. Membrane depolarisation reverses the operation of the $3Na^{+}/Ca^{2+}$ exchanger, leading to a rapid influx of Ca^{2+} (Siesjo et al., 1989). Ultrastructural studies demonstrated that preincubation with 1μM tetradotoxin (TTX), 10 minutes prior to onset of anoxia, allows complete axonal recovery (Waxman et al., 1994). This evidence proposes that Na^{+} channels are directly coupled to Ca^{2+} entry and is something that requires further investigation. Calcium-mediated injury, although via different routes, may be a common pathogenic factor involved in both grey (Choi et al., 1987; Rothman and Olney 1978; Choi 1988) and white matter damage after brain injury (For review see Stys 1998).

Alterations in axolemma permeability have also been implicated in axonal injury after TBI. Povlishock and colleagues demonstrated moderate TBI evoked alterations in axolemmal permeability to horseradish peroxidase, which is normally excluded from the axolemma, such that the peroxidase tracer flooded into injured axons in amounts proportional to the severity of injury (Pettus et al., 1994). Thus transient defects in the axonal membrane may lead to a disruption of ionic and osmotic homeostatic mechanisms and extracellular Ca^{2+}, which is usually rigorously controlled in the intra-axonal environment, may accumulate in damaged axons (Povlishock 1993; Pettus et al., 1994; Povlishock et al., 1997). In mild TBI axonal permeability changes are thought to be reversible (Graham 1996). However, in moderate to severe TBI ionic imbalances occur so that the axoplasm cannot fully restore ionic and osmotic homeostasis contributing to axonal cytoskeletal breakdown. There may be initial abnormalities that occur within the first few minutes after injury known as mechanoporation, where small pores are created in the lipid bylayer (Gennarelli 1997). These mechanopores are thought to allow Ca^{2+} to leak into the cell down its concentration gradient. Electrophysiological studies have demonstrated transient depolarisation of axons after stretch injury in the guinea pig optic nerve (Tomei et al., 1990) Cytochemical evidence

also supports such Ca^{2+} influx in the same model (Maxwell et al., 1995) with alterations in the membrane pump Ca-ATPase and ecto-Ca-ATPase activity being detected.

Once there is an elevated concentration of axoplasmic calcium it can activate a number of deleterious pathways that lead to damage (Figure 1.4). Elevated cytosolic calcium contributes to cell death by activating lipases which breakdown membranes, nucleases which induce DNA fragmentation and proteases, such as calpains which can cause cytoskeletal breakdown. In addition, raised axoplasmic Ca^{2+} could also interact with pathogenic mechanisms such as oxidative stress (see 1.5.3) (Silver and Erecinska 1990).

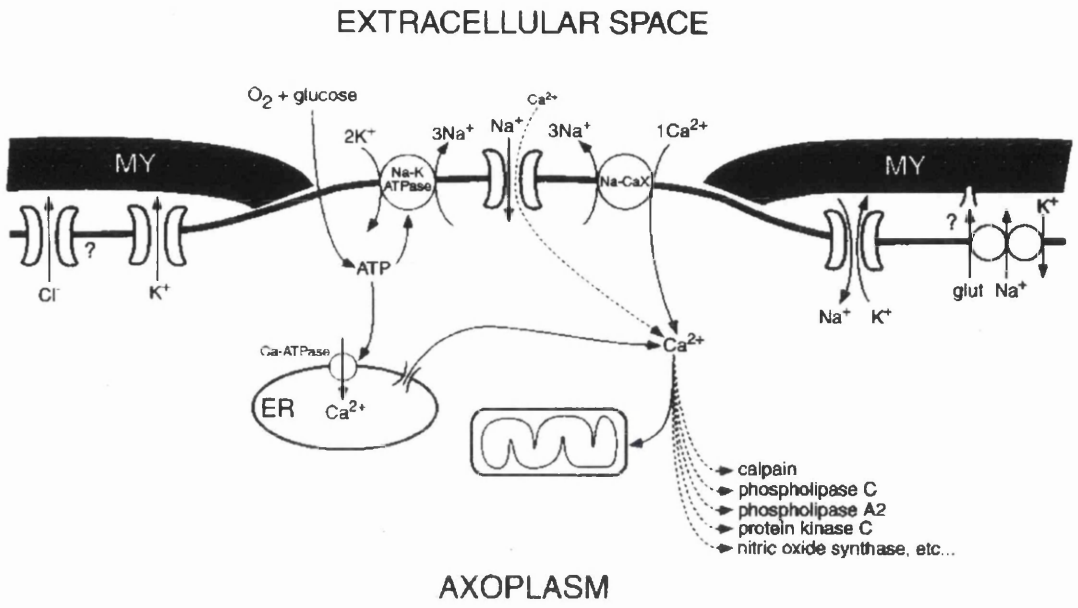

Modified from Stys (1998)

Figure 1.4 Calcium entry into the axon

A diagrammatic illustration of the sequence of interrelated events leading to the influx of calcium into the axon. Acute brain injury leads to alterations in axolemma permeability disrupting ionic homeostasis and encouraging Ca^{2+} to flow into the cell down its concentration gradient through ion channels located on the membrane. Elevated cytosolic calcium will then lead to the activation of a variety of enzymes which could contribute to axonal dysfunction and damage (1.5.2).

Abbreviations: My, myelin; ATP, adenosine triphosphate; ER, endoplasmic reticulum.

1.5.2 Calpains

Calcium activated neutral proteases were first identified in rat brain (Gurof 1964) and subsequently renamed "calpains". There are two specific isoforms, μ-calpain and m-calpain, constitutively expressed in the mammalian brain. Within neurons, there are higher levels of μ-calpain in the somatodendritic region and lower levels within myelinated axons (Perlmutter et al., 1990) while m-calpain is located mainly in axons (Hamakubo et al., 1986) and is thought to be a constituent of myelin (Li and Banik 1995). Calpains are thought to participate in the turnover of cytoskeletal proteins, regulation of kinase activities, transcription and long term potentiation under normal physiological conditions. These two isoforms are structurally homologous with a catalytic 80kDa subunit and a smaller 30kDa subunit, it still remains to elucidate as to whether it stabilises (Yoshizawa et al., 1995) or enhances catalytic activity (Tsuji and Imahori 1981). The primary difference between μ and m-calpain is the concentration of Ca^{2+} required to activate them. μ-Calpain requires micromolar while m-calpain requires millimolar concentrations of calcium to be activated. At the resting cytoplasmic Ca^{2+} concentration, both forms are inactive and become activated when cytosolic Ca^{2+} increases (see above) after acute brain injury. The highest level of calpains is in the cytosol, however, when the enzymes are activated they translocate to the phospholipid membrane. Phospholipids reduce the concentration of calcium required to activate calpain (Suziki et al., 1995). Under pathological conditions membrane disruption increases the amount of phospholipids present in the cytosol thus, enhancing calpains local proteolytic effects. Calpain activation following acute brain injury have been proposed to play a role in the final common neuropathogenic pathway, affecting cytoskeletal proteins, membrane proteins and various regulatory and cell signalling proteins (Figure 1.5).

Figure 1.5 Calpains contribute to degradation of cytoskeletal and cellular proteins

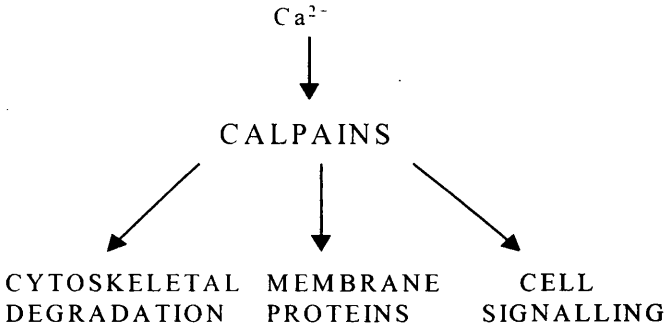

Calpain activation and calpain-mediated breakdown of the cytoskeleton has been proposed as a mediator of damage in a variety of animal models of stroke and TBI. Extensive research has demonstrated cytoskeletal breakdown in a variety of TBI models. Neurofilament breakdown (NF-L and NF-H) has been demonstrated in neuronal cell bodies after controlled cortical impact (Posmantur et al, 1994) and fluid percussion injury (Saatman et al., 1996) in the rat. Breakdown of the microtubule protein, β-tubulin was evident in both grey and white matter while dephosphorylated tau was increased in the cortex and subcortical white matter underlying a subdural haematoma (Fitzpatrick et al., 1997). Increased calpain-mediated spectrin breakdown products were also detected in both grey (Kampfl et al., 1996; Saatman et al., 1996) and white matter (Saatman et al., 1996; Fitzpatrick et al., 1997) after injury. Neurofilament breakdown and calpain activation have been demonstrated within myelinated fibre tracts in a rat model of spinal cord injury (Banik et al., 1997a). Protein degradation in grey matter (Inzuka et al., 1990; Pettigrew et al., 1996) and the axonal cytoskeleton (Dewar and Dawson 1996; Yam et al., 1998) have been reported in models of cerebral ischaemia. There was also evidence of increased calpain-mediated spectrin breakdown products in animal models of focal cerebral ischaemia (Hong et al., 1994; Bartus et al., 1995) and global ischaemia (Roberts-Lewis et al., 1994; Bartus et al., 1998). The importance of calpain-mediated cytoskeletal breakdown mediating the process of acute brain damage is supported by the early appearance after injury of cytoskeletal changes and calpain activation in both models of TBI and cerebral ischaemia cytoskeletal

breakdown in grey and white matter with concomitant increase of calpain-mediated breakdown products is evident. Thus, calpain-mediated injury may represent a final common pathway leading to brain damage, regardless of whether the initial cerebral insult is traumatic or ischaemic.

As well as the calpain-mediated breakdown of the cytoskeleton, calpains have been proposed to interact with other pathogenic processes. Calpains induce the irreversible conversion of xanthine dehydrogenase to xanthine oxidase (Fridovich 1970; McCord 1985; Sussman and Bulkly 1990). Xanthine oxidase in turn catalyses the oxidation of xanthine producing superoxide anion (O^{2-}) accelerating oxidative stress (Figure 1.6).

Figure 1.6 Calpains irreversibly inhibit xanthine dehydrogenase subsequently increasing superoxide anions

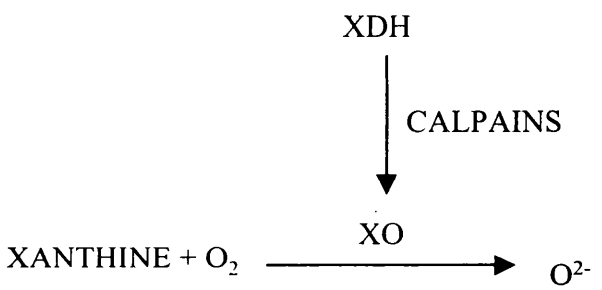

1.5.3 Oxidative stress

In several chronic degenerative disorders such as, Alzheimer's disease, Huntington's disease and Parkinson's disease oxidative stress has been implicated as pathogenic mechanism involved. Oxidative stress has also been proposed to play a major role in the pathogenesis of neuronal cell death following cerebral ischaemia and trauma. Reactive oxygen species are unstable and attack critical cellular components essential for ion homeostasis, membrane integrity and protein synthesis. Oxidative stress has been shown to contribute to neuronal cell body death in grey matter following acute brain injury (Watson et al., 1984; Doopenberg et al., 1998; see reviews Flamm et al., 1978; Chan 1994; Murphy et al., 1999; Love 1999) however, there is little evidence in the literature indicating a role for oxidative stress in white matter damage following acute brain injury.

1.5.3.1 Reactive oxygen species

Within the central nervous system, energy is derived from mitochondrial oxidative phosphorylation. Uncoupling of oxidative phosphorylation occurs within minutes after the onset of ischaemia. (Siesjo et al, 1981; Rachle 1983). Oxidative phosphorylation generates ATP and reduces molecular oxygen to water by the sequential addition of four electrons and four hydrogens. This process occurs within the electron transport chain. There is evidence to indicate that the ubiqinone-cytochrome b region serves as a site of oxygen radical production in the brain under such reducing conditions (Cino and Del Maestro 1989).

The brain consumes 1/5 of the body's total oxygen supply (Siddiqi et al., 1996). This coupled with a high lipid content and its relative paucity of antioxidants (Coyle and Puttfarcken 1993) in the brain could contribute to the production of reactive oxidative species (ROS). ROS can be divided into free radicals; superoxide anion ($O_2^{\bullet-}$) and hydroxyl radical (OH•) and non-radical oxygen species such as hydrogen peroxide (H_2O_2) and hypochlorous acid. ROS readily donate or extract electrons from other molecules evoking cellular damage. Amongst ROS they differ in their potencies (Figure 1.7). Superoxide anion production is not always detrimental, in fact, phagocytes produce superoxide anions to kill certain bacterial strains made by neutrophils (Halliwell and Gutterridge 1986).

Figure 1.7 Reactive oxygen species order of reactivity

$$OH\bullet > H_2O_2 .> O_2^{-} > 0_2$$

The superoxide anion can act as either a strong reducing or weak oxidising agent causing significant tissue damage. However, superoxide is reduced to hydrogen peroxide and oxygen by the metalloenzyme family of superoxide dimutases (SOD) (Figure 1.8A). There are 3 different types of SOD enzymes, Cu/Zn-SOD present in the cytosol, Mn-SOD in the mitochondria and Ec-SOD in the extracellular space (Siesjo et al, 1989). Endogenous antioxidants and scavenging enzymes play major a role in the intracellular defence against oxygen radical damage. Transgenic mice overexpressing

these SOD isoforms have demonstrated a protective role against hypoxic ischaemic insults (Wei 1989; Rosenbaum et al., 1994; Truelove et al., 1994). Hydrogen peroxide is then catalysed to water by a heme protein, catalase, (Figure 1.8B) located in peroxisomes and the inner mitochondrial membrane. Hydrogen peroxide can also be detoxified by the glutathione system (Schraufstter 1985) which is dependent on the maintenance of a sufficient metabolic potential via glucose utilisation. Unlike catalase, glutathione peroxidase (GPx) will convert any hydroperoxide and not just hydrogen peroxide (Juurlink 1997). GPx is present in the cytosol and mitochondria but not within peroxisomes. The glutathione (GSH) redox cycle is a protective system that will minimise cell damage from oxidative stress (Figure 1.8C). Loss of antioxidant activity due to a deficiency in GSH was directly related to mitochondrial damage in the brain (Jain et al, 1991).

Figure 1.8 Role of antioxidants

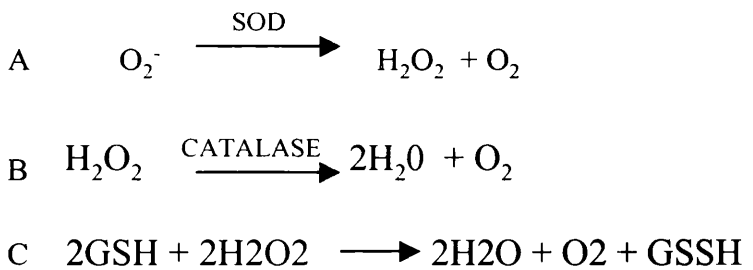

Under pathological conditions oxidative phosphorylation fails and energy stores become depleted very rapidly leading to an excess production of O_2- anions (Siesjo 1978; Doopenberg et al., 1998). It is during this period that endogenous antioxidants can become saturated or their function compromised.

Hydrogen peroxide acts as a poor oxidising agent as its outer orbital is filled. However, unlike superoxide, hydrogen peroxide can diffuse easily across cell membranes. Catalase and GPx cannot remove excess hydrogen peroxide which then allows hydrogen peroxide to accumulate in tissues and spontaneously dismutate to the hydroxyl radical (Beckman 1994). Hydrogen peroxide can catalyse certain transition metals iron or copper to produce an extremely toxic hydroxyl radical (OH•). The hydroxyl radical is thought to cause the most extensive cellular damage, with rate

constants on the order of 10^9 to 10^{10} $m^{-1}s^{-1}$, they react within 5 molecular radi of their production (Dykens 1994).

The production of hydrogen peroxide and the hydroxyl radical is enhanced by the availability of transition metal ions. Iron is an excellent catalyst as it can exist in more than one valance. The ferrous ion (Fe^{3+}) is the stable form while the ferric ion (Fe^{2+}), is capable of transferring electrons and facilitating free radical generation. Iron ions catalyse the production of hydrogen peroxide from superoxide and then to the hydroxyl radical in the overall Haber-Weiss reaction (Figure 1.9).

Figure 1.9 Haber-Weiss reaction

$$O_2^- + H_2O_2 \xrightarrow{Fe^{2+}/Fe^{3+}} OH\bullet + OH^- + O_2$$

The ubiquity of iron within the CNS means that it needs to be tightly controlled in a bound or stored form. At physiological pH 7.4, iron is bound to transferrin in plasma or stored as soluble ferritin. However, if cerebral pH falls to 5.6 or below as occurs following ischaemia (Smith et al., 1986) this will induce the release of free iron (Siesjo et al., 1985; Rehncrona et al., 1989; Bralet et al., 1992), increasing catalysation of free radicals. This process is also thought to be catalysed by copper ions but their distribution within the CNS is unknown. Therefore, the distribution of iron within the CNS is important particularly to cells with a high iron content, for example, oligodendrocytes.

1.5.3.2 Reactive nitrogen species

Nitric oxide (NO) is a gaseous chemical that exists in the CNS. NO is no more reactive than oxygen but its metabolism yields a family of potentially dangerous species collectively known as reactive nitrogen species (RNS). NO is generated from nitrogen and oxygen catalysed by calcium dependent nitric oxide synthase (NOS) (Moncada et al., 1991) (Figure 1.10).

The exact identity of the species generated NO•; NO^+ or NO^- (Stamler et al., 1992) depends on the local redox milieu, pH and temperature (Patel et al., 1999) and the

production of RNS is accelerated by excess intracellular calcium (see 1.7.1) that occurs after acute brain injury (Sato et al., 1993; Tominaga et al., 1993). NO• has an unpaired electron and out competes SOD for superoxide (Beckman and Crow 1993) and reacts at near diffusion limited rates with superoxide to form the peroxynitrite anion (ONOO-) (Beckman et al., 1990; Huie and Padmaya 1993; Squarito and Pyror 1995; Crow and Beckman 1996). Peroxynitrite can be protonated to form the potent oxidising agent peroxynitrous acid (Beckman and Koppenol 1996) (ONOOH) (Figure 1.11). Peroxynitrite formation does not require transition metals and thus oxidative stress can continue even without the presence of iron.

Figure 1.10 Synthesis of nitric oxide and reactive nitrogen species

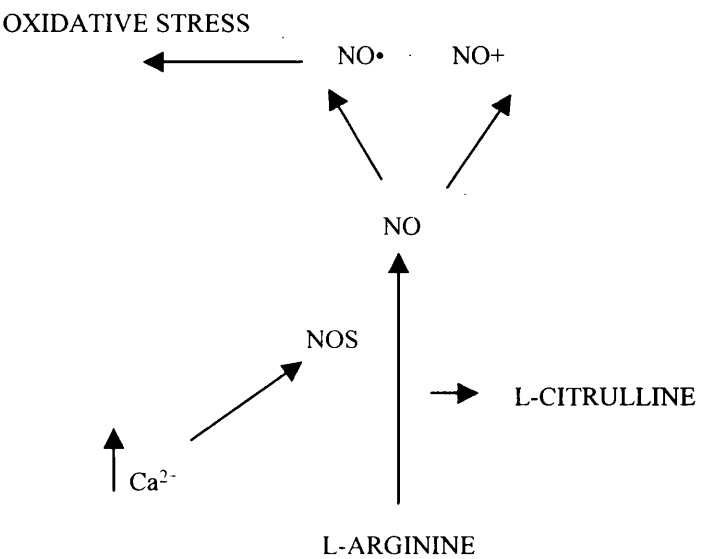

Diagrammatic representation of production of NO from L-arginine catalysed by calcium dependent NOS, either producing NO^+ or NO• which is involved in oxidative stress.

Figure 1.11 Generation of peroxynitrite and peroxynitrous acid

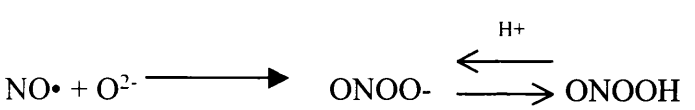

Peroxynitrite attacks cellular components which are critical for respiration and signal transduction and which possess tyrosine residues or thiol moieties. Peroxynitrite can initiate lipid peroxidation by abstracting hydrogen atoms from polyunsaturated fatty acids resulting in nitrated lipids and accelerating the cascade of oxidative stress (Radi et al., 1991; Darely-Usmar et al., 1992; Rubbo et al., 1994).

Respiratory enzymes involved in the electron transport chain are altered by peroxynitrite thus increasing the production of superoxide anions (Castro et al., 1994; Hausladen et al., 1994; Bouton et al., 1997). Peroxynitrite inactivates the active site of Mn-SOD (MacMillian and Thompson 1999) but not Cu/Zn SOD (Smith et al., 1992) and thus can contribute to mitochondrial dysfunction. There is evidence of peroxynitrite mediated necrotic (Zingarelli et al., 1996) and apoptotic (Vaux et al., 1994) cell death. Peroxynitrite nitrates tyrosine residues and can be detected by specific monoclonal antibodies. Nitrotyrosine residues detected by immunohistochemistry were evident in infarcted regions after focal cerebral ischaemia (Fukuyama et al.,1998) and in ischaemia-reperfusion injury (Malinski et al., 1993; Kumura et al., 1995). Proteins that have been nitrated are more susceptible to proteolysis suggesting that there maybe a link between proteolytic enzymes, e.g calpains, and oxidative stress. While ROS and RNS can cause direct damage to key proteins and DNA they have another potentially long lasting effect on membrane lipid bilayers by initiating lipid peroxidation.

1.5.4 Lipid peroxidation

Lipid peroxidation is a self-propagating process in which hydroxyl radicals and peroxynitrite anions readily attack lipid membranes. Membranes rich in polyunsaturated fatty acids (PUFAs) are more susceptible to attack by free radicals than mono or saturated fatty acids because their double bonds allow easy removal of hydrogen atoms. Peroxidation continues by abstracting a methylene hydrogen atom from fatty acid side chains leaving behind a C centred radical lipid which combines with oxygen to form a peroxyradical (Braughler and Hall 1989a; Braughler and Hall 1989b) (Figure 1.12).

Figure 1.12 Lipid peroxidation

$$\text{LIPID-H} + \text{RADICAL} \rightarrow \text{LIPID} + \text{RADICAL-H}$$

$$\text{LIPID} + O_2 \longrightarrow \text{LIPID-}O^{2-}$$

$LipidO_2^{\bullet-}$ is a peroxyradical which attacks membranes, receptors and enzymes and is converted into lipid hydroperoxides by removal of methylene carbons from adjacent PUFAs, which are toxic and unstable. Lipid hydroperoxides decompose into more stable complex aldehydes that are extremely cytotoxic. (Esterbauer 1991; Halliwell 1992; Siddiqi et al., 1996; Marskberry 1997). Important PUFAs that yield hydroxyalkenels with or without iron ions are omega-6 PUFAs. These include linoleate acid; γ linoleate acid and arachidonic acid with arachidonic acid yielding the highest levels of hydroxyalkenel: 2-hydroperoxynonenal, 4,5-hydroxydecenal and 4-hydroxynonenal (4-HNE) (Comporti 1985; Comporti 1989) (Figure 1.13).

Figure 1.13 4-hydroxynonenal

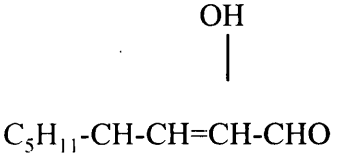

Aldehdye by-products are themselves cytotoxic and may also prolong the initial free radical attack. Unlike free radicals, aldehydes are longer lived and can easily diffuse from their site of origin and thus attack both intracellular and extracellular targets.

4-HNE is an electrophilic species that covalently binds to cysteine, histidine and lysine residues in amino acids by Michael nucleophilic addition (Firguet et al., 1994). Alternatively, it can form pyrolle adducts (Montine et al., 1997a; Mattson 1998) with proteins such as, neurofilaments, microtubule associated proteins and glial fibrillary acidic protein (Montine et al., 1996a; Mattson et al., 1997).

1.5.4.1 Cytotoxic effects of 4-hydroxynonenal

4-HNE cytotoxicity has been studied predominantly *in vitro* in a variety of tissue types. 4-HNE not only damages cells directly but initiates biochemical changes that could produce cellular damage. Endothethial cells exposed to 4-HNE displayed significant cytotoxic defects (Karlburber 1997) that may have an important effect on the blood brain barrier (BBB). BBB permeability defects could allow an influx of oxygen to brain tissue thus escalating production of ROS, which could then lead to brain tissue damage. Mitochondrial inhibition by 4-HNE increased superoxide anions in cortical synaptosomes (Keller et al., 1997). Topical application of 4-HNE induced relaxation of pre-contracted cerebral arteries and this was partially prevented by L-NAME. This suggests that 4-HNE might interact with nitric oxide affecting the cerebral vasculature (Martinez et al., 1994).

Ion homeostasis is an important factor following acute brain injury and 4-HNE can increase intracellular calcium levels indirectly. The Na^+K^+-ATPase transporter is an integral membrane protein and is susceptible to both intra and extracellular concentrations of 4-HNE. 4-HNE causes irreversible damage to the transporter (Siems et al., 1996) and disruption of the membrane potential causes an influx of Ca^{2+}. A slow progressive increase in calcium influx was observed in hippocampal slices within 2 hours of 4-HNE exposure (Mark et al., 1997). 4-HNE binds to the GLT1 glutamate uptake transporter on astrocytes (Springer et al., 1997; Keller et al., 1997; Blanc et al., 1998). If 4-HNE were present then accumulation of glutamate in the surrounding microenvironment would augment secondary excitotoxicity in adjacent more vulnerable cells.

Most of the above findings have been characterised in culture *in vitro*, however, there is recent data demonstrating that the lipid peroxidation by-product, 4-HNE is toxic *in vivo*. Intracerebral injection of 4-HNE into the basal forebrain induced perikaryal damage (Bruce-Keller et al., 1998). In a model of spinal cord injury an increase in 4-HNE immunoreactivity was detected in white matter tracts rostrocaudal from the site of injury (Springer et al, 1997). However, there is no evidence available indicating that 4-HNE is toxic to cerebral white matter.

AIMS OF THESIS

Extensive research has demonstrated that the neuronal perikaryon in grey matter is vulnerable following acute brain injury. The introduction of this thesis has outlined the importance of axons and oligodendrocytes and their vulnerability following acute brain injury. There are number of non-receptor mediated mechanisms that have been discussed in the introduction that might be involved in the pathogenesis of white matter damage. A number of these processes can be either initiated at the point of injury or as a consequence of primary injury and work either independently or in interaction with other pathogenic processes. A hypothesised scheme is illustrated below (Figure 1.14).

Figure 1.14 Cascade of pathogenic factors involved in axonal damage after acute brain injury

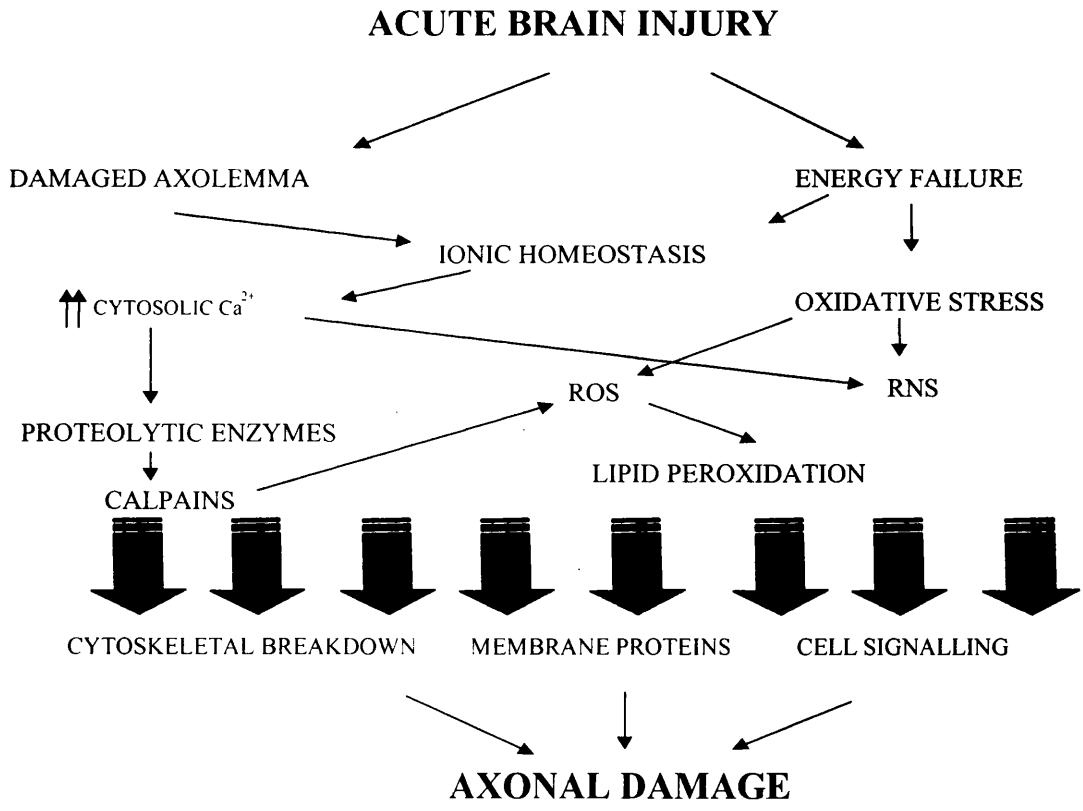

The specific aims of this thesis were:

1. To determine if cytoskeletal proteins associated with the axonal cytoskeleton were degraded in the corpus callosum after human head injury.

2. To determine whether calpains were activated in the corpus callosum after human head injury.

3. To determine if there were pathological changes in white matter following systemic injection of a mitochondrial inhibitor, 3-nitropropionic acid in the rat.

4. To determine if intracerebral injection of 4-hydroxynonenal in the rat was toxic to both grey and white matter *in vivo.*

5. To determine if 4-hydroxynonenal was toxic to oligodendrocyte cultures *in vitro.*

CHAPTER II

METHODS AND MATERIALS

2.1 TISSUE COLLECTION

2.1.1 Human brain tissue

The head-injured patients in this study had been managed by the Department of Neurosurgery at the Institute of Neurological Sciences, Glasgow. In each case a full autopsy was carried out, during which, 11 anatomical defined regions in each cerebral hemisphere were dissected from a 1cm coronal slice of unfixed brain at the level of the lateral geniculate bodies. This allowed the selection of multiple samples for freezing in isopentane and storing at -80°C until neurochemical analysis (Dewar and Graham 1996). Thereafter the specimen was immerse fixed in 10% formal saline for at least 3 weeks before dissection, using a previously described protocol (Adams et al., 1980). Comprehensive histological studies were carried out at the level parasaggital gyrus thereby allowing close correlation between observations deriving from the adjacent frozen and paraffin embedded brain slices. Material was acquired to the tissue bank according to MRC guidelines and was approved by local hospital ethics committee.

Tissue from the corpus callosum (Figure 3.1) of all head-injured and controls (Table 3.1) was dissected from frozen blocks of the parasaggital region and homogenised for Western blot analysis (see 2.2). Adjacent formalin fixed material was paraffin embedded and cut into 8μm sections for histology and immunohistochemistry (see 2.3.1).

2.2 WESTERN BLOTTING

2.2.1 Tissue homogenisation

Human corpus callosum tissue (see 2.1.1) was homogenised with a Polytron in 10 volumes of ice-cold HEPES buffer: 5mM HEPES; 0.32M sucrose; pH 8; 5mM benzamidine; 2mM β.mercaptoethanol; 3mM EGTA; 0.5mM $MgSO_4$; 1mM sodium vanadate; 0.1mM phenylmethylsulfonyl fluoride; 2μg/ml leupeptin; 5μg/ml pepstatin and 2μg/ml aprotinin (modified from Masliah et al., 1990). Homogenates were centrifuged for 5 minutes in a bench microfuge (Beckman, microfuge E) and the

supernatant collected. The supernatant was stored at -20°C for either protein assay or gel electrophoresis. Protein content of the supernatant was determined to 1mg/ml according to Lowry et al., 1951, using bovine serum albumin as the standard (Figure 2.1). Standards and tissue samples were prepared simultaneously in a 1:1 mixture of 2% copper sulphate; potassium sodium tartate; sodium carbonate and Folin's reagent. Absorbance readings from a spectrophotometer (Pharmacia. Ultraspec III) were taken at 680nm and the protein concentration of tissue samples derived from BSA standards. Protein samples were prepared in Laemmli sample buffer; 0.1M Tris HCl pH8; 0.1% bromophenol blue, 5M urea, 5% DTT, 5%SDS (Laemmli 1970).

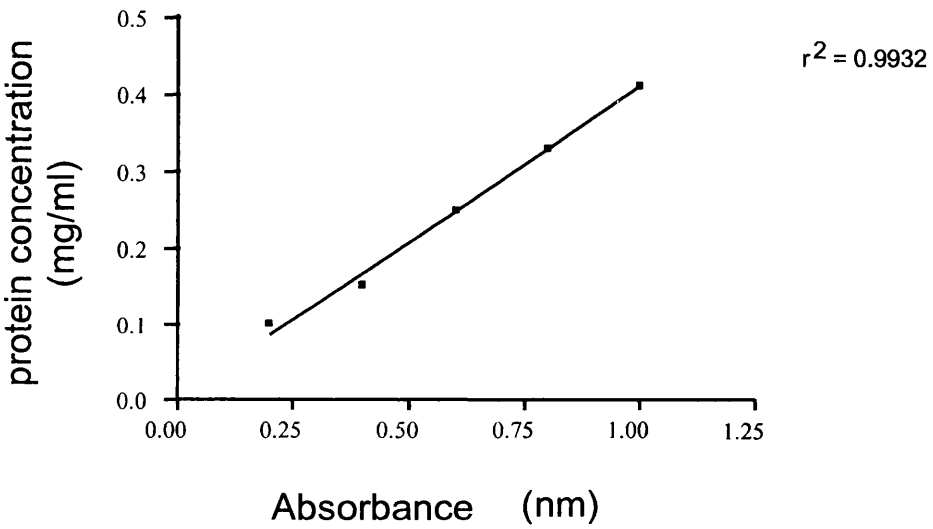

Figure 2.1 Bovine serum albumin protein standard curve

Linear regression curve demonstrates that absorbency at 680nm increases in a linear manner with increasing BSA (mg/ml) protein concentration. Absorbency values for all Western blotting experiments (Chapter III) were then derived from the curve to determine the protein concentrations of each sample.

2.2.2 Sodium dodecyl sulphate polyacrylamide gel electrophoresis (SDS-PAGE)

Protein samples diluted in Laemmli sample buffer (Laemmli 1970) were firstly boiled for 5 minutes to denature proteins, placed on ice and then separated by sodium dodecyl sulphate polyacrylamide gel electrophoresis (SDS-PAGE). Gels were prepared with either 12% protogel or 8% gradient gel (see appendix 2) in a sandwich of two glass plates (Bio-Rad). The resolving gel was prepared first then topped with a 3% stacking gel the gels were polymerised with N,N,N'N'- tertramethylethlenediamine (TEMED). 25μg protein were loaded to each lane in the stacking gel and separated through the gel in a water cooled gel tank (Bio-rad) at 12mV overnight in 0.19M glycine, 0.024 M Tris base and 10% SDS. Biotinylated and prestained molecular weight standards were loaded alongside the protein samples to determine the bands were at the correct molecular weight. Proteins were then transferred to nitro-cellulose membranes detection (Schleicher and Schuell, 0.45μm) for alkaline phosphates using a water-cooled tank blot transfer cell at 80v for 3h in 0.19M glycine, 0.024 M Tris base and 20% methanol.

2.2.3 Coomassie blue staining of gels

Gels were stained with 40%, 10% acetic acid and 0.1% coomassie blue overnight at room temperature. The following day the gel was destained in a 40% methanol and 10% glacial acetic acid solution and this allowed visualisation of protein bands to confirm transfer and equal loading of samples.

2.2.4 Immunoblotting

Blots were incubated in Tris-buffered saline, (TBS) (20mM Tris, HCl pH7.5, 0.5M sodium chloride, 0.2% Tween-20, (TBS-T) containing 3% dried non-fat milk for 2 hours at room temperature. Blots were washed 3 x 10 minutes in TBS-T then incubated in primary antibody overnight at 4°C. Dilutions of primary antibodies are shown in Table 2.1. Blots were washed for 3 x 10 minutes in TBS-T and incubated with biotinylated anti-mouse secondary antibody for monoclonal antibodies (1:250) and biotinylated anti-rabbit secondary antibody for polyclonal antibodies (1:250) for 1 hour. Blots were washed in TBS-T for 3 x 10 minutes. The blots were re-incubated for 1 hour with streptavidin-alkaline phosphatase (1:1500 in TBS-T with 3% dried non-fat milk).

Immunoreactivity was then visualised using an alkaline phosphatase substrate kit (Bio-Rad).

2.3.4 Quantitative analysis of immunoreactivity of blots

The optical density (OD) of protein bands on the developed blots was quantified using an MCID image analyser (Imaging Research, Canada). The instrument was calibrated using Kodak gelatin filters of known OD (Figure 2.2). Calibration allows the relative optical density for protein bands to be calculated.

Increasing protein concentrations, detected by SBAbS2, a polyclonal antibody that detects calpain-mediated spectrin breakdown products were measured to confirm that with an increase in protein concentration there was an increase in relative optical density value (Figure 2.3). From the relative optical density values shown in figure 2.3, 25μg of protein was taken as the optimal protein concentration (Figure 2.4). For the experiments described in Chapter III 25μg protein was loaded for all controls and head-injured patients.

Primary antibodies Table 2.1

Antibody	Company	Clone	Host	Blocking Serum	IH	WB
A2B5	Boehringer Mannheim	A2B5-105	Mouse	Horse	1:100	
β-APP	Boehringer Mannheim	22C11	Mouse	Horse	1:500*	
β-tubulin	Sigma	JDR.3B8	Mouse	Horse		1:750
GalC	Boehringer Mannheim	mGalC	Mouse	Horse	1:100	
GFAP	Sigma	G-A-5	Mouse	Horse	1:4000	
4-HNE	Calbiochem		Rabbit	Goat	1:2000*	
Mn-SOD	Calbiochem		Rabbit	Goat	1:300	
NF68	Sigma	NR4	Mouse	Horse	1:400	1:1000
NF200	Sigma	NE14	Mouse	Horse		1:2000
NF200	Sigma	N52	Mouse	Horse	1:400	1:1000
SBAbS2	SKB		Rabbit	Goat	1:10,000	1:20,000
Spectrin	Chemicon		Mouse	Horse	1:1000	
SNAP-25	Serotec	SP12	Mouse	Horse	1:750	
Tau 1	Gift		Mouse	Horse		1:1000
μ calpain	Chemicon		Mouse	Horse		1.1000

*: microwave with citric acid pH6; WB; Western blotting; IH: immunohistochemistry;
SKB: SmithKline Beecham, SBAbS2 antibody was a gift from SmithKline Beecham
Tau 1 antibody was a gift from Prof. B.Anderton

Characterisation of cells in culture:Anti-A2B5 = 0-2A progenitor; Anti-GalC = differentiated oligodendrocytes and GFAP = astrocytes. *Cytoskeletal proteins:* β-APP = a fast axonal transport protein; β-tubulin = β-tubulin; 4-HNE =4-HNE modifed proteins; NF86 = neurofilament (NF) light subunit (independent of phosphorylation); NF200 (clone NE14) NF heavy subunit dependent on phosphorylation state; NF200 clone N52 = NF heavy subunit independent of its phosporylation state; SBAbS2 = calpain-mediated spectrin breakdown products; Spectrin = brain spectrin, SNAP-25 = a fast axonal transport protein and Tau 1 = dephosphorylated tau. *Enzymes:* Mn-SOD = Manganese superoxide dismutase; μ-calpain = inactive and active isoforms

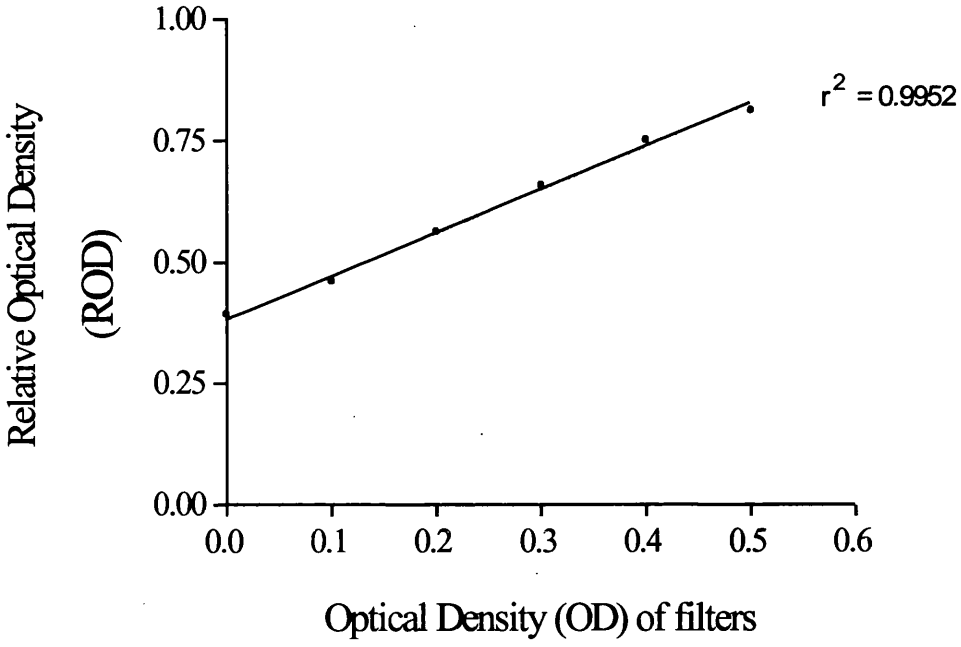

Figure 2.2 Calibration curve for optical density filters

Before measuring protein band of sample, background of the blot was calibrated using Kodak gelatin filters of known optical density. On the x axis 0.0 is the OD value for the background of the blot, 0.1 – 0.6 is the increase in OD filters. Calibration of the imaging system allows the relative optical density for protein bands to be calculated.

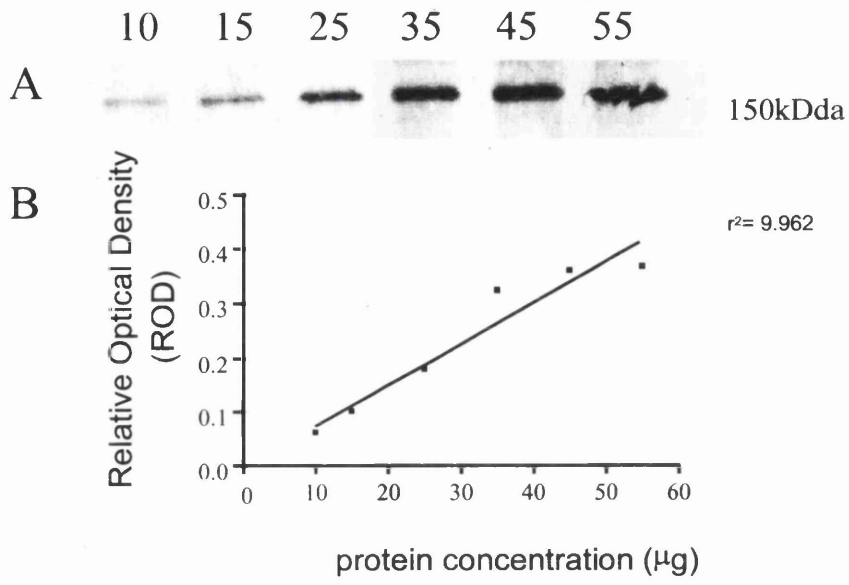

Figure 2.3 Linear regression of protein concentration versus optical density

The panel in A) shows a Western blot of SBAbS2 immunoreactivity in the corpus callosum of a control patient showing the signal produced with increasing protein concentrations. The quantitative data in B) demonstrates increasing protein concentrations produces a linear increase in relative optical density.

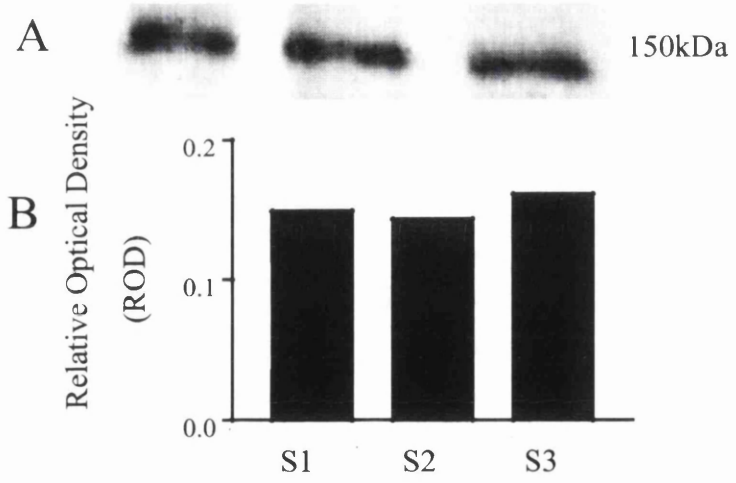

Figure 2.4 Optical density values for 25µg protein

The panel in A) shows a Western blot of SBAbS2 immunoreactivity demonstrating repeated loading of 25µg protein for a control patient. The quantitative data in B) shows equivalent relative optical density values all three protein samples loaded. S1, S2, S3 = protein sample in triplicate.

2.3 IMMUNOHISTOCHEMISTRY

2.3.1 Single label immunohistochemistry on paraffin sections

Tissue sections from rat and human studies were dewaxed in histoclear for 10 minutes and dehydrated in 100% alcohol for 10 then 5 minutes. Tissue sections were pretreated for 30 minutes in 3% hydrogen peroxide in methanol to block endogenous peroxidase. Sections were then rinsed in running tap water for 5 minutes and then washed in 50mM phosphate buffer saline (PBS). Sections were then incubated for 1 hour with 10% normal serum (Table 2.1) 0.5% bovine serum albumin in PBS to reduce non-specific binding. Sections were incubated in primary antibody overnight at 4°C (Table 2.1) then washed in PBS 2 x 5 minutes the next day. Sections were then incubated for 1 hour in biotinylated secondary antibodies: biotinylated anti-mouse secondary antibody for monoclonal antibodies (1:100) and a biotinylated anti-rabbit secondary antibody for polyclonal antibodies (1:100) (Table 1). Avidin-biotin complex (ABC) was prepared 1 hour before use. Following incubation with secondary antibody tissue sections were washed 2 x 5 minutes in PBS and then incubated in ABC for 1 hour. Finally sections were washed in PBS 2 x 5 minutes then developed using 3'3' diaminobenzidine tetrahydrochloride (DAB) as the chromagen. In all immunohistochemistry protocols, negative controls were performed by omitting the primary antibody (Figure 2.5).

2.3.2 Fluorescent labelling

Immunohistochemistry on oligodendrocyte cultures (see 2.7.2) to characterise O-2A cell lineage and the presence of astrocytes was detected using fluorescence. Cells were post-fixed in 4% paraformaldehyde for 15 minutes. Blocking solution was applied to reduce non-specific binding for 1 hour and then incubated with primary antibody (Table 2.1) overnight at 4°C. The next day cultures were washed in PBS and incubated for 1 hour with fluorescein isothiocynate (FITC) and mounted in an aqueous media with anti-fading agent.

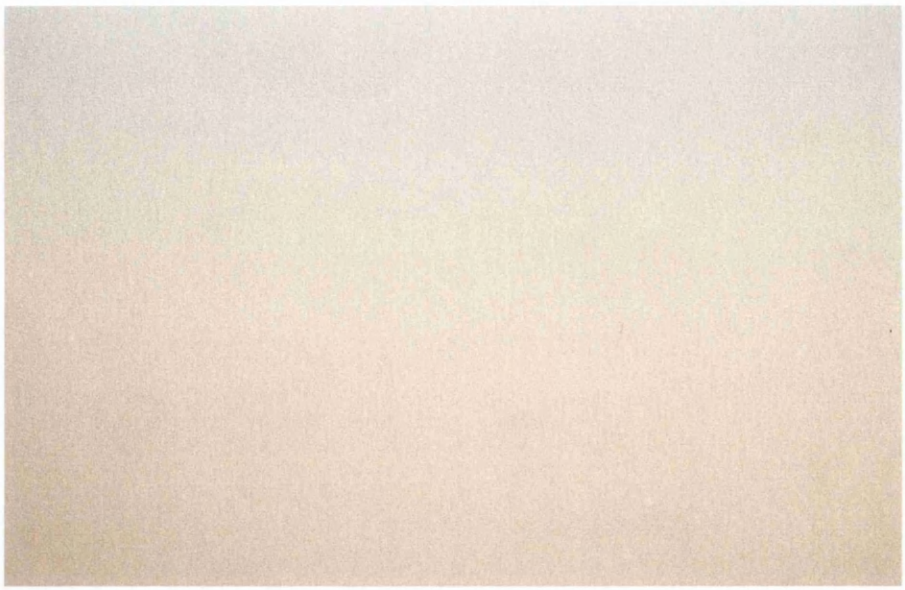

Figure 2.5 Immunohistochemistry negative control

The scanned image shows the absence of immunostaining when the primary antibody was omitted. This indicates the specificity of primary antibody binding. A negative control was included in all immunohistochemical experiments. X400 Magnification

2.4 AN EXPERIMENTAL MODEL OF OXIDATIVE STRESS

2.4.1 Systemic injection of 3-nitropropionic acid

Male adult Sprague-Dawley rats (Charles River), weighing between 300-320g, were individually housed before and after injection of 3-nitropropionic acid (3-NPA). Rats (n=4 or 5 per group) were injected intraperitoneally with 10, 15, 20 or 30mg/kg 3-NPA dissolved in sterile distilled water (pH 7.4 with 5M NaOH) or vehicle (sterile distilled water). Animals were monitored for any unusual behavioural changes, e.g motor deficits, over a 24 hour period. Rats were deeply anaesthetised with 5% halothane and 30% oxygen/70% nitrous oxide and transcardially perfused fixed with 0.9% saline and then 4% paraformaldehdye 24 hours after injection. Rats were decapitated the heads post-fixed for 24 hours in 4% paraformaldehyde the brains were removed and post fixed for a further 48 hours before being processed through a series of dehydrating and clearing agents and then paraffin embedded (see 2.4.2). 5μm microtome sections were collected onto poly-L-lysine slides for histology and immunohistochemistry.

2.4.2 Rat tissue processing I

Fixed rat brains were placed supine in a stainless steel matrix and cut into coronal blocks. For the 3-nitropropionic acid study (Chapter IV), blocks were cut rostrocaudally through the brain although the region of neuropathological interest was at the level of the caudate nucleus. The block was placed in a cassette (Surgipath) and processed through a series of dehydrating, clearing and waxing agents (Shandon Citadel 1000 automatic processor). Cassettes were first placed in 50% absolute alcohol for 30 minutes then 70% absolute alcohol, 30 minutes; 90% absolute alcohol, 30 minutes; 100% absolute alcohol twice for 30 minutes and then clear through three separate histoclear tanks for 30 minutes each and then 30 minutes in paraffin wax at 60'C and finally in a vacuum containing paraffin wax for 1 hour. Blocks were removed from cassettes and cooled before cutting. 5μm microtome sections were collected onto poly-L-lysine coated slides for histology and immunohistochemistry.

2.5 AN EXPERIMENTAL ANIMAL MODEL OF LIPID PEROXIDATION

2.5.1 Intracerebral injection of 4-hydroxynonenal, ethanol and artificial cerebrospinal fluid

Male Sprague Dawley rats (Harlan Olac, UK) weighing between 290-330g were housed together before surgery and individually housed afterwards, throughout the 24 hour recovery period. Animals were anaesthetised with 5% halothane and 70% nitrous oxide/30% oxygen in a perspex box and placed in a David Kopf stereotaxic frame (Clark Electromedical). A stereotaxic face mask was fitted over the snout and halothane, (1-2%) was administered for duration of the experiment. An incision was made in the scalp and Bregma exposed. A craniotomy was made with a dental drill and using a Hamilton syringe 0.5μl 64mM 4-hydroxynonenal (4-HNE), vehicle (ethanol) or artificial cerebrospinal fluid (aCSF) was injected into the subcortical white matter. 4-HNE, ethanol and aCSF were injected at the stereotaxic co-ordinates (A/P = -0.26mm from Bregma, L/M = 2mm and D/V = 3mm) at a rate of 0.1μl/min. The needle was left in place for 10 minutes before removal to allow diffusion of the injectate away from the needle tip. The scalp was sutured and 2mls of sterile saline was given subcutaneously. Aureomycin (Cyanamid) was applied topically to the scalp to prevent infection. Animals were allowed to recover for a period 24 hours and during this period monitored for any gross behavioural changes. Animals were then re-anaesthetised with 5% halothane 70% nitrous oxide/30% oxygen in a perspex box and then transcardially perfused with 0.9% saline and 4% paraformaldehyde. Rats were decapitated and the heads post-fixed in 4% paraformaldehyde, the brains removed and post fixed for a further 48 hours before being processed through a series of dehydrating, clearing and waxing agents and embedded in paraffin. 5μm microtome sections were collected onto poly-L-lysine slides for histology and immunohistochemistry.

2.5.2 Rat tissue processing II

For the 4-hydroxynonenal study (Chapter V), rat brains were cut rostrocaudally, and placed in cassettes (Surgipath) and hand processed for paraffin embedding. First blocks were placed in 50% absolute alcohol for 3 hours; 70% absolute alcohol, 3 hours; 90% absolute alcohol overnight, on the second day cassettes were transferred in to 100% absolute alcohol twice for 3 hours and then into a mixture of absolute alcohol and

xylene for 1 hour, fresh xylene replaces the mixture for 1 hour and then the cassettes remained in xylene overnight. On the final day the cassettes were removed from xylene and put in paraffin wax for 3 hours and transferred to new paraffin wax for 4 hours. Blocks were then embedded and cooled before cutting. 5μm microtome sections were collected onto poly-L-lysine coated slides for histology and immunohistochemistry.

2.6 HISTOLOGY

2.6.1 Haematoxylin and eosin staining

Histological analyses were performed on rat paraffin tissue sections. Paraffin sections were dewaxed and rehydrated through a series of graded alcohols before washing in water. The sections were then placed in haematoxylin for periods of between 1-10 minutes, washed in water, differentiated in hydrochloric acid/1% methlyated spirits and washed thoroughly in water. Following incubation in Scots tap water for 1 minute, sections were then stained in eosin for 2-5 minutes, washed in water, dehydrated through the alcohols before 5 minutes in histoclear and then mounted onto coverslips with DPX.

2.6.2 Cresyl fast violet and luxol fast blue staining

Rat tissue sections were dewaxed in histoclear for 10 minutes and rehydrated in absolute alcohol for 2 minutes. Sections were then washed in methylated spirits and incubated overnight in luxol fast blue. Sections were washed in running water to remove excess stain and then differentiated in lithium carbonate (few dips), re-washed in running water and then re-incubated with cresyl fast violet overnight. Following this, sections were washed in running water and differentiated in acetic acidified methylated spirit. Finally, sections were dehydrated through graded alcohols, cleared in histoclear and mounted onto coverslips with DPX.

2.7 CELL CULTURE

2.7.1 Preparation of mixed glial cultures

All cell culture procedures were carried out under sterile conditions. Postnatal (1-3 days) Sprague-Dawley rats were killed by intraperitoneal injection of 0.1ml sodium pentobarbitone, decapitated and the heads placed in 70% ethanol. Skulls were removed using fine sterile foreceps and whole brains placed in Hanks Balanced Salt Solution without calcium and magnesium (HBSSw/oCaMg). Cerebral hemispheres were separated along the median fissure and the hippocampus and meninges removed with the aid of a dissecting microscope using transillumination and placed in fresh HBSSw/oCaMg. Culture media was drained and the neopallia finely chopped into small cubes. Cells were enzymatically dissociated using 2000U/ml collagenase, 0.25% trypsin and 0.02% ethylenediaminetetraacetic acid (EDTA) incubated at 37°C (5% /CO_2/95%/O_2) for 20 minutes. Cells were then incubated with soya bean trypsin-DNAse inhibitor for a few minutes and then 3 mls of HBSSw/oCaMg was added. Cells were then triturated, firstly through a 10ml pipette (10x); 21G needle (5x) and finally through a 23G needle (3x) to obtain a single cell suspension. The cell suspension was then centrifuged at 1000 rpm for 7 minutes (Hettich zentrifugen, Universal 16/16R). The supernatant was removed carefully and 2-3mls of 20% fetal calf serum in Dulbecco's Modified Eagles Medium (20% FCS-DMEM) was added and triturated through a 5ml pipette, a 23G followed by a 25G needle (3 times each). Cell density was determined by trypan blue exclusion (2.7.5). Trypan blue is a specific dye that is only taken up into the cell if cell membrane integrity has been compromised. A 1:10 dilution of the cell suspension (10µl), 20% FCS-DMEM (140µl) and 0.4% trypan blue (40µl) was prepared and 40µl of mix pipetted onto a haemocytometer. Cells were counted at x400 magnification using an inverted phase contrast microscope (Lecia DMIL). Only phase bright cells were counted, and blue stained cells were excluded.

Cells were then plated at 6 x 10^6 per $75cm^3$ flask. Culture medium was changed after 4 days to 10% FCS-DMEM and every 3-4 days thereafter until cells were 80% confluent or a maximum of 12 days old. Under these conditions a monolayer of polygonal type 1 astrocytes bed down while phase bright O-2A progenitor cells reside on top of this layer. The unique properties of mixed glia cells growing together allowed us to obtain

pure oligodendrocyte cultures. The adhesion of O2-A progenitors to the astrocytic layer is weaker than adhesion of the astrocytes to the culture flasks, up to 12 days after initial plating.

2.7.2 Preparation of oligodendrocyte cultures

To obtain oligodendrocyte cultures a modified method of McCarthy and De Vellis (1980) shaking protocol was used. Mixed culture flasks were shaken on an orbital shaker (Forma Scientific, Life Sciences International) at 150 rpm for 90 minutes, this allowed removal of unwanted debris and microglia. The cultures were then re-incubated with fresh 10% FCS-DMEM for 1 hour. Cultured flasks were then re-shaken at 260rpm for 18-22 hours, this allowed detachment of O-2A progenitors. The media collected from the shaken flasks was poured through a 10μm mesh which had been soaked with 70% ethanol. Residual cells were obtained from flasks rinsed with a small volume of unsupplemented DMEM. Sieved media was then centrifuged at 2000rpm for 10 minutes and the supernatant discarded. Sato's media (1-2 mls) was added to the pellet prior to trituration (23G then 21G needle). Cell density was determined by trypan exclusion as described for mixed glia cells (see 2.7.1). Cells were plated at 2 x 10^2 on poly-L-lysine coverslips. Cultures were incubated (37°C (5% /CO2/95%/O_2) for 7 days being fed every 2 days with fresh Sato's media. Seven day old oligodendrocytes were then treated with different toxins thought to play a biological role in oxidative stress (see 2.7.4; 2.7.5).

2.7.3 Characterisation of 0-2A cell lineage

The sequential process and changes in phenotype during maturation and differentiation of 0-2A cell lineage can be labelled by immunohistochemistry. Using specific antibodies that recognise cell surface antigens at different stages of oligodendrocyte development (Figure 2.8). Anti-A2B5 detects the initial proliferating bipolar cell that can then be differentiated into either an oligodendrocyte or type-2 astrocyte. Oligodendrocytes immunolabelled with anti-galactocerebroside while type-2 astrocytes are detected by anitbodies against glial fibrial acidic protein (GFAP).

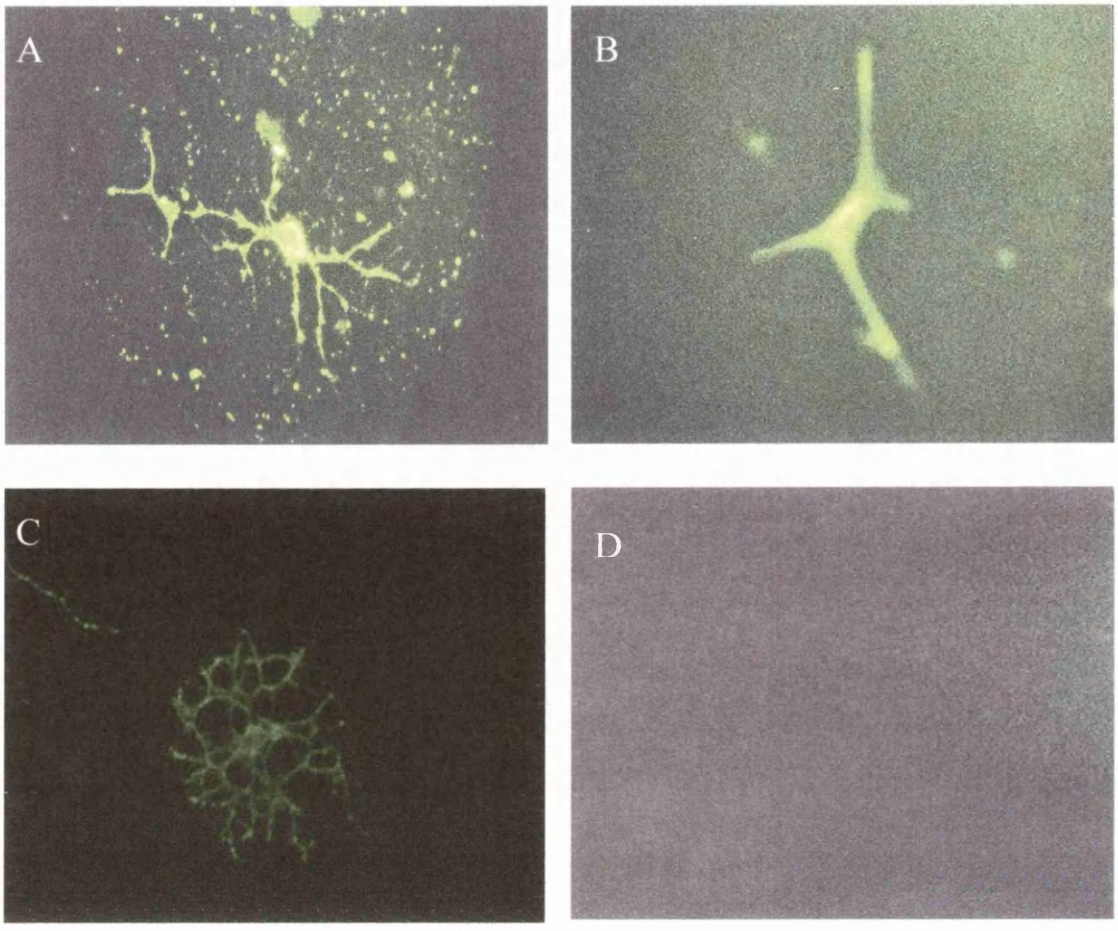

Figure 2.6 Immunodetection of O-2A progenitors and their differentiation into either type-2 astrocytes or oligodendrocytes *in vitro*

Representative photographs of A) O-2A progenitors visualised by A2B5 antibody (2 days in culture) B) GFAP positive type 2-astrocyte (7 days in culture) C) oligodendrocyte labelled with the galactocerebroside antibody (7 day in culture) and D) omission of primary antibody. O-2A progenitors can divide into either oligodendrocytes or type-2 astrocytes depending on the culture media. Magnification X400

2.7.4 Glucose/glucose oxidase treatment

Following characterisation of cultures, the first study was to evaluate an experimental paradigm which has been previously reported to detect oligodendrocyte cell death using similar oligodendrocyte cultures (Kim and Kim 1991). Oligodendrocyte cultures were taken at 7 days and were first washed in minimum Eagles medium (MEM) for 2 x 5 minutes, then incubated in MEM + 0.5% glucose for 30 minutes at 37°C (5%/CO2 95%/O_2). 20mU/ml glucose/glucose oxidase was dissolved in 0.05M sodium acetate buffer pH 5.1 and added to cultures for 1, 2 or 4 hours (Kim and Kim 1991). This particular experiment was chosen because incubation with glucose/glucose oxidase enzymatically generates a free radical system. Glucose oxidase in a glucose environment produces hydrogen peroxide directly at a slow continuous rate (Rubin and Faber 1984) (Figure 2.7). Control cultures contained MEM + 0.5% glucose for each time point. Cell viability was assessed using trypan blue and cell death calculated (see 2.7.5).

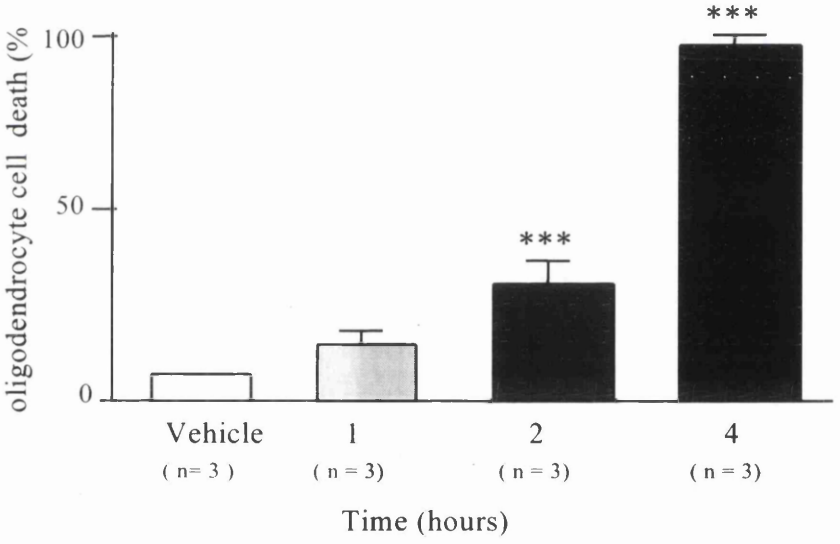

Figure 2.6 Glucose/glucose oxidase kills oligodendrocytes in a time dependent manner

20mU/ml glucose oxidase plus 0.5% glucose time dependently increased oligodendrocyte cell death over 1, 2 and 4 hours. There was a significant increase in the percentage of oligodendrocyte cell death following 2 and 4 hours. Data are mean + SEM. One way ANOVA post tested with Student's t test and corrected with Bonferroni. The data replicate the findings by Kim and Kim 1991. Vehicle = MEM +0.5% glucose at the longest time point, 4 hours.

2.7.5 Calculating percentage of oligodendrocyte cell death

Oligodendrocytes cultures grown on coverslips were treated with various toxins after seven days in culture and the cell viability determined by trypan blue exclusion. At the end of the experiment, cultures were incubated in a 1:1 mix of 0.4% trypan blue: HBSS for 10 minutes then washed in phosphate buffered saline (PBS) for 2 x 2 minutes and then post fixed with 3% glutaraldehyde in 0.1M phosphate buffer for 1 hour. Coverslips were then mounted in an aqueous mounting media; (8g polyvinyl alcohol, 0.2M Tris-HCl pH8.5, 20ml glycerol and 1-2.5% 1,4 diazoabicyclo(2,2,2) octane). To ascertain cell viability a 1cm square graticule was placed in 10 randomly selected areas in each coverslip. The number of dead, trypan blue positive, and number of live, phase bright cells, were counted using a phase contrast microscope (Lecia) at X200 magnification. The percentage cell viability was expressed as the number of dead cells (C_D) minus the number of live cells (C_L) divided by the total number of cells (C_T) (Figure 2.7).

Figure 2.8 Calculating percentage of oligodendrocyte cell death

$$\% \text{ cell death} = \frac{C_D - C_L}{C_T}$$

2.7.6 4-Hydroxynonenal treatment

Seven day old oligodendrocyte cultures were washed with Sato's for 2 x 5 minutes and then incubated at 37°C (5%/CO2 95%/O_2) with 1, 10 or 50μM 4-hydroxynonenal or vehicle (0.2% ethanol) for 1, 2 or 4 hours. 4-HNE concentrations (1-50μM) are within the range known to be generated in cells exposed to $FeSO_4$ and other insults that induce membrane lipid peroxidation (Esterbauer et al 1991; Mark et al 1997). Trypan blue exclusion assessed cell viability as described for glucose/glucose oxidase (see 2.1.6). Morphological changes of cultured oligodendrocytes was also assessed as an endpoint and assessed using immunohistochemistical labelling of a monoclonal antibody against the cytoskeletal protein, spectrin (see 5.3.2).

CHAPTER III

CYTOSKELETAL BREAKDOWN IN THE CORPUS CALLOSUM OF HEAD-INJURED PATIENTS AND ALTERATIONS IN CALPAIN ACTIVITY

3.1 INTRODUCTION

Diffuse axonal injury (DAI) is an important type of pathology in patients who sustain a blunt head injury, being the commonest cause of coma in the absence of an intracranial mass lesion (Graham et al., 1995; Graham and Gennarelli 1997). Irreversible axonal damage was once thought to occur solely at the moment of injury and there is general consensus that axons are primarily vulnerable to mechanical loading (Povlishock and Christman 1995; Gennarelli 1997). However, it is now recognised that although a proportion of axons may become severed at the time of injury, so called primary axotomy, many axons undergo secondary or delayed axotomy (Graham and Gennarelli 1997; Maxwell et al., 1997). The processes leading to secondary axotomy, during which axons undergo a sequence of reactive changes which precedes physical disconnection, is thought to occur over a period of 12 hours or longer in humans (Gentleman et al., 1993; Grady et al., 1993; Blumbergs et al, 1994; Blumbergs et al., 1995; Christman et al., 1994) indicating a potential window of opportunity for therapeutic intervention. In order to exploit this it is essential to determine the pathogenic mechanisms, which lead to axonal damage after head injury.

Disruption of ionic homeostasis with a concomitant increase in $(Ca^{2+})i$ occurs after acute brain injury (Choi 1988; Siesjo and Bengtsson 1989; Shapira et al., 1989; Fineman et al., 1993). Raised $(Ca^{2+})i$ can activate the neutral proteases μ and m-calpain the substrates for these enzymes being cytoskeletal proteins essential for axonal structure and function. In grey matter after experimental traumatic brain injury (TBI) in the rat, a loss of cytoskeletal proteins was detected after injury (Posmantur et al., 1994; Saatman et al., 1996; Fitzpatrick et al., 1997) and cytoskeletal changes were also observed after focal ischaemia (Inuzuka et al., 1990; Dewar and Dawson 1996). Evidence of calpain activation by an increased amount of calpain-mediated spectrin breakdown products in neurons were also evident in experimental models of TBI (Kampfl et al., 1996), focal ischaemia (Bartus et al., 1995) or global ischaemia (Roberts-Lewis et al., 1994; Bartus et al., 1998). There is also evidence of these breakdown products in myelinated fibre tracts in the rat after experimental TBI (Saatman et al., 1996; Newcomb et al., 1997; Fitzpatrick et al., 1997). Thus, calpain-mediated breakdown may represent a final common pathway leading to neurodegeneration, regardless of whether the initial cerebral insult is traumatic or

ischaemic. However, although there is compelling evidence for this pathogenic mechanism in experimental animal models, evidence that these events occur in human head injury is currently lacking.

3.2 AIM

Therefore the aim of this study was to determine cytoskeletal protein integrity and alterations in calpain activity in the corpus callosum from post-mortem brains from patients who died following a blunt head injury.

3.3 MATERIALS AND METHODS

Fresh brain tissue was obtained post-mortem from 10 patients (6 males; 4 females) who died following a head injury and 6 control patients (3 males; 3 females) who died of causes other than head injury and who had no other CNS pathology (Table 3.2). Tissue of the corpus callosum was dissected out from frozen parasaggital blocks (Figure 3.2). The survival times after injury in the head-injured group ranged from 4h to 12.5 days (Table 3.3). There were no significant differences between head-injured patients and controls for age or post-mortem delay (Table 3.1) (time between death of the patient and freezing of the tissue). There were no clinical or neuropathological criteria applied to the inclusion or exclusion of the head–injured cases for this study.

Table 3.1 Statistical data for age and post-mortem delay

	Head-injured	Control
Age	47.7 ± 5.6	59.1 ± 3.1
Post-mortem delay	57 ± 6.7	49 ± 4.6

Data are mean ± SEM.

Fresh frozen corpus callosum tissue was homogenised (see 2.2.1) and protein content determined (Lowry 1970). 25μg of protein were separated by SDS-PAGE and detected by Western blotting (2.2). Gels were: 10% for μ-calpain; 12.5% for tau, NF68, β-tubulin, (both Protogel, National Diagnositics). Gradient gels were 8% for NF200 and calpain-mediated spectrin breakdown products, detected by SBSbS2 (Prosieve, Flowgen) (see appendix). Biotinylated and prestained molecular weight standards (Bio-Rad) were loaded alongside the protein samples, transferred and detected, to ensure proteins bands detected were at the correct molecular weight. Optical density of protein bands were measured (see 2.2.4). Data are presented as mean ± standard error of the mean (SEM) for control and head-injured groups. Significant differences between head-injured patients and controls were determined by unpaired, two-tailed Students t test.

Table 3.2 Case details of head-injured and control patients

Case	Age	Sex	Survival	Cause of Death	PM Delay
H1	59	F	<24	Raised ICP after head injury	72
H2	44	M	55	Raised ICP after head injury	68
H3	20	F	96	Raised ICP after head injury	36
H4	28	F	10	Multiple injuries including head injury	34
H5	47	M	80	Raised ICP after head injury	69
H6	27	M	264	Raised ICP after head injury	34
H7	69	F	91	Raised ICP after head injury	46
H8	61	M	11.5	Raised ICP after head injury	36
H9	51	M	300	Raised ICP after head injury	67
H10	21	M	216	Raised ICP after head injury	67
N1	77	F		Ischaemic heart disease	42
N2	62	M		Pulmonary embolism	54
N3	29	F		Pulmonary embolism	48
N4	52	M		Ischaemic heart disease	63
N5	71	M		Aspiration pneumonia	57
N6	64	F		Ischaemic heart disease	31

Abbreviations: H, head injury; N, control; F, female; M, male; ICP, intracranial pressure. NP, not present. Survival time for the head-injured cases is the number of hours between the time of injury and death. Post-mortem (PM) delay is the number of hours between death and freezing of the tissue.

Table 3.3. Principal neuropathological features of head-injured and control patients.

Case	Skull Fracture	Intracranial haematoma	Contusions	DAI	Swelling	Ischaemic brain damage
H1	N	Bilateral(R>L)SDHs	Min	-	R	R.ACA/R.MCA
H2	Y	Bilateral SDH (E)	Mod	1	L	L.ACA/LMCA
H3	Y	N	Mod	3	Bilateral	Diffuse
H4	Y	N	Min	-	L	Diffuse
H5	N	LSDH (E)	none	-	Bilateral	Diffuse
H6	Y	R ICH (E)	Min	1	N	-
H7	Y	R & L SDHs	Mod	1	L	-
H8	Y	LSDH (E)	Mod	-	N	R.ACA.MCA.BZ
H9	Y	LSDH (E)	Mod	-	L	L.ACA
H10	N	LSDH (E)	Mod	3	Bilateral	Diffuse
N1	N	N	N		N	
N2	N	N	N		N	
N3	N	N	N		N	
N4	N	N	N		N	
N5	N	N	N		N	
N6	N	N	N		N	

Abbreviations: H, head injury; N, controls; L, left; R, right; SDH, subdural haematoma; E, surgically evacuated; DAI, diffuse axonal injury; ICH, intra cerebral haematoma; ACA, anterior cerebral artery; MCA, middle cerebral artery; BZ, boundary zone.Grading of DAI as described previously (Adams etal., 1989) and contusions (Adams et al., 1985).

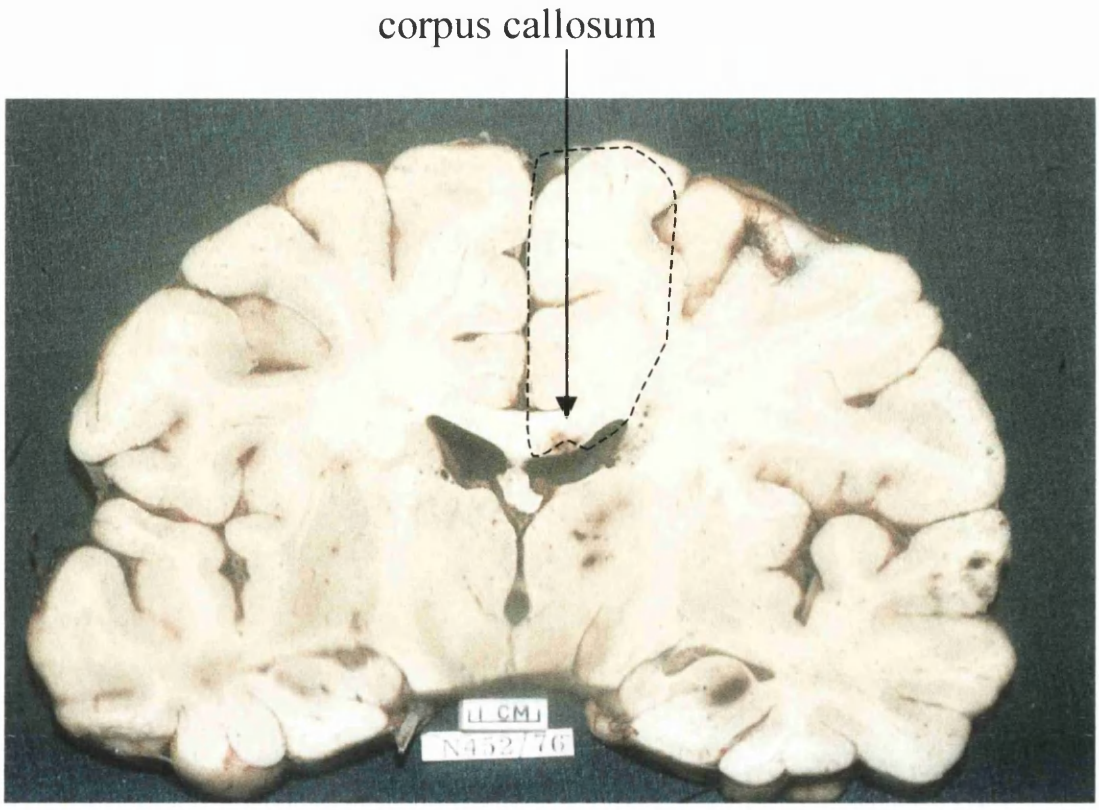

Figure 3.1 Coronal brain slice of a human head-injured patient

Formalin-fixed coronal brain slice of a human head-injured patient. The dotted line illustrates the parasagittal block from which the corpus callosum was dissected from the frozen samples. The arrow indicates the corpus callosum, a white matter commissure, where axonal damage is frequently observed following head injury in man (Adams et al., 1989; McKenzie et al., 1996). This head-injured case shows evidence of a contusion within the corpus callosum, the area of neuropathological interest. The dissected tissue was homogenised and stored at -20°C prior to Western blotting.

3.3.1 Assessment of axonal damage

To determine if there was axonal damage in the corpus callosum, sections were cut from the formalin-fixed, paraffin-embedded blocks adjacent to the fresh-frozen blocks. Sections of corpus callosum from all head-injured patients and controls were processed for amyloid precursor protein (β-APP) immunostaining as described previously (Gentleman et al., 1995). The amount and distribution of β-APP immunoreactivity was

then graded and given a score rating on a scale of 0-3, as described previously (Gentleman et al., 1995) (Table 3.2). The amount and distribution of hypoxic brain damage was also assessed: it was severe when the lesions were diffuse, mutli-focal or large infarcts in the distributions of arterial territories, and moderate when lesions were limited to the arterial boundary zones, singly or combination with sub-total infarction in the distribution of the cerebral arteries (Graham et al., 1989). The ability to attribute β-APP immunoreactive axons to either DAI or in association with infarction is based on interpretation of the different patterns of immunoreactivity. These findings when taken in conjunction with the more widely based neurohistological assessment in man and allowed the β-APP immunoreactivity to be interpreted as being due either to DAI or to other types of axonal injury associated infarction often in association with internal herniation. This part of the work was carried out by Professor D.I. Graham, neuropathologist at the Southern General Hospital, Glasgow. β-APP immunostained sections were graded by E. McCracken.

Adjacent sections of corpus callosum from all head-injured and control cases were immunostained for calpain-mediated spectrin breakdown products, detected by polyclonal antibody SBAbS2. SBAbS2 detects spectrin eptiopes specifically cleaved by μ/m calpain. SBAbS2 stained sections were also analysed and given a score according to the amount and distribution of immunostaining as above.

3.4 RESULTS

3.4.1 Cytoskeletal proteins

In the corpus callosum of the head-injured patients there was a marked reduction in the levels of NF200 protein immunoreactivity compared to controls. Using clone NE14, the antibody which detects only phosphorylated NF200, there was an approximately 80% reduction in immunoreactivity in the head-injured patients, compared to the controls (Figure 3.2). In the case of the N52 antibody, which detects NF200 independent of the phosphorylation state of the protein, there was a 40% reduction in immunoreactivity in the head-injured patients compared to the controls (Figure 3.3). In addition to these marked changes in NF200 levels in the head-injured cases there was also a significant reduction in NF68

immunoreactivity in the corpus callosum of the head-injured patients compared to the controls, NF68 immunoreactivity in the head-injured patients being reduced by 50% (Figure 3.4). Thus, in the head-injured patients there was a marked degradation of both high and low molecular weight neurofilament triplet proteins in the corpus callosum. In contrast, microtubule associated proteins were not as prominently affected compared to neurofilament triplet proteins in the head-injured patients. β-tubulin immunoreactivity was not significantly different between the head-injured patients and the controls (Figure 3.5). Tau 1, a monoclonal antibody which only recognises a non-phosphorylated epitope within tau, demonstrated a modest reduction of immunoreactivity to dephosphorylated tau in the head-injured group compared to the controls (Figure 3.6), although the difference was not statistically significant.

3.4.2 Calpain

Both 80- and 76kDa forms of the μ-calpain were detected in the corpus callosum of both controls and head-injured patients (Figure 3.7). The 80kDa form of μ-calpain is thought to reflect the inactive form of the enzyme while the 76kDa form reflects the active component (Kishimoto et al., 1989). In the head-injured patients, there was a significant reduction in the levels of the 80kDa form of μ-calpain compared to the controls while there was no difference between the two groups in the 76kDa form (Figure 3.7). The ratios of 76:80kDa forms between the head-injured (1.5) and control (1.4) groups were not different. Calpain-mediated spectrin breakdown products, as detected by the SBAbS2 antibody, were present in the corpus callosum of both the controls and the head-injured patients (Figure 3.8). However, there was a significant increase in the optical density of the 150kDa band detected by SBAbS2 in the head-injured patients compared to the controls (Figure 3.8).

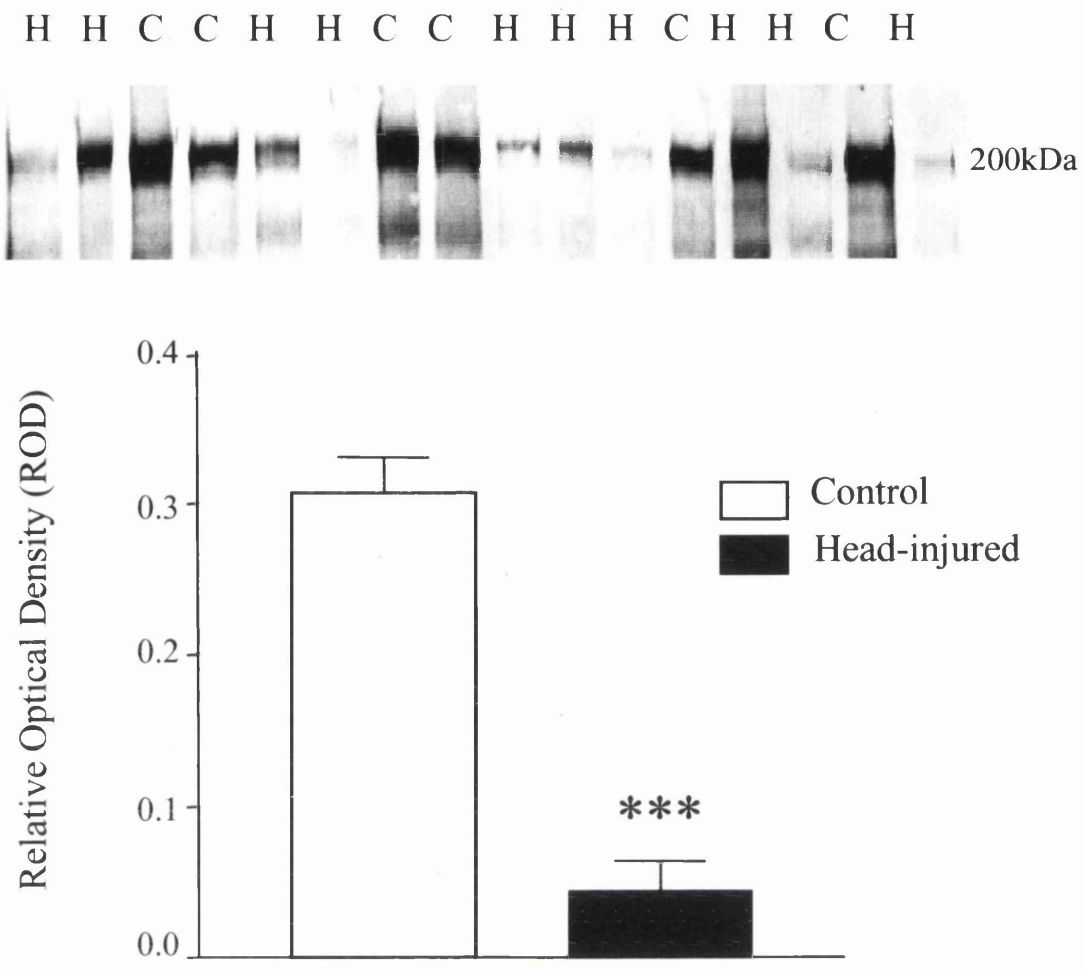

Figure 3.2 Western blot and quantitative data for neurofilament 200kDa dependent on phosphorylation state

Phosphorylated NF200 detected by antibody NE14 in samples of corpus callosum from head-injured and control patients. H – head-injured, C – control. The clone NE14 only detects phosphorylated NF200 proteins. The top panel shows a Western blot of NE14 immunoreactivity in all head-injured and control cases. H - head-injured patient, C - control. The graph in the bottom panel shows the quantitative data derived from optical density measurements of the blot. There was an 80% reduction in immunoreactivity in head-injured patients, compared to controls. Data are mean + SEM, *** $p<0.001$, unpaired Student's *t* test.

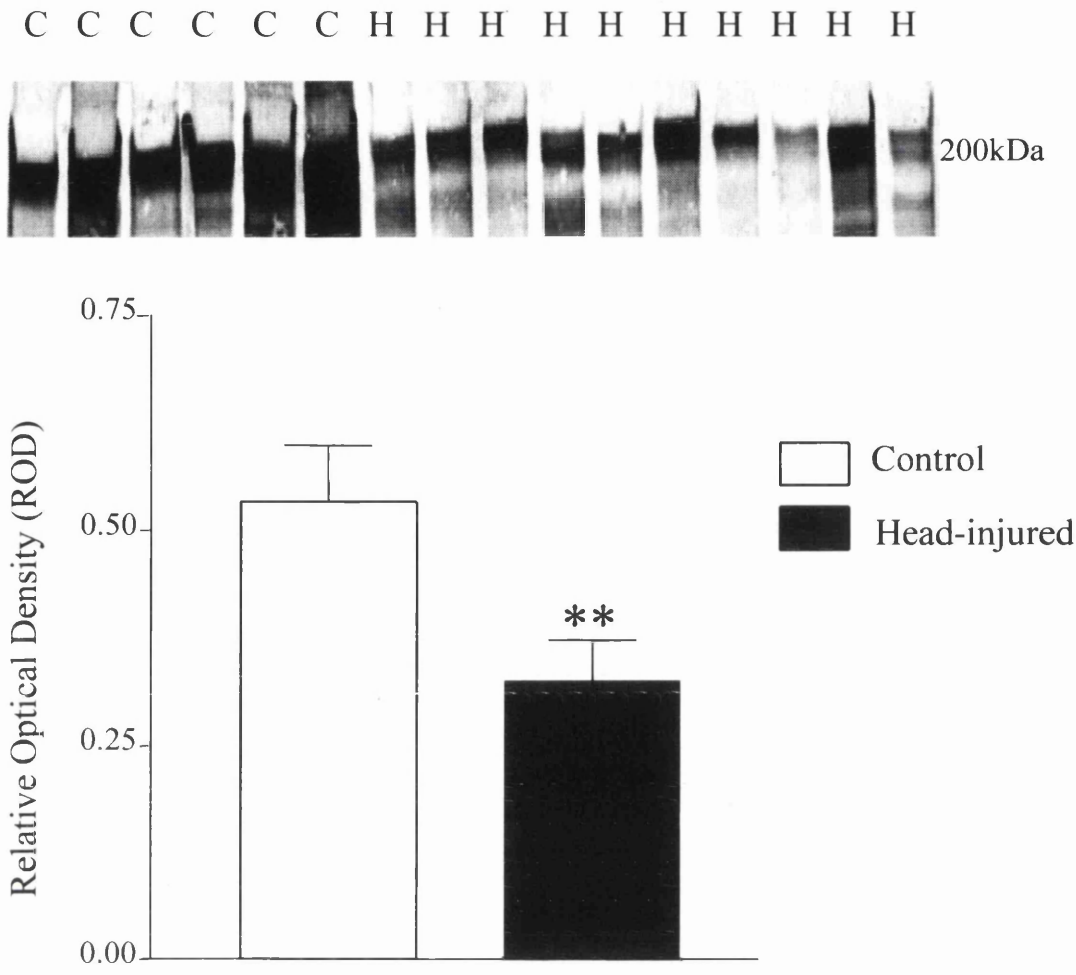

Figure 3.3 Western blot and quantitative data for neurofilament 200kDa independent of phosphorylation state.

The top panel shows the Western blot of antibody N52 which detects NF200 independent of phosphorylation state in all head-injured and control patients. H – head-injured C- control. The graph in the bottom panel shows the quantitative data derived from optical density measurements. There is a 40% reduction in the head-injured group compared to the controls. Data are mean + SEM, ** $p<0.01$, unpaired Student's *t* test.

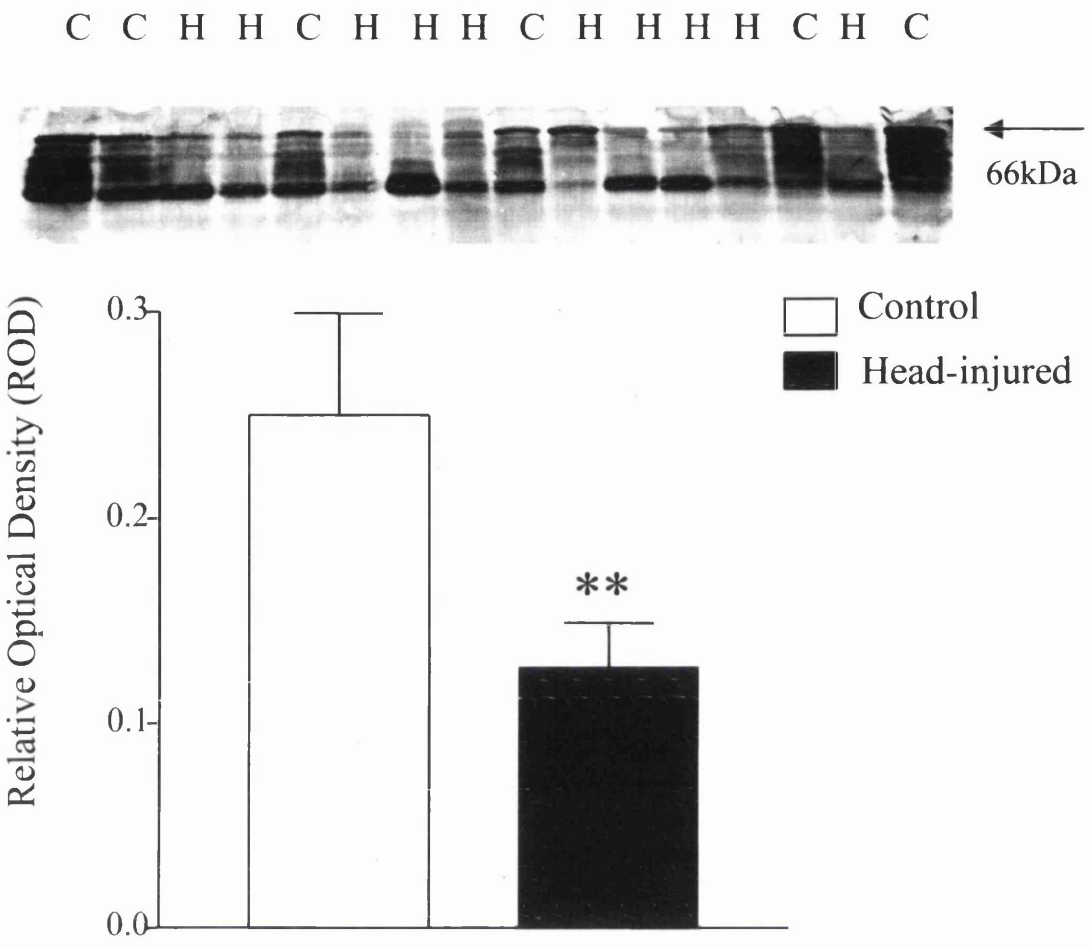

Figure 3.4 Western blot and quantitative data for neurofilament 68kDa

The top panel shows a Western blot of NF68 immunoreactivity in all head-injured patients and controls. H - head-injured patient, C - control. 66kDa represents the biotinylated molecular weight standards and the band measured for 68kDa is indicated by the arrow. The graph in the bottom panel shows the quantitative data derived from optical density measurements of the blot as described in the methods section. There is a 50% reduction in NF68 protein levels in the head-injured group compared to the control group. Data are mean + SEM; ** $p < 0.01$, unpaired Student's *t*-test.

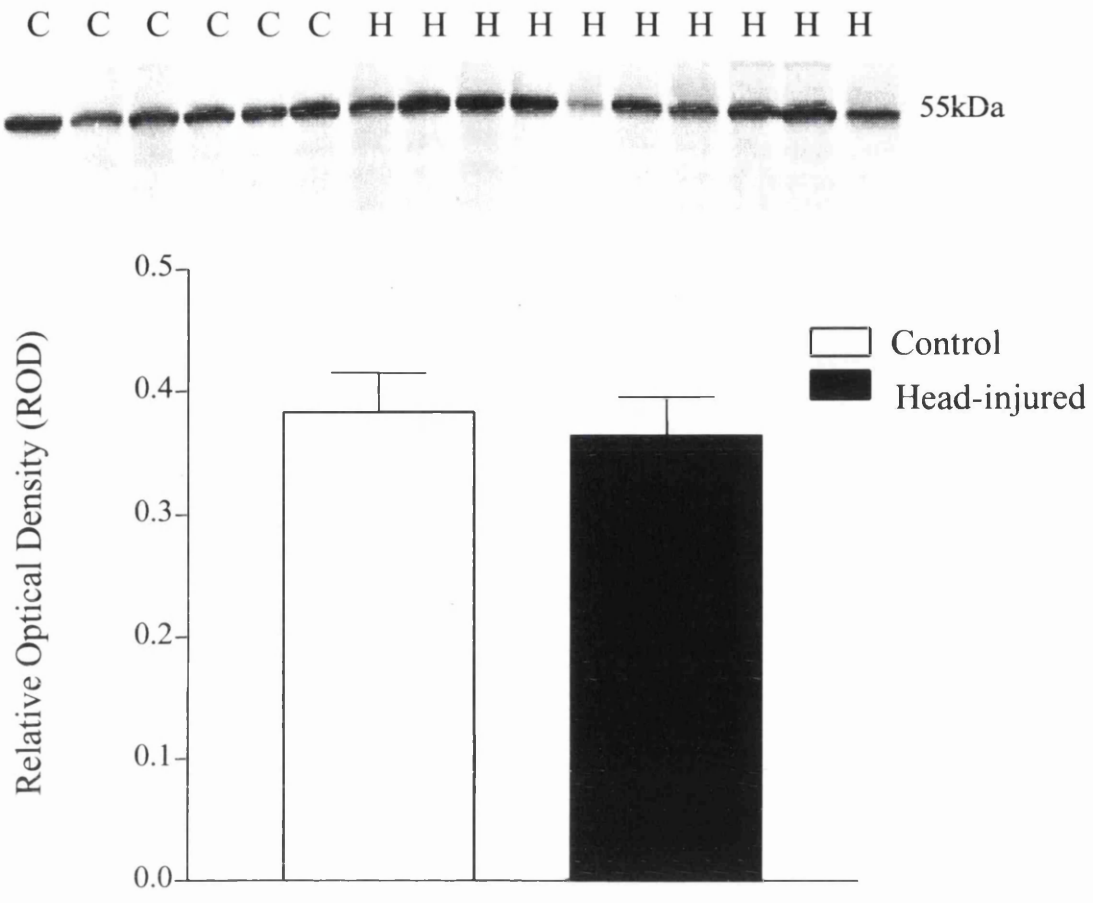

Figure 3.5 Western blot and quantitative data for β-tubulin

The top panel shows a Western blot of β-tubulin immunoreactivity in all head-injured patients and controls. H - head-injured patient, C - control. The quantitative data in the bottom panel shows that there was no significant difference in the levels of β-tubulin immunoreactivity between the head-injured patients and controls. Data are mean + SEM, unpaired Student's *t*-test.

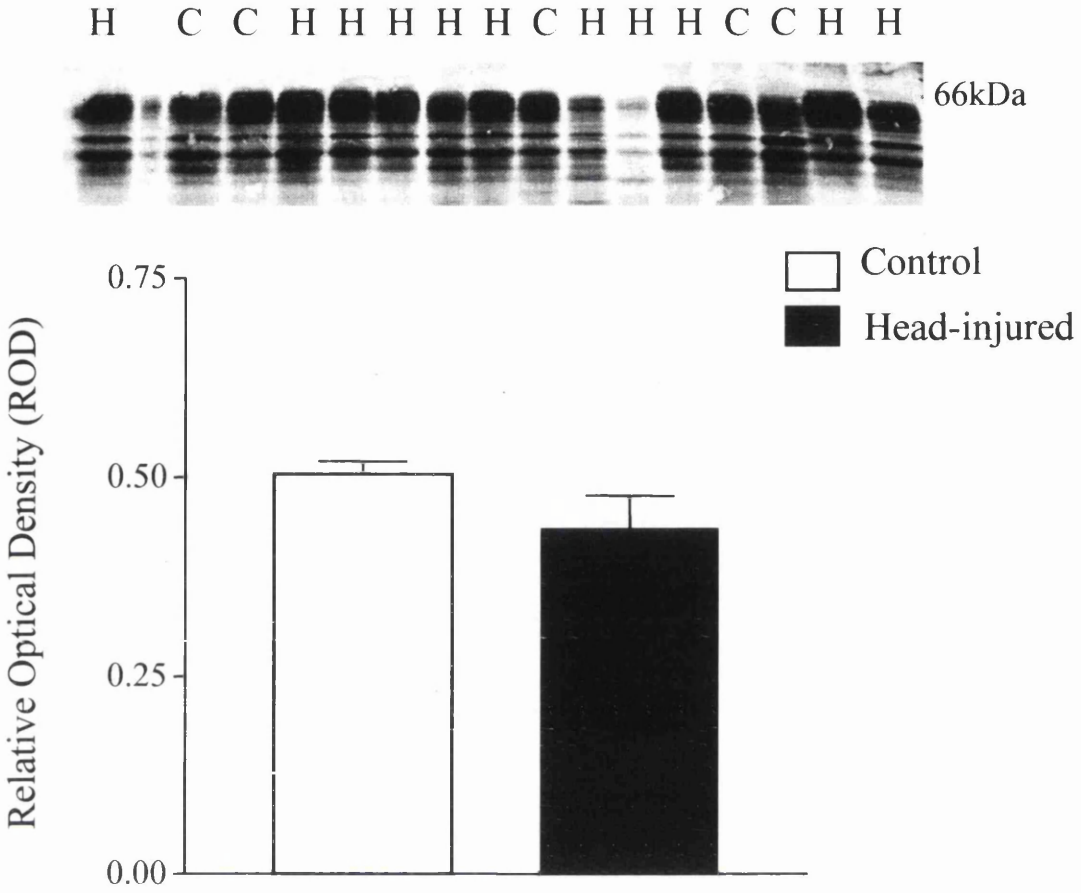

Figure 3.6 Western blot and quantitative data for Tau 1.

Dephosphorylated tau, detected by the monoclonal antibody Tau 1 in samples of corpus callosum from head-injured and control patients. 66kDa represents the molecular weight standards. Since tau has various isoforms all bands were measured. The top panel shows a Western blot of Tau 1 immunoreactivity in all head-injured and controls. H - head-injured patient, C - control. The graph in the bottom panel shows the quantitative data. Tau 1 immunoreactivity was slightly reduced in the head-injured patients compared to the controls, however this was not statistically significant. Data are mean + SEM, unpaired Student's *t*-test.

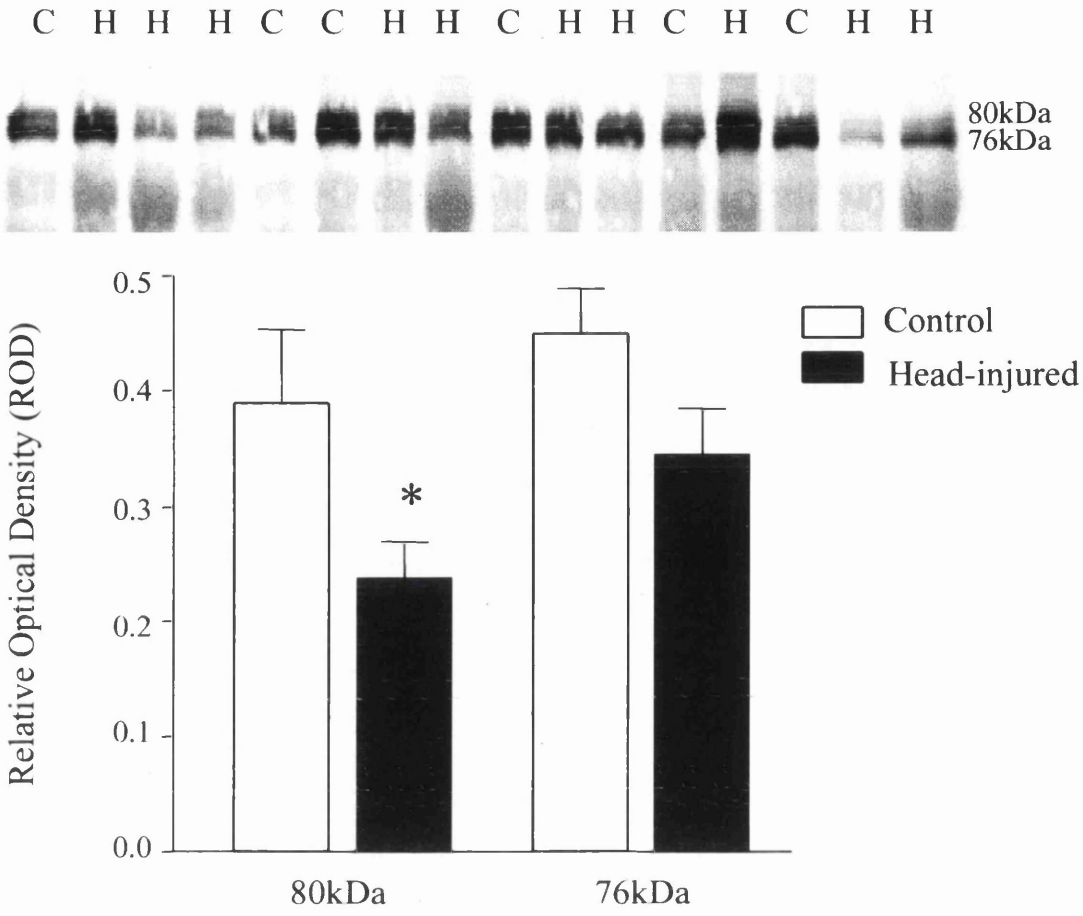

Figure 3.7 Western blot and quantitative data for μ-calpain

μ-Calpain immunoreactivity in the corpus callosum from head-injured and control patients. Optical density measurements were made of both the 80kDa and 76kDa bands. The Western blot in the top panel shows that both the inactive 80kDa and active 76kDa subunit of μ-calpain are present in both head-injured patients and controls. H - head-injured patient, C - control. The quantitative data reveals that the levels of 80kDa μ-calpain immunoreactivity were significantly lower in the head-injured patients compared to the controls. Data are mean + SEM. * $p < 0.05$ unpaired Student's *t*-test.

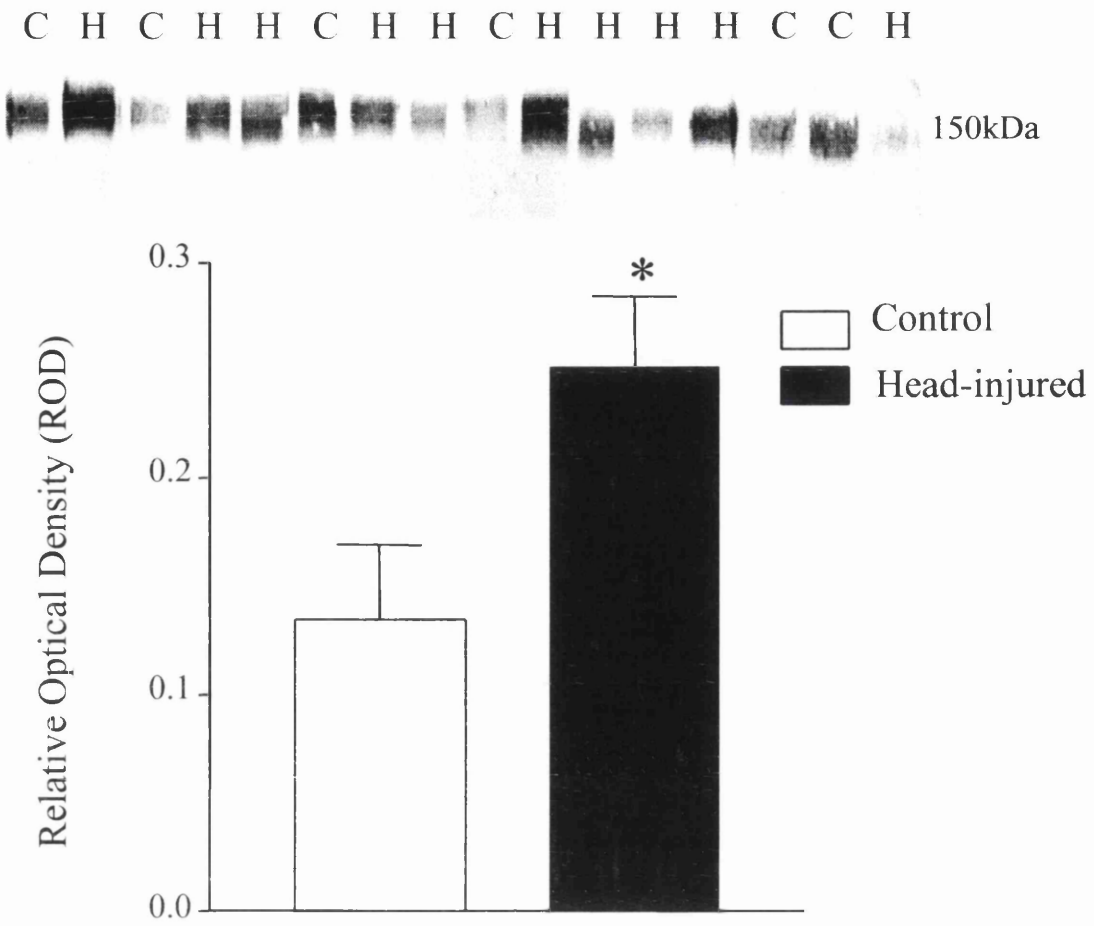

Figure 3.8 Western blot for quantitative data for SBAbS2

The polyclonal antibody, SBAbS2, detected calpain-mediated spectrin breakdown products. H - head-injured patient, C - control. The quantitative data demonstrates that compared to controls, there was a 45% increase in μ/m-calpain-mediated spectrin breakdown products in the head-injured patients. Data are mean + SEM. * $p < 0.05$ unpaired Student's *t* test.

3.4.3 β-Amyloid precursor protein immunohistochemistry

β-APP-immunostained sections from formalin-fixed blocks adjacent to those used for Western blotting were examined by microscopy. β-APP immunoreactive axons were present in varying amounts in the corpus callosum of 9 out of the 10 head-injured patients but were absent from all control cases (Table 3.2). The different patterns of β-APP-stained axons due to DAI or infarction are shown in Figure 3.9. β-APP staining in axons damaged due to DAI shows widely distributed, multifocal swellings and or bulbs within white matter tracts that are not in association with haemorrhage or infarcts (Figure 3.9B). In contrast, the immunoreactivity seen at the edge of an infarct shows a different pattern consisting of a much greater concentration of abnormal profiles that often orientate across a straight or "Z-shaped" line (Figure 3.9A). In 5 of the head-injured patients the pattern of β-APP immunoreactive axonal profiles, when taken in conjunction with associated infarction and the interpretation of the multiple samples taken for diagnostic purposes, was consistent with DAI (H2,H3,H6,H7,H10 in Table 3.2). In another 3 patients, the pattern of β-APP-stained axons was consistent with either arterial territory or boundary zone infarction but not DAI (H1, H8, H9 in Table 3.2). In patient H5 there was some β-APP staining in association with diffuse hypoxic damage and in the remaining patient (H4) there was no APP staining of axons, although there was diffuse hypoxic brain damage. Thus, in the head-injured group there was evidence of axonal damage due to survival mechanisms; either DAI or infarction alone, or a combination.

3.4.2 Calpain-mediated spectrin breakdown products immunohistochemistry

There was no detectable calpain-mediated spectrin breakdown products immunoreactivity in any of the control patients. All head-injured patients were immunopositive for calpain-mediated spectrin breakdown products. Staining appeared fragmented along axons within the white matter of head-injured patients (Figure 3.10). Using the same criteria to grade each section (see 3.3.3), the data shows that there is a correlation between the amount of β-APP immunoreactivity and calpain-mediated spectrin breakdown products in head-injured patients (Table 3.4 and Figure 3.11).

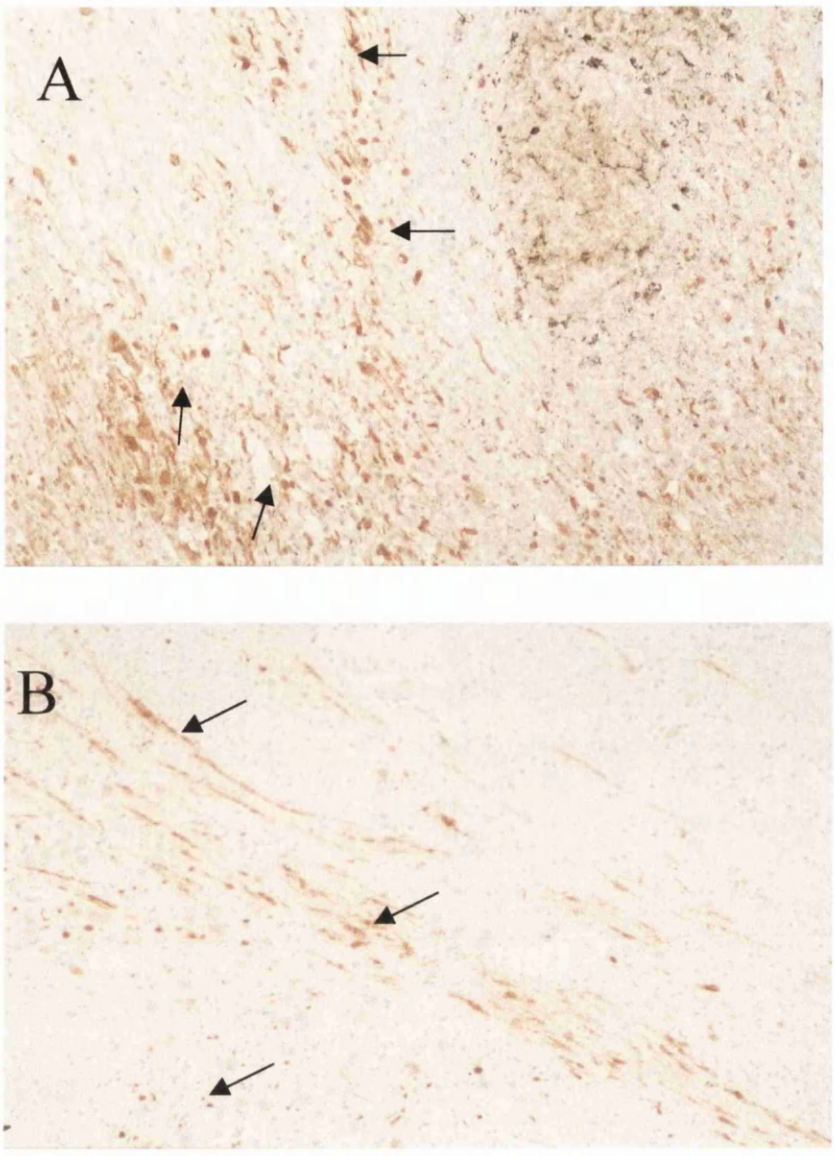

Figure 3.9 Pattern of β-amlyoid precursor protein immunopositive axonal swellings in patients who sustained a head injury

β-APP immunostained sections of human corpus callosum taken from formalin-fixed blocks adjacent to the fresh-frozen samples used for Western blotting. A) Arrows indicate the edge of an infarct in the corpus callosum. There is a clustering of immunoreactive axons that define the margin of an ischaemic lesion. B) Diffuse axonal injury in corpus callosum. In contrast to figure A the immunoreactive axons are not clustered but random and widely distributed throughout the corpus callosum. X400 Magnification.

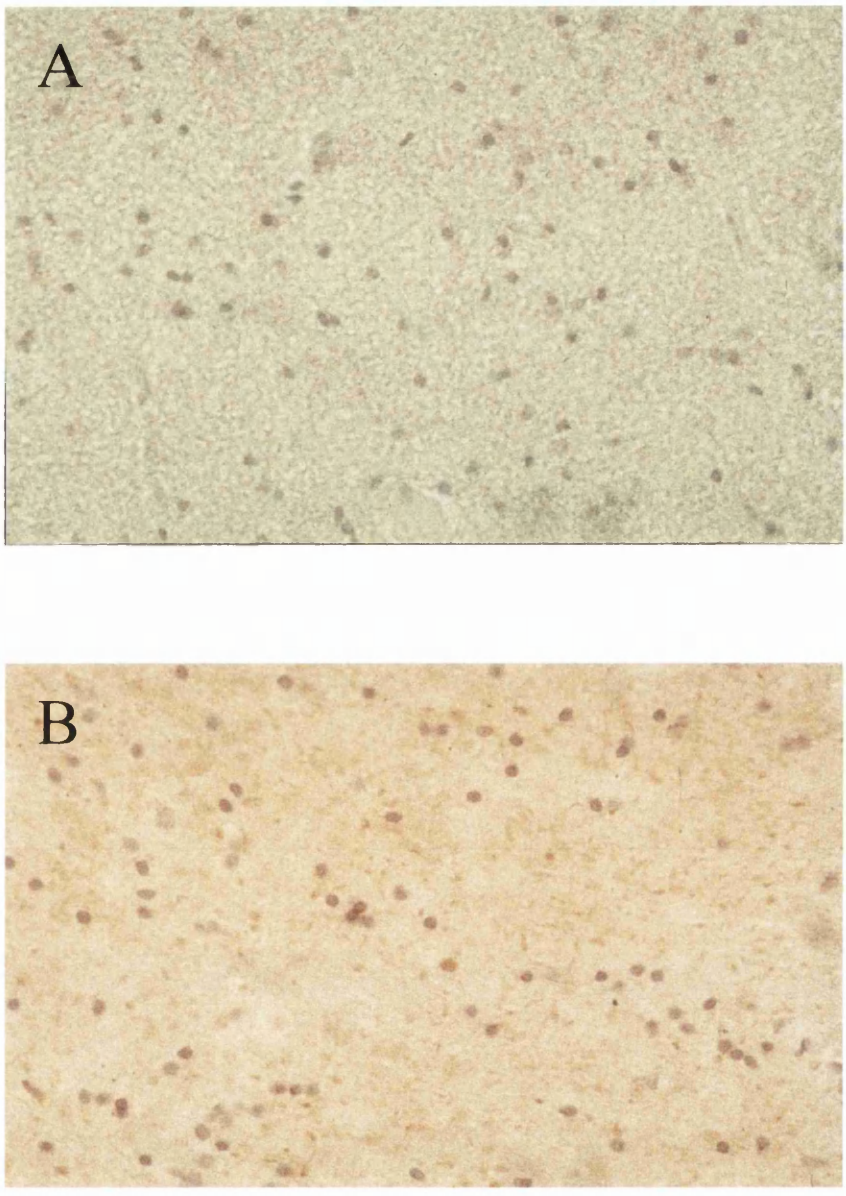

Figure 3.10 Calpain-mediated spectrin breakdown products in a control and head-injured patient

Adjacent sections to β-APP stained sections were immunostained for calpain-mediated spectrin breakdown products detected by the polyclonal antibody SBAbS2 in A) control and B) head-injured patient. There was no evidence of SBAbS2 immunoreactivity in any of the control patients. All head-injured cases immunostained with SBAbS2 demonstrated an increase in calpain-mediated spectrin breakdown products in white matter. X400 Magnification.

Table 3.4 Scores of β-amyloid precursor protein and SBAbS2 immunoreactivity

Case	Grading of β-APP	Grading of SBAbS2
H1	2	2
H2	3	3
H3	2	2
H4	0	0
H5	1	0
H6	1	2
H7	3	2
H8	3	3
H9	1	1
H10	3	3

Staining was classified as: 0 not present; 1 minimal; 2 moderate; 3 intense.

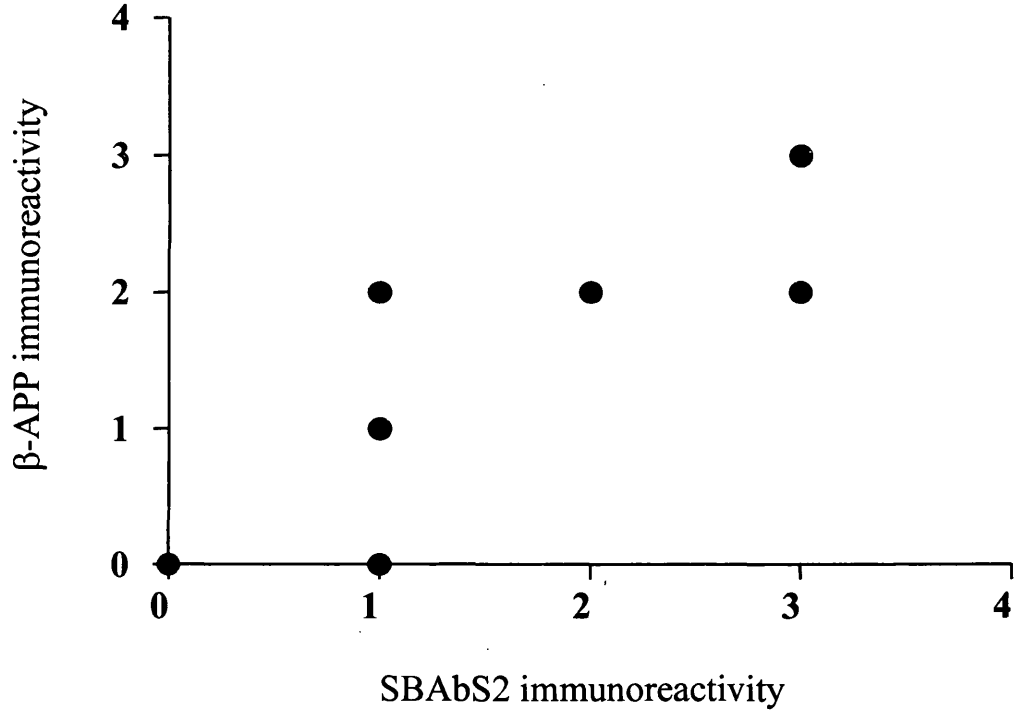

Figure 3.11 Correlation between the amount and distribution of β-amyloid precursor protein accumulation and calpain-mediated spectrin breakdown products

The graph shows the relationship between the semi-quantitative scores for β-APP and SBABS2 immunostaining in head-injured patients. There was no β-APP or SBAbS2 immunoreactivity observed in any of the control patients. There were three head-injured patients with a score of three for both β-APP and SBAbS2 immunoreactivity and two patients had scores of two for both β-APP and SBAbS2 immunoreactivity.

3.5 DISCUSSION

The present study demonstrates that in the corpus callosum after blunt head injury in human patients, there are marked changes in proteins which are essential in maintaining the structural integrity of axons. The data indicate a marked loss of immunoreactivity to both NF200 and NF68 neurofilament proteins in head-injured patients compared to controls. In contrast, β-tubulin and the microtubule-associated protein, tau, were not affected to the same extent as the neurofilament proteins in the head-injured patients. Neurofilaments may therefore be more vulnerable than microtubules, in the corpus callosum of head-injured patients. Concomitant with these marked alterations in neurofilament proteins, the study also demonstrates increased levels of calpain-mediated spectrin breakdown products in the corpus callosum of head-injured patients, which suggests calpain activation. Thus, the data is consistent with the hypothesis that calpain-mediated cytoskeletal breakdown occurs in the corpus callosum after head-injury in human patients.

In the present study two different antibodies were used to detect changes in NF200 in the corpus callosum : N52 which detects NF200 independent of its phosphorylation state and NE14 which detects only the phosphorylated form of NF200. The most striking difference between head-injured patients and controls was detected using the antibody against the phosphorylated form of NF200, with a reduction of approximately 80% compared to controls. Loss of NE14 immunoreactivity may therefore indicate dephosphorylation of NF200. Dephosphorylation of the normally highly phosphorylated sidearms of neurofilaments has been proposed to cause the compaction of neurofilaments in myelinated axons after TBI in experimental animals (Yaghmai and Povlishock 1992, Pettus et al., 1994, Povlishock 1997, Ononkwo et al., 1998). Both assembly/disassembly and proteolysis of neurofilaments is influenced by their phosphorylation state (Goldstein et al., 1987, Schlaepfer et al., 1987, Nixon and Sihag, 1991). Pant (1988) examined phosphorylated and dephosphorylated neurofilaments extracted from bovine spinal cord and showed that dephosphorylated neurofilament proteins were more susceptible to calpain-mediated proteolysis than phosphorylated proteins. The mechanisms which may contribute to protein dephosphorylation after head injury are, as yet, unknown, although dysregulation of phosphatase and kinase activities are likely to arise as a consequence of alterations in axolemmal permeability

(Pettus et al 1994). In the present study, evidence of neurofilament degradation in the corpus callosum of head-injured patients was also found. Using the antibody N52, which detects NF200 independent of its phosphorylation state, a significant reduction in immunoreactivity in the corpus callosum of head-injured patients compared to controls was detected. Taken together the data is consistent with both dephosphorylation and degradation of NF200 in the corpus callosum after head injury in humans. NF68 immunoreactivity was also observed in the corpus callosum of head-injured patients indicating that NF68 is also degraded in myelinated fibre tracts after head injury in humans. NF68 was significantly reduced in the corpus callosum, detecting NF68 independent of its phosphorylation state. Degradation of both NF200 and NF68 neurofilament proteins have been demonstrated in the cerebral cortex underlying the site of injury after controlled cortical impact in the rat (Posmantur et al., 1994).

In contrast to the marked changes in neurofilament proteins in the corpus callosum of head-injured patients, proteins involved in the structure and function of microtubules were relatively unchanged compared to controls. The levels of β-tubulin immunoreactivity were no different between the two groups and there was only a modest reduction in the levels of the microtubule-associated protein tau, as detected by the Tau 1 antibody. Tau 1 detects only dephosphorylated tau and therefore the small reduction in signal in the head-injured patients could be consistent with either changes in the phosphorylation state of the protein or degradation. However, the results indicate that proteins associated with microtubules are less susceptible to the effects of head injury at least in the corpus callosum of the human brain. In animal models of TBI early and marked changes in axonal microtubules have been reported, using electron microscopy as an endpoint (Jafari et al., 1997; Pettus et al., 1994; Pettus et al., 1996; Maxwell, 1997). Thus, although there was no marked changes in β-tubulin or tau using Western blotting this cannot rule out that the axonal microtubular structure was unaffected. Microtubules play a dynamic role in the axon being involved in fast axonal transport, the process through which β-APP is moved along the axon (Koo et al., 1990). Thus, the presence of β-APP accumulations within axons of the corpus callosum in nine of the 10 head-injured patients examined in our study suggests that fast axonal transport was disrupted in β-APP-positive axons. Depolymerisation of tubulin structure, in the

absence of the degradation of the β-isoform or changes in other microtubule-associated proteins may contribute to the cessation of fast axonal transport.

Based on data from experimental animal studies, breakdown of the cytoskeleton after head injury has been attributed to the overactivation of calpains (Kampfl et al., 1997). The data from this study demonstrates that both the inactive (80kDa) and active (76kDa) forms of μ-calpain are present in the corpus callosum of head-injured patients. There was a reduction in the level of the 80kDa form in the head-injured patients in comparison to the controls, while there was no significant difference between the two groups in the 76kDa form. There was no difference between the groups in the ratio of the active: inactive forms of the enzyme. In addition, however, there was an increase in the levels of calpain-mediated spectrin breakdown products in the corpus callosum of the head-injured patients. Thus, it is possible that calpain may be involved in spectrin degradation in axons after head injury. The polyclonal antibody SBAbS2 used in this study is analogous to Ab38, and specifically detects calpain-mediated spectrin breakdown products (Robert-Lewis et al., 1994). Calpain-mediated spectrin breakdown products immunostained sections illustrated axonal fragmentation in the white matter tracts of the corpus callosum. Increased immunostaining of subcortical white matter with the Ab38 antibody has been reported within 90 minutes of lateral fluid percussion injury in the rat (Saatman et al., 1996a) although this was not observed until 24 hours after controlled cortical impact in the rat (Newcomb et al, 1997). The majority of the head-injured patients in this study had survived for longer than 24 hours after their primary injury and the limited size of the group examined did not permit analyses to determine the time course of relative changes in calpain levels, activation and neurofilament protein loss. However, it is interesting to note that spectrin associates specifically with a 30kDa fragment from the amino terminus of neurofilament (Nixon and Sihag 1991). Therefore, it might be speculated that if spectrin is rapidly degraded by calpains, and neurofilaments are freed from the spectrin cytoskeleton, this may have an impact on the susceptibility of neurofilament proteins to pathological mechanisms after injury.

Calpain-mediated breakdown of the cytoskeleton has also been implicated in the pathogenesis of ischaemic brain damage (Roberts-Lewis et al., 1994; Hong et al., 1994;

Bartus et al., 1995). In any given head-injured patient changes in axons may be present for various reasons only some of which can be attributed to trauma per se (Gennarelli et al., 1998, Graham and Gennarelli 1997) In patients who die after head-injury a principal cause of axonal damage is ischaemia in association with haemorrhage and the complications of internal herniation due to raised intracranial pressure (Graham etal., 1989; Graham et al., 1987). Therefore, in the assessment of axonal damage after trauma it is necessary to undertake a comprehensive neurohistological study of multiple bilateral brain regions in order to determine not only the presence of axonal damage but also its distribution, and to determine the relationship between it and the various other pathologies of traumatic brain injury. This task has been greatly facilitated with the advent of immunohistochemistry and in particular for amyloid precursor protein (Gentleman et al., 1993, Sherrif et al., 1994, McKenzie et al., 1996; Blumbergs et al., 1989) which is both sensitive in the detection of axonal changes and the identification of abnormalities within a few hours of injury. By this means it is now possible to identify the presence of DAI and to determine its severity (Adams et al., 1989; Gentleman et al., 1995). The use of β-APP immunohistochemistry in this study determined a number of important aspects of axonal damage. First, the head injury patients had lived long enough for changes to have developed (minimal survival of 4 hours). Secondly, that the variable post mortem interval (range from 34 to 72 hours) did not alter the sensitivity of the method, thirdly it identified β-APP-positive immunoreactive axons in the corpus callosum in nine of the 10 head-injured patients and fourthly the distribution of the axonal changes to be determined and correlated with the presence of hypoxic brain damage including infarction. In this way it was possible to attribute the axonal changes in the corpus callosum to either DAI, infarction or a combination of both.

It has been previously demonstrated that abnormalities in cytoskeletal proteins and β-APP accumulation occur in myelinated fibre tracts after a focal ischaemic insult in the rat (Dewar & Dawson, 1995; Yam et al., 1997; Yam et al., 1998) while others have reported accumulation of β-APP in white matter at the margin of an ischaemic lesion in human brain (Oghami et al., 1992; Suenaga et al., 1994, Jendroska et al., 1997). Due to the limited number of patients in subgroups of the head-injured patients we did not make a formal analysis comparing those with ischaemia or diffuse axonal damage alone. However, the percentage reduction compared to controls in neurofilament signal

was similar in patients who had diffuse or ischaemic damage (approximately 80% in each subgroup) as was the percentage increase in calpain-mediated spectrin breakdown products (40% in each subgroup). Thus, in head-injured patients cytoskeletal disruption and accumulation of β-APP in axons of the corpus callosum may be a consequence of either primary traumatic or secondary ischaemic injuries. However, the mechanism by which these types of pathologies are manifest may involve overactivation of calpains. Both β-APP and calpain-mediated spectrin breakdown products were graded semi-quantitatively according to their immunoreactivity. In the head-injured patients there was a close correlation between the two scores, reinforcing the suggestion that calpain activity is involved in axonal degeneration. Thus calpain inhibition may prove to be a potent therapeutic strategy for attenuation of both neuronal and axonal damage, due to either trauma or after a stroke.

From this study and other research it can be speculated that calpain-mediated proteolysis is involved in cytoskeletal breakdown following acute brain injury. However, it is possible that axonal damage is not solely due to calpains and that other mechanisms could be involved in axonal degeneration. Another important mechanism thought to play a major role in acute brain injury is oxidative stress. Calpains may have an integral link to increasing free radicals and free radicals can increase the autolysis of calpains indirectly by increasing intracellular Ca^{2+} (Figure 3.12).

Therefore in the next part of the thesis experimental studies were undertaken to examine the role of oxidative damage and its association with calpain activation in axonal damage

Figure 3.12 Cascade of biochemical events after human head injury

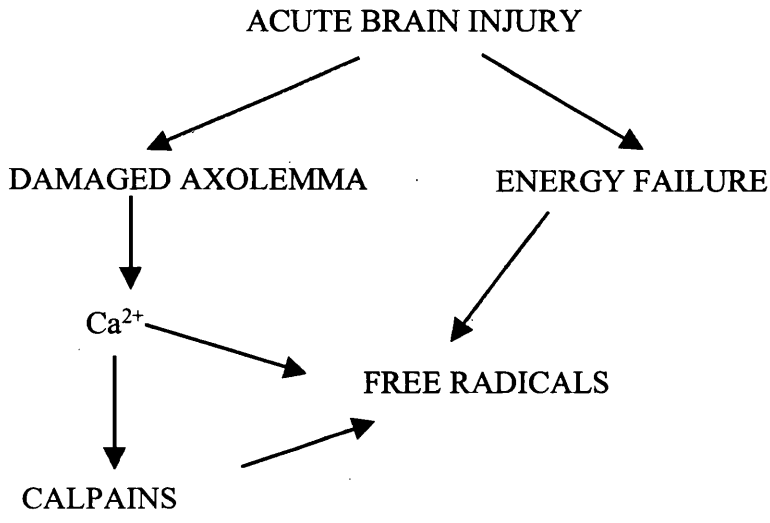

The diagram illustrates that following head injury alterations in axolemmal permeability leads to Ca^{2+} activated proteases, calpains. However, it also proposes that primary mechanisms, calpain activation and free radicals could have a complex interaction.

CHAPTER IV

WHITE MATTER DAMAGE FOLLOWING SYSTEMIC INJECTION OF THE MITOCHONDRIAL INHIBITOR 3-NITROPROPIONIC ACID

4.1 INTRODUCTION

Oxidative stress has been proposed to play a major role in the pathogenesis of neuronal cell death following acute brain injury (Watson et al., 1984; Doopenberg et al., 1998; see reviews Flamm et al., 1978; Chan 1994; Murphy et al., 1999; Love 1999). One of the major cellular organelles responsible for excessive production of superoxide ions is the mitochondria (Dugan et al., 1995; Piantadosi and Zhang 1996). During ischaemia, oxidative phosphorylation becomes uncoupled leading to decreased ATP synthesis and increased superoxide production (Cino & Del Maestro 1989; Shigenaga et al., 1994). Rapid catalysis of superoxide anion can be reduced to hydrogen peroxide and then catalysed to the potent hydroxyl radical in the presence of Fe^{+} ions. Endogenous antioxidants become saturated and cannot remove excess radicals that then go onto enhance the oxidative stress cascade. Although, there is an overwhelming body of evidence proposing a role for oxidative stress in perikaryal damage there is little evidence in the literature suggesting that white matter is vulnerable to oxidative stress.

3-Nitropropionic acid (3-NPA) is a plant myotoxin, which is an irreversible inhibitor of succinate dehydrogenase in the Krebs cycle and complex II of the electron transport chain (Alston et al., 1977; Coles et al., 1979; Alexi et al., 1998) (Figure 4.1). This toxin impairs energy metabolism and increases lactate (Brouillet et al., 1993; Tsai et al., 1997) and has been shown to produce selective striatal lesions in both experimental animal models and in man (Ludolph et al., 1991). Hippocampal slices treated with 3-NPA demonstrated both a rapid necrotic cell death that was NMDA receptor-dependent and a delayed non NMDA-receptor dependent apoptotic cell death (Pang and Geddes 1997). Systemic injection of 3-NPA *in vivo* induces generation of free radicals (Schulz et al., 1996).

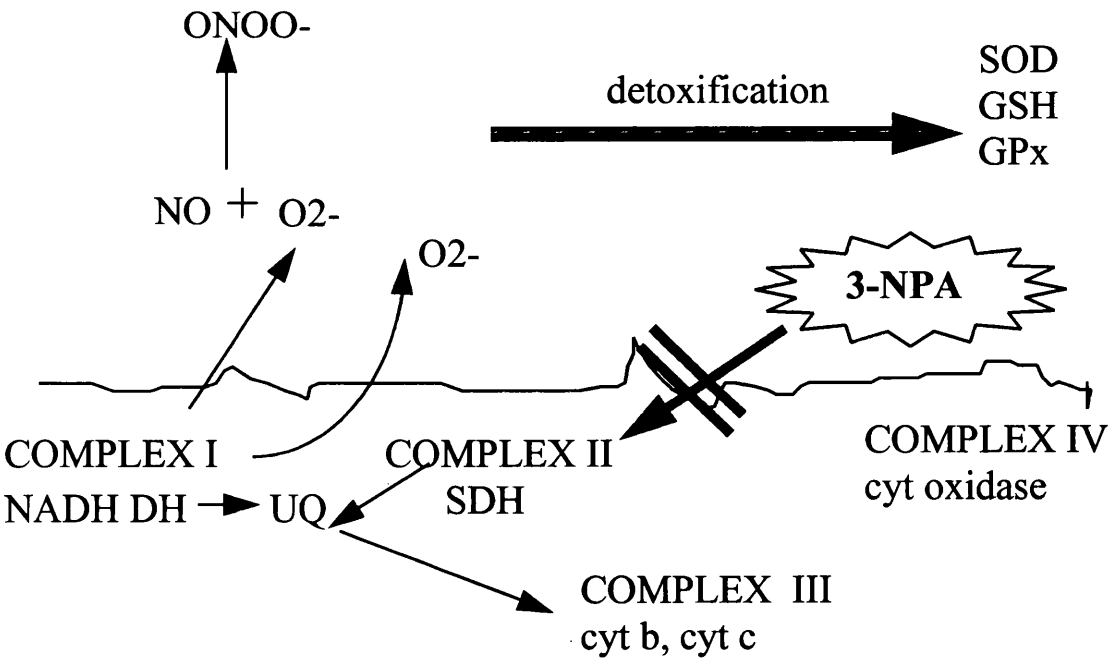

Figure 4.1 Electron transport chain located on the inner mitochondrial membrane
Modified from Murphy et al., 1999.

The diagram illustrates the electron transport chain where oxidative phosphorylation occurs. 3-Nitropropionic acid inhibits succinate dehydrogenase at complex II, thus elevating the production of superoxide anions which in turn causes oxidative stress.

4.2 AIM

To determine if oxidative stress played a role in axonal cytoskeletal breakdown and alterations in calpain activity, 3-nitropropionic acid was systemically injected into rats.

4.3 MATERIALS AND METHODS

Animals received an intraperitoneal injection of 10,15, 20 or 30mg/kg 3-NPA or sterile water (n = 4/5 per group) and were transcardially perfused with 4% paraformaldehyde 24 hours later. Rats were decapitated and heads post-fixed for 24 hours. Brains were removed and post-fixed for a further 48 hours and then brains were processed for paraffin embedding (see 2.4.2). 5μm sections were cut for histology and stained with cresyl fast violet and luxol fast blue. Cresyl fast violet staining was used to determine

morphological changes detected in the neuronal perikarya and similar changes have been described in other studies after systemic injection of 3-NPA (Beal et al., 1995). Luxol fast blue staining was used to determine if there were histological changes in myelinated axons. To determine if there were changes in the axonal cytoskeleton rat brain sections were immunostained with the transport proteins β-APP and SNAP-25. Adjacent sections were stained with the polyclonal antibody SBAbS2 to detect if there were alterations in calpain activity. Rat brain sections were also stained with Mn-SOD to confirm the role of oxidative stress in this model.

4.3.1 Assessment of axonal damage

Immunostained sections from each group, taken at the level of the anterior commissure, were analysed microscopically and each section scored according to the amount and distribution of immunoreactive axons within the striatum. A score of 0 was given to sections with no immunostaining; 1 for minimal immunoreactivity; 2 for moderate staining and 3 for dense immunostaining. Each section was graded blind to the identity of the treatment of the animal.

4.3.2 Assessment of glial cell staining

A 1cm square graticule was used to count the oligodendrocyte-like cells immunopositive for calpain-mediated spectrin breakdown products in three different loci along the subcortical white matter at the level of anterior commissure (Figure 4.2). Oligodendrocytes were identified by their characteristic morphology of a small soma and thin rim of cytoplasm. Cells were counted and expressed as cells per mm^2.

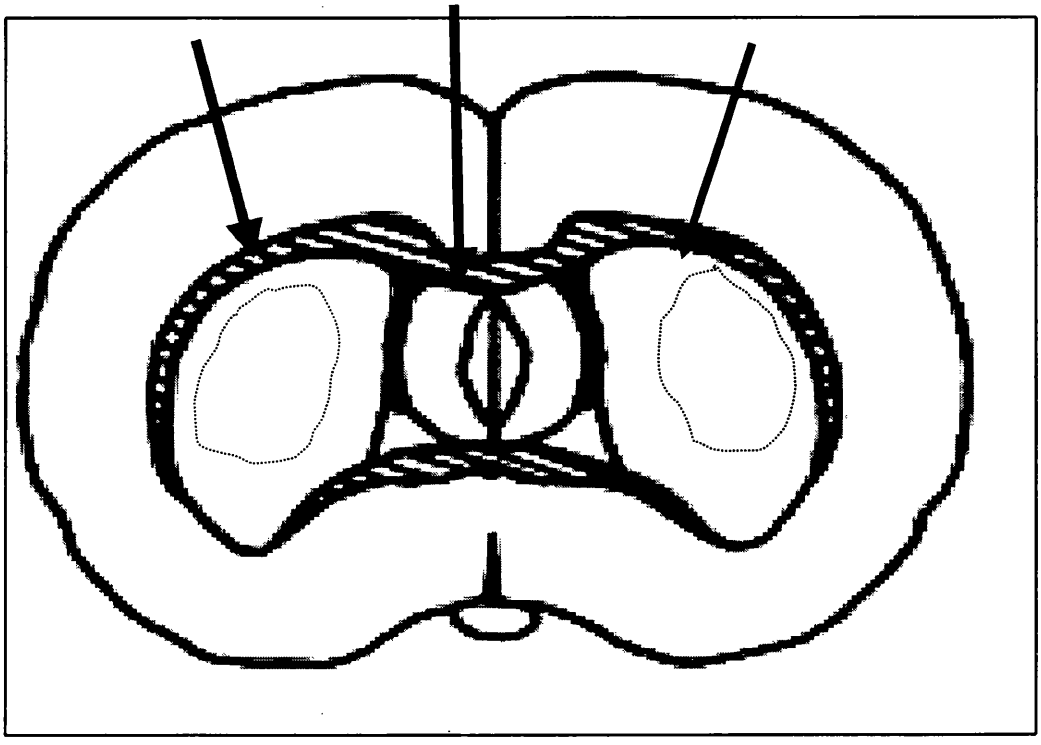

Figure 4.2 Rat brain section at the level of the anterior commissure

Neuronal perikaryal damage was observed bilaterally within the dorsolateral region of the striatum at all concentrations of 3-NPA systemic injection. There was no neuronal perikaryal damage observed in the cortex. Dotted lines represent the areas of neuronal damage. In the 3-NPA treated groups oligodendrocyte-like cells were immunopositive for calpain-mediated spectrin breakdown products, detected by SBAbS2 only in the subcortical white matter. The density of these cells was determined at the points indicated by the arrows.

4.4 RESULTS

4.4.1 Histology

Morphological changes in neuronal perikarya were observed at all the concentrations of 3-NPA administered. However, the most severe histological changes were observed following systemic injection of 30mg/kg 3-NPA, the highest concentration. Therefore only photographic data from vehicle and 30mg/kg treated groups is presented in this chapter. For 10, 15 and 20mg/kg 3-NPA immunostained sections see appendix 3. Morphologically normal spherical-shaped neurons and axons within the striatum were observed in the vehicle treated animals (Figure 4.3A). In contrast, systemic injection of 3-NPA at all concentrations produced a bilateral lesion in the striatum while no neuronal damage was observed in the cortex. Throughout the lesion there were shrunken neurons and disrupted myelinated fibre tracts (Figure 4.3B). Cresyl fast violet and luxol fast blue stained sections demonstrated a typical pattern of 3-NPA induced neurotoxicity (Beal et al., 1993; Brouillet et al., 1993; Wuulner et al., 1994; Borlongan et al., 1995).

4.4.2 Axonal pathology

There was no evidence of β-APP accumulation in axons in the vehicle treated animals (Figure 4.4A). Accumulation of protein was detected after 3-NPA injection only within the myelinated fibre tracts of the striatum. Intense widespread β-APP immunoreactive axonal swellings were observed in the 30mg/kg treated group (Figures 4.4B). There was no evidence of SNAP-25 immunoreactivity in the vehicle treated group (Figure 4.5A). A striking increase in the density of SNAP-25 immunoreactive axonal swellings and bulbs within the myelinated fibre tracts was observed in animals injected with 30mg/kg 3-NPA (Figure 4.5B). All β-APP and SNAP-25 immunoreactive axons were restricted to the myelinated fibre tracts in the striatum. Axonal pathology was anatomically coincidental with the neuronal lesion. Using the scoring system described in 4.3.1 there was a concentration dependent increase in axonal pathology, reflected in β-APP (Figure 4. 6) and SNAP-25 (Figure 4.7) accumulation in the 3-NPA treated animals. The amount of β-APP (Table 4.1) and SNAP-25 (Table 4.2) immunoreactivity varied between animals within each group.

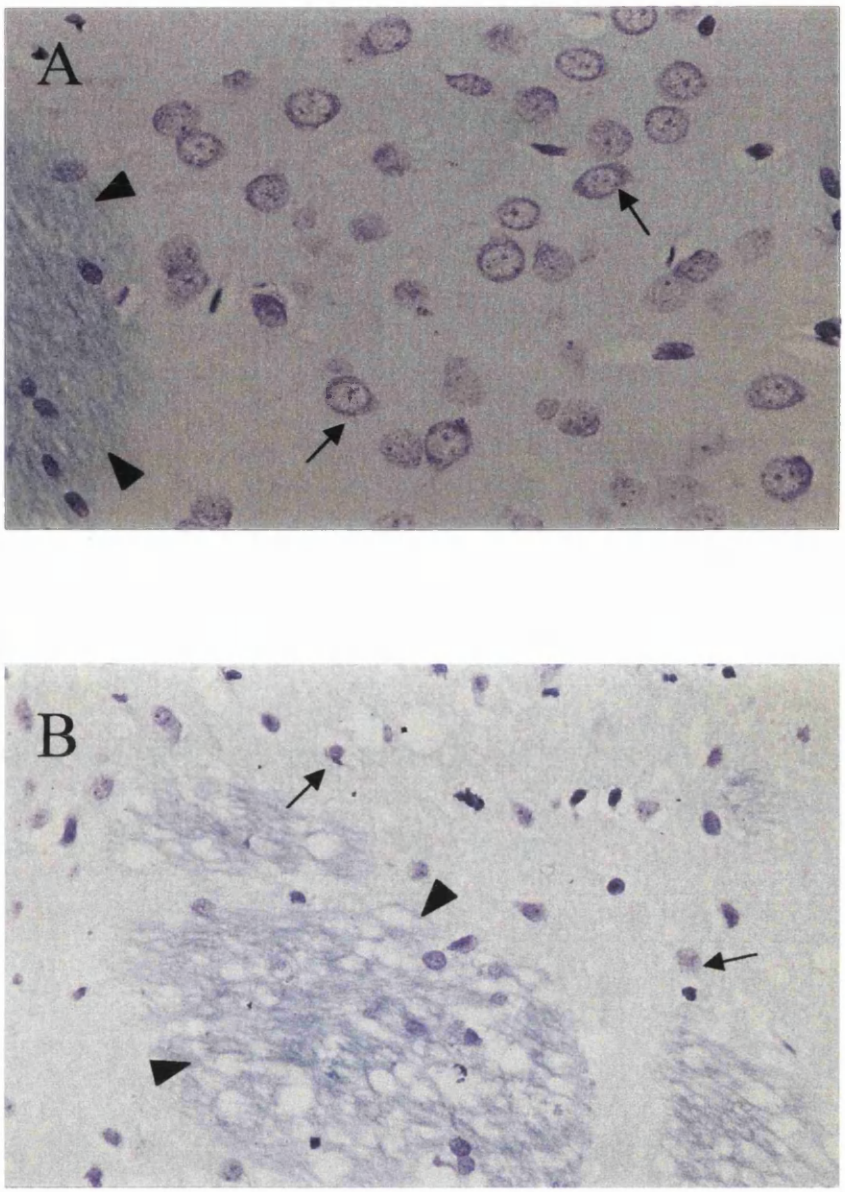

Figure 4.3 Morphological changes in the striatum following systemic injection of 3-nitropropionic acid

Cresyl fast violet and luxol fast blue histology in A) vehicle and B) 30mg/kg 3-NPA treated rat. In the vehicle treated rats neuronal perikarya exhibited the characteristic morphology of normal neurons (arrows) while myelinated axons had a smooth regular appearance (arrow heads). In 30mg/kg 3-NPA treated animals there was shrinkage of neuronal perikarya in the striatum (arrows). Myelinated axons stained with luxol fast blue had a disrupted appearance compared to the vehicle within the striatal white matter bundles (arrow heads). X400 Magnification.

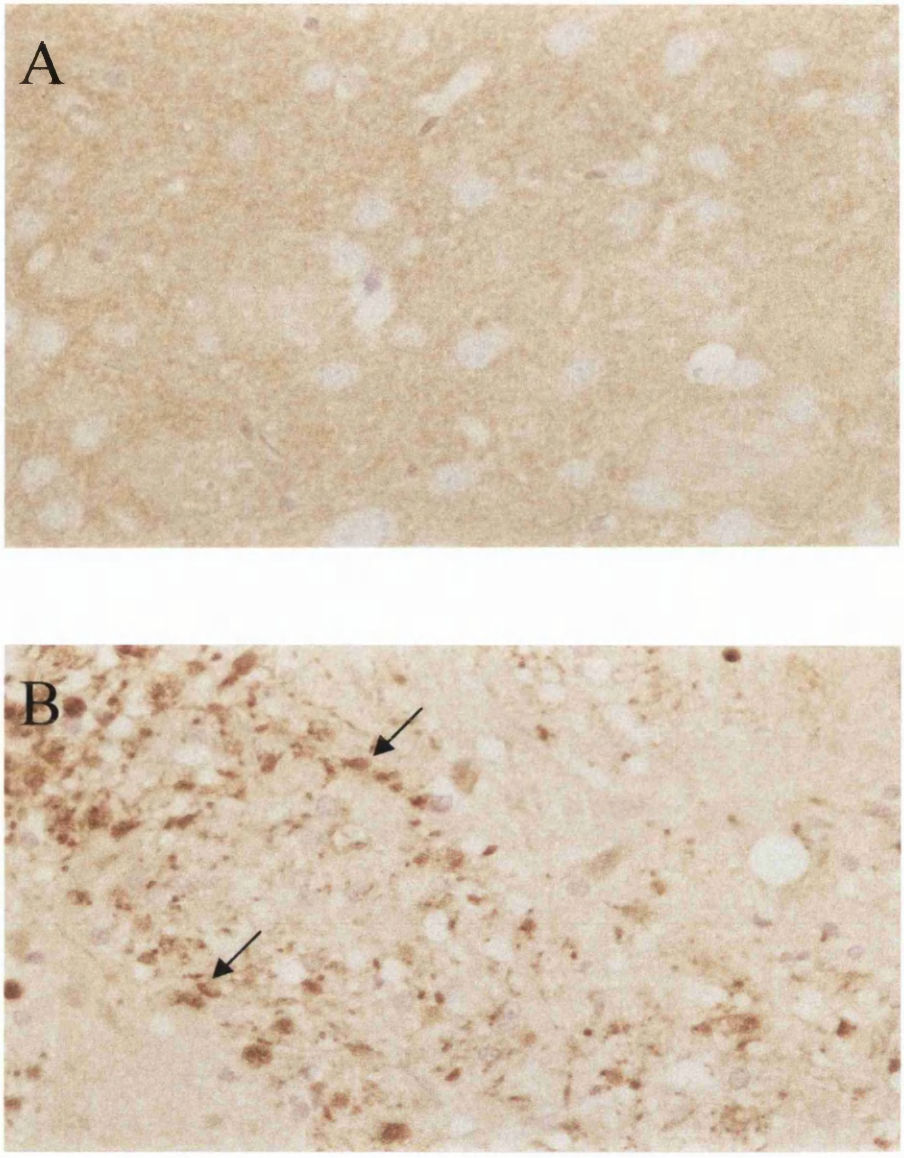

Figure 4.4 β-amyloid precursor protein immunohistochemical staining in the striatum following systemic injection of 3-nitropropionic acid

β-APP, immunostaining in A) vehicle and B) 30mg/kg treated animals. No β-APP immunostaining was evident in axons in the vehicle treated group, This was a typical of pattern of immunoreactivity that was given a score of 0. In the 30mg/kg treated animals β-APP immunoreactivity demonstrated axonal bulbs and swellings in the striatal white matter tracts. This was a typical pattern that represents a score of 3. The arrows indicate β-APP axonal bulbs. X 400 Magnification.

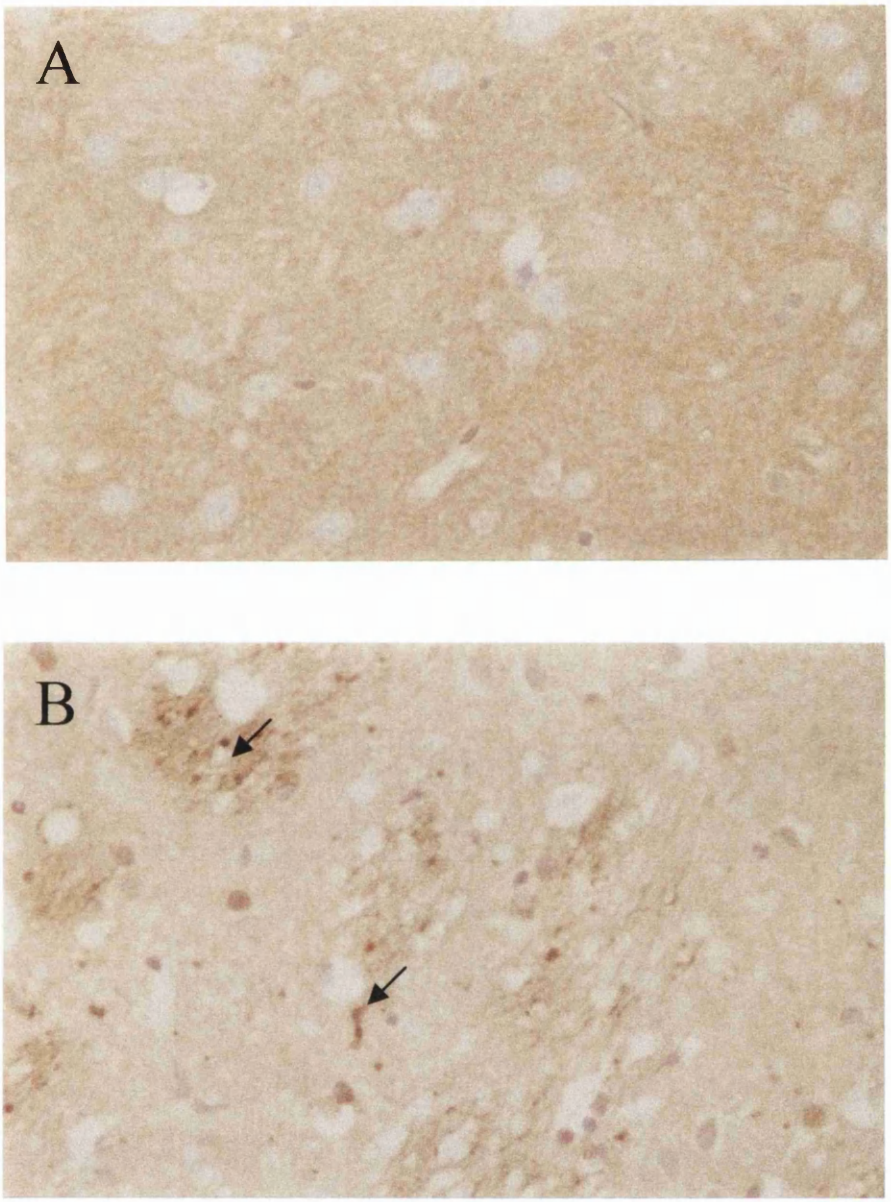

Figure 4.5 SNAP-25 immunohistochemical staining in the striatum following systemic injection of 3-nitropropionic acid

SNAP-25 immunostaining in A) vehicle and B) 30mg/kg 3-NPA treated rat. There was no SNAP-25 immunostaining in the vehicle treated group. This was a typical pattern of immunoreactivity that was given a score of three SNAP-25 immunoreactivity accumulated in myelinated fibre tracts of the striatum in 30mg/kg treated animals. This was a typical pattern of immunoreactivity that was given a score of 3. The arrow indicates SNAP-25 axonal bulbs. X400 Magnification.

Table 4.1 Scores of β-amyloid precursor protein immunoreactivity following 3-nitropropionic acid injection

Animal No	Vehicle	10mg/kg	15mg/kg	20mg/kg	30mg/kg
1	0	0	1	2	3
2	0	1	0	1	3
3	0	0	1	1	3
4	0	1	1	2	3
5	0		1	1	3

Staining was classified: 0, not present; 1, minimal; 2, moderate, 3, intense β-APP accumulation;

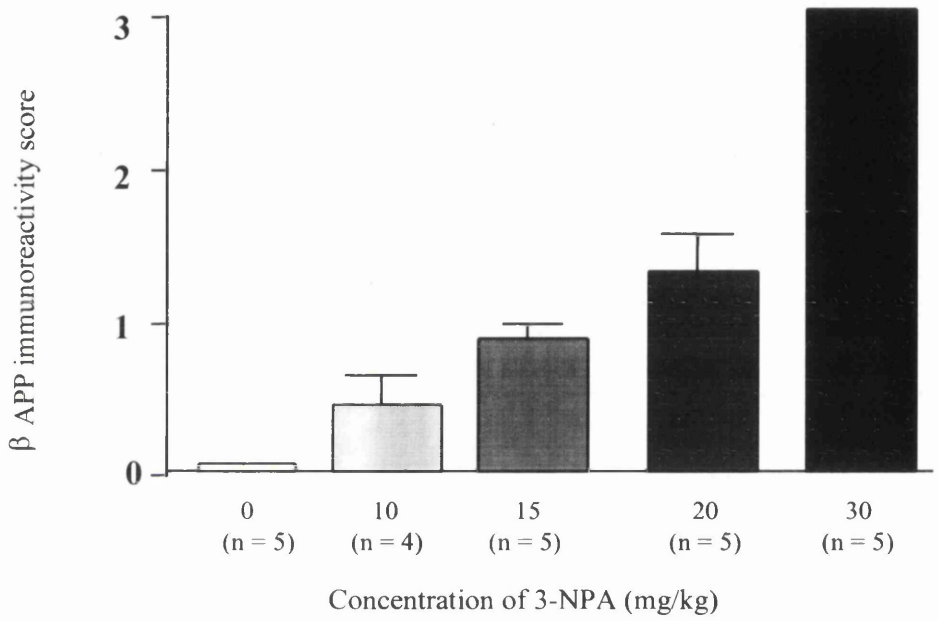

Figure 4.6 β-amyloid precursor protein accumulation following increased concentrations of 3-nitropropionic acid

β-APP immunoreactive sections were graded and given a score of either 0 = none; 1 = minimal; 2 = moderate and 3 = intense immunostaining. There was no β-APP immunoreactivity in axons in vehicle treated animals and only one animal out of four and three out of five in 10 and 15mg/kg 3-NPA treated animal, respectively, demonstrated any evidence of β-APP immunoreactivity. Animals treated with 20mg/kg 3-NPA all had evidence of β-APP immunoreactive swellings although this varied in the intensity of immunostaining. All five animals in 30mg/kg 3-NPA treated groups demonstrated bilateral β-APP accumulation throughout the white matter bundles in the striatum and all scored three. Data are mean + SEM. Kruskal-Wallis test $p<0.0007$

Table 4.2 Scores of SNAP-25 immunoreactivity following 3-nitropropionic acid injection

Animal No	Vehicle	10mg/kg	15mg/kg	20mg/kg	30mg/kg
1	0	0	0	1	3
2	0	1	1	1	2
3	0	0	1	2	2
4	0	0	0	1	2
5	0		0	0	3

0, not present; 1, minimal; 2, moderate, 3, intense SNAP-25 accumulation;

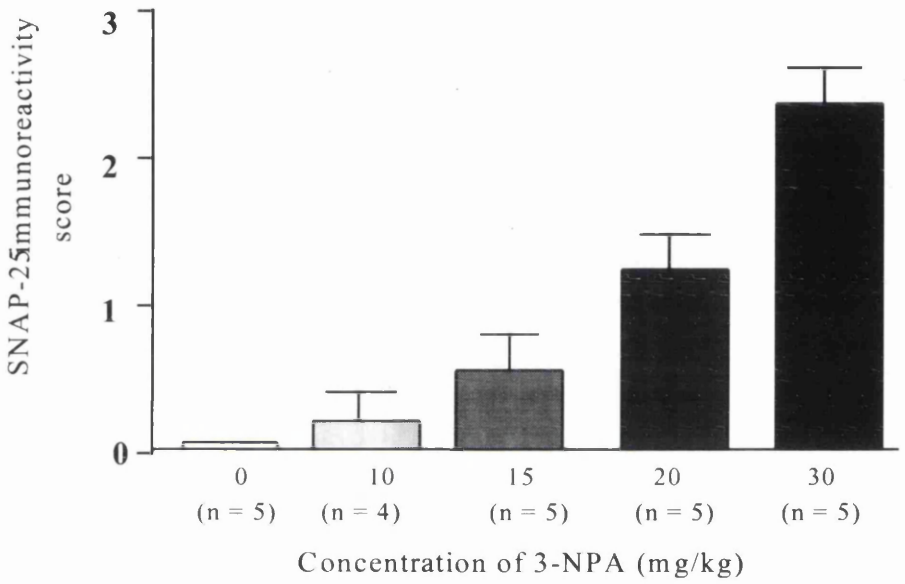

Figure 4.7 SNAP-25 accumulation following increased concentrations of 3-nitropropionic acid

SNAP 25 immunoreactive sections were graded and given a score of either 0 = none; 1 = some; 2 = moderate and 3 = intense immunostaining in axons. The data shows that there is no immunostaining in the vehicle treated group and that only one out of four and two out five animals in the 10 and 15mg/kg 3-NPA treated group, respectively had evidence of SNAP-25 accumulation. SNAP-25 immunoreactive axons were present in four out the five animals in the 20mg/kg treated group, although the amount of SNAP-25 ranged not present, to some to moderate between animals. The amount of SNAP-25 immunostaining varied between animals but all five animals in the 30mg/kg treated group had evidence of SNAP-25 immunoreactivity within the striatum. Data are mean + SEM. Kruskal-Wallis test $p<0.0023$

4.4.3 Calpain-mediated spectrin breakdown products immunohistochemistry

The polyclonal antibody, SBAbS2 specifically detects calpain-mediated spectrin breakdown products. In the vehicle treated animals only a few immunopositive oligodendrocyte-like cells were present within the subcortical white matter (Figure 4.8A and Figure 4.9). In the 3-NPA treated animals there was a concentration dependent increase in the density of SBAbS2 immunopositive cells present in the subcortical white matter at the level of the anterior commissure (Figure 4.8B and Figure 4.9). The number of oligodendrocyte-like cells which were positive for SBAbS2 was increased three-fold in the 30mg/kg treated animals compared to the vehicle treated animals. There was evidence of SBAbS2 immunopositive oligodendrocyte-like cells in the myelinated fibre tracts within the striatum, however, these cells were only present in the 30mg/kg treated animals and were therefore not counted. There was evidence of these cells in the myelinated fibre tracts of the striatum only in the 30mg/kg treated group and therefore these cells were not counted.

4.4.4 Manganese superoxide dismutase immunohistochemistry

Manganese superoxide dismutase (SOD-2) is located within the mitochondria. The mitochondria is a subcellular source of ROS (Dugan 1995) and Mn-SOD detoxifies ROS produced under normal physiological conditions. In the vehicle treated group there was a basal level of Mn-SOD immunoreactivity present within the subcortical white matter and striatum (Figure 4.10A). In the 3-NPA treated animals there was a concentration dependent increase in Mn-SOD immunoreactivity in the striatum (Figure 4.10B). There was no increase in Mn-SOD observed in the subcortical white matter in any of the 3-NPA treated groups.

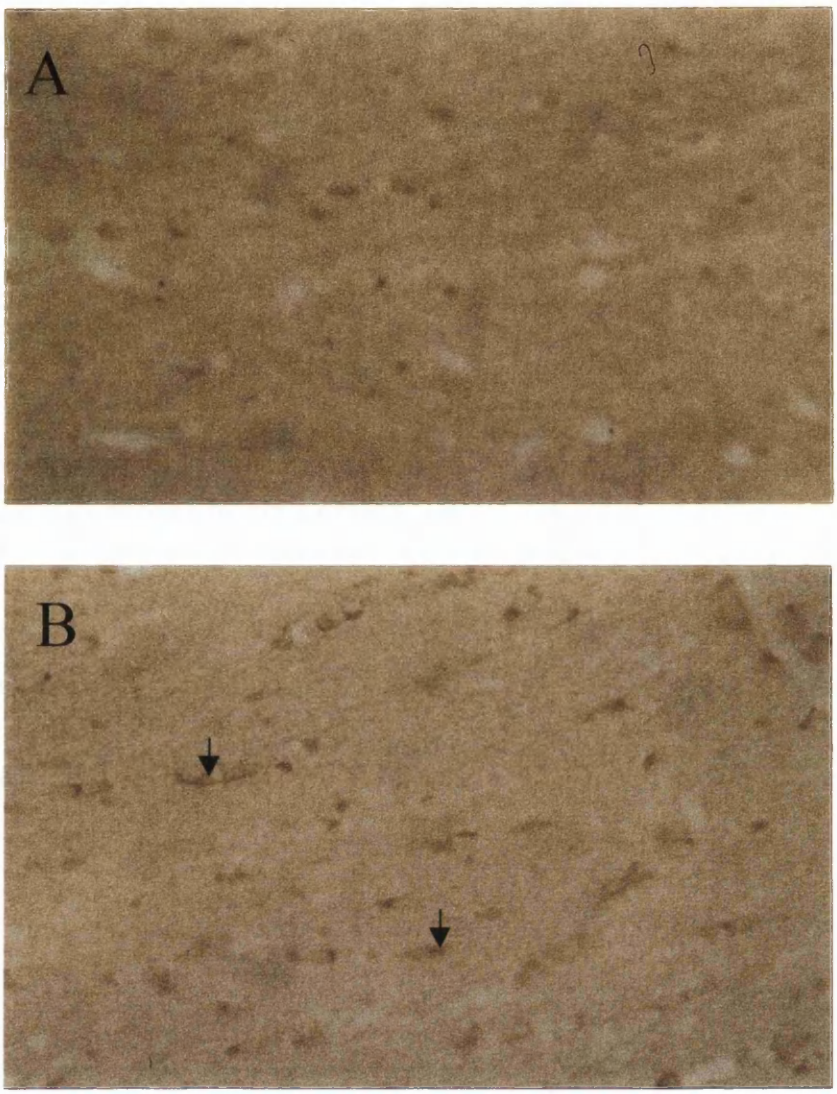

Figure 4.8 Immunohistochemical staining of calpain-mediated spectrin breakdown products in the subcortical white matter following systemic injection of 3-nitropropionic acid

The polyclonal antibody, SBAbS2 detected calpain-mediated spectrin breakdown products in oligodendrocyte-like cells in A) vehicle and B) 30mg/kg 3-NPA treated rat. Negligible staining of oligodendrocyte-like cells was evident in the subcortical white matter in vehicle treated group. However, there was intense SBAbS2 immunostaining of oligodendrocyte-like cells in the 30mg/kg 3-NPA treated group. The arrow indicates a typical positively stained oligodendrocyte with the characteristic small soma and thin rim of cytoplasm. X400 Magnification.

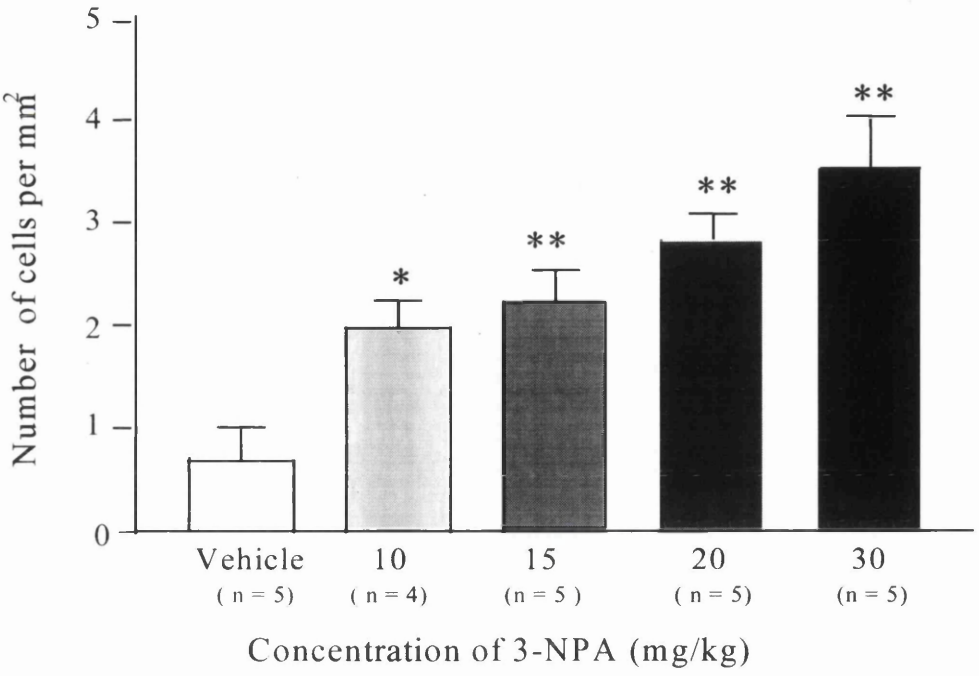

Figure 4.9 Quantitative data representing SBAbS2 immunopositive oligodendrocyte-like cells following systemic injection of 3-nitropropionic acid

Oligodendrocyte cells were counted in the subcortical white matter at the level of the anterior commissure at three specified regions (Figure 4.2). Cells were counted microscopically using a 1cm square graticule at x400 magnification and expressed as the number of cells per mm^2. The data show that there was a concentration dependent increase in the number of SBAbS2 immunopositive oligodendrocyte-like cells. Data are mean + SEM. one way ANOVA post-tested with Students *t* test and corrected with Bonferroni.

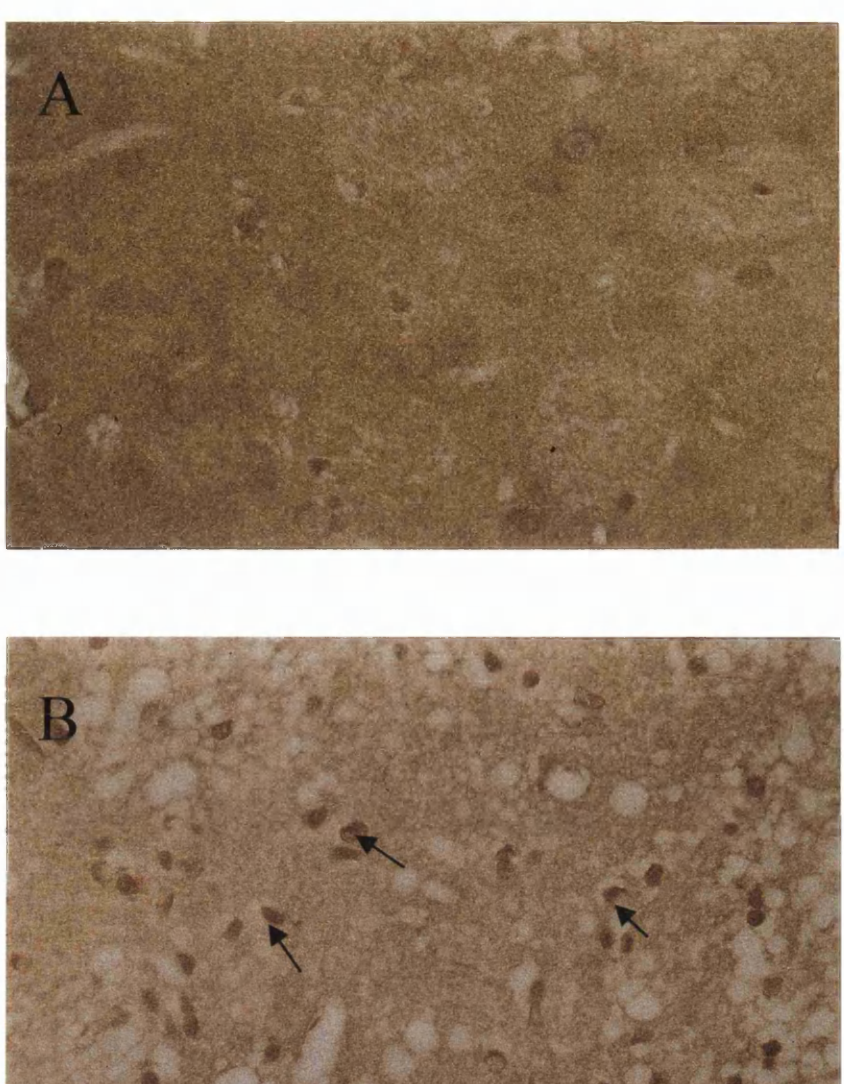

Figure 4.10 Manganese superoxide dismutase immunostaining following systemic injection of 3-nitropropionic acid

Mn-SOD immunoreactivity in the striatum of A) vehicle and B) 30mg/kg 3-NPA treated rat. There was some evidence of Mn-SOD immunostaining in the vehicle treated animals within the striatum. In contrast to the vehicle treated animals, Mn-SOD immunoreactvity was increased in the 30mg/kg treated group throughout the striatum. Mn-SOD appeared to be present in neuronal cells but not in axons. The arrow indicates Mn-SOD positive necrotic neurons. X400 Magnification.

4.5 DISCUSSION

Systemic injection of 3-nitropropionic acid induced marked pathological changes in myelinated axons in the striatum. There was a concentration dependent increase in the amount and distribution of axonal pathology reflected by the accumulation of the axonally transported proteins β-APP and SNAP-25. The gallyas silver staining technique, another method used to identify axonal damage, detected changes in axonal pathology up to two days post-injection of 3-NPA (Miller and Zaborszky 1997). In the present study, semi-quantitative analysis revealed no protein accumulation in either the subcortical white matter or the striatal fibre tracts in the vehicle treated group. Minimal immunoreactivity of both β-APP and SNAP-25 in the 10 or 15mg/kg 3-NPA treated animals was apparent and axonal damage detected by β-APP and SNAP-25 was slightly increased following 20mg/kg 3-NPA. However, after 30mg/kg 3-NPA two out of the five animals had moderate SNAP-25 staining and an intensely stained profile of axonal pathology was present in the other remaining three animals. In contrast, all five animals treated with 30-mg/kg 3-NPA demonstrated intense widespread accumulation of β-APP in the fibre tract bundles of the striatum. Scoring the amount and distribution of β-APP and SNAP-25 accumulation in axons revealed that the extent of axonal pathology was related to the concentration of 3-NPA administered. Using a similar paradigm, Brouillet et al., 1998 demonstrated a concentration dependent reduction in succinate dehydrogenase staining in the striatum following systemic injection of 3-NPA. However, in the present study the type of axonal pathology present in the striatum was not evident in the subcortical white matter. Structural alterations in the somatodendritic cytoskeleton are induced by intracerebral injection of 3-NPA. A loss of MAP-2 immunoreactivity was observed after 3-NPA treatment indicating a disruption of the cytoskeleton that is essential for stability and maintenance of dendritic and perikaryal structure and function. Thus, components of both the axonal and perikaryal cytoskeleton could be vulnerable to free radical mediated damage induced by 3-NPA.

Other mechanisms have also been proposed as pathogenic mediators involved in 3-NPA induced damage. Pang (1997) detected two different types of cell death in hippocampal slices after 3-NPA treatment: a rapid necrotic cell death that was NMDA receptor dependent and a delayed non NMDA-receptor dependent apoptotic cell death (Pang and

Geddes 1997). This suggests that mitochondrial dysfunction could induce a number of different pathogenic factors. Impaired energy metabolism reduces the amount of ATP available, leading to membrane depolarisation and this will relieve the Mg^{+} block on the NMDA receptor (Riepe et al., 1995; Greene et al., 1998). NMDA receptor activation by glutamate leads to Ca^{2+} influx. Calcium overload could in turn lead to activation of calpains suggesting a mode of action in grey matter. In the previous chapter of the thesis breakdown of the axonal cytoskeleton was associated with an increased activation of calpains after human head injury. However, after 3-NPA treatment in the rat, calpain-mediated spectrin breakdown products were not present within damaged axons. This contrasts with the findings in patients who had sustained a blunt head injury where there was evidence of calpain-mediated damage within axons. This suggests that 3-NPA administration in rats did not cause calpain activation in axons. Thus the axonal pathology induced by 3-NPA may reflect other actions of free radicals on the axonal cytoskeleton. By contrast, calpain-mediated spectrin breakdown products were increased in oligodendrocyte-like cells after 3-NPA treatment. Geddes et al., 1994, reported that intracerebral injection of 3-NPA induced calpain activation within neurons and this supports the suggestion that there is an interaction between oxidative stress and calpain activation, at least in neurons and oligodendrocytes. The oxidative stress cascade can increase the amount of intracellular Ca^{2+} (Dykens 1994; Desphande et al., 1997; Silver and Ercinska 1990) which could lead to calpain activation. Immunopositive oligodendroctyes was restricted to the subcortical white matter and was not present in the myelinated fibre tracts of the striatum where axonal damage was evident. However, increased calpain-mediated spectrin breakdown products were detected in oligodendrocytes in the striatum in response to the highest concentration of 3-NPA. Although, there were reduced levels of succinate dehydrogenase activity in the corpus callosum after 3-NPA treatment in the rats (Brouillet et al., 1998) this study did not distinguish between axons and oligodendrocytes and thus may explain why there was no protein accumulation in axons in the subcortical white mater. Therefore, this data suggests that neurons, axons and glia cells could have different sensitivities to pathogenic mechanisms. Therefore, although mitochondrial inhibition constitutes the primary insult after 3-NPA injection (Takamatsu et al., 1998) secondary mechanisms such as calpains, excitotoxity and oxidative stress may also be responsible for cellular damage.

There was a concentration dependent increase in the amount and distribution of Mn-SOD cellular staining in the striatum following 3-NPA treatment. A basal level of Mn-SOD immunopositive cells was present in the vehicle treated group. In the 30mg/kg treated group Mn-SOD immunoreactive cells appeared to be coincident with necrotic neurons within the striatum. Immunostaining did not appear to be increased in the subcortical white matter in any of the 3-NPA treated animals. This result concords with a previous study which demonstrated increased levels of Mn-SOD and the cytosolic Cu/Zn-SOD enzymes in the striatum following 3-NPA injection (Binienda et al.,1998). Both studies indicate that the levels of endogenous antioxidants are increased after 3-NPA treatment. Although, 3-NPA induced pathological changes, antioxidant enzymes may become overwhelmed by the intensity of free radical production and this may lead to tissue damage. There was a difference in the type of pathology observed in the striatum and the subcortical white matter yet they both had similar reductions in succinate dehydrogenase activity after 3-NPA administration (Brouillet et al., 1998). Therefore following 3-NPA injection, axonal damage in the striatum could be due to oxidative stress whereas the increased number of oligodendroctye-like cells in the subcortical white matter could be due to calpain activation. Furthermore, the presence of β-APP accumulation in axons within the striatum but not in axons within the subcortical white matter suggests that there may also be a differential tissue response to 3-NPA as well as multiple mechanisms involved.

Initiation of the self-propagating process, lipid peroxidation, may also enhance 3-NPA neurotoxicity. Systemic injection of 30mg/kg 3-NPA significantly increased the amount of free fatty acids, a marker of lipid peroxidation (Binienda et al., 1997). Reduction of the nitro moiety on 3-NPA produces superoxide anions (Fu et al., 1995) and these anions can undergo reactive changes to form either the hydroxyl radical or peroxynitrite anions, which can in turn induce lipid peroxidation. Therefore, a complex interacting cascade of pathogenic mechanisms leading to white matter damage could be hypothesised (Figure 4.11). In the next study the ability of the lipid peroxidation by product, 4-hydroxynonenal to induce axonal or oligodendrocyte damage was determined.

Figure 4.11 Cascade of biochemical events after acute brain injury

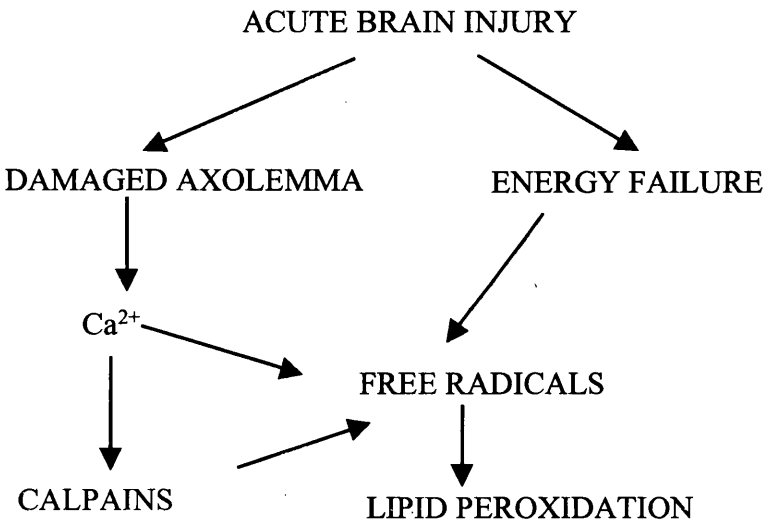

The digram illustrates a more complex interaction between pathogenic mediators than demonstrated in Figure 3.12. Oxidative cascade could contribute to cellular damage through initiation of the self-propagating process, lipid peroxidation.

CHAPTER V

THE LIPID PEROXIDATION BY-PRODUCT 4-HYDROXYNONENAL IS TOXIC *IN VIVO* AND *IN VITRO*

5.1 INTRODUCTION

Lipid peroxidation is an autocatalytic event that continues by abstracting hydrogen atoms from polyunsaturated fatty acids (Radi et al., 1991; Darely-Usmar 1992; Rubbu et al., 1994; Braughler and Hall 1989a; Braughler and Hall 1989b). As well as a long lasting effect on membrane integrity, lipid peroxidation releases an aldehyde cytotoxic by-product, 4-hydroxynonenal (4-HNE) (Esterbauer et al., 1991) which may itself contribute to cellular damage. 4-HNE has been shown *in vitro* to covalently bind to cytoskeletal proteins (Montine et al., 1996a; Mattson et al., 1997), ionic transporters (Siems et al., 1996) and neurotransmitter transporters (Springer et al., 1997; Keller et al., 1997; Blanc et al., 1998). These actions could lead to increased production of reactive oxygen and nitrogen species (Kinter and Roberts 1996; Karlbuber et al., 1997; Keller et al., 1997; Martinez et al., 1997) increased levels of intracellular calcium or induce excitotoxicity (Springer et al., 1997; Keller et al., 1997; Blanc et al., 1998). Increased 4-HNE immunoreactivity was present in white matter tracts surrounding the site of impact in a rat model of spinal cord injury (Springer et al 1997) and this lipid peroxidation product has been shown to be directly toxic to neuronal perikarya both *in vitro* and *in vivo*. (Bruce-Keller et al., 1998). However, it is not known if 4-HNE is toxic to white matter.

5.2 AIM

The aims of this study were threefold. Firstly, to determine if exogenous 4-HNE damages axons *in vivo*. Secondly, to determine if exogenous 4-HNE is toxic to oligodendrocytes in culture *in vitro* and thirdly to determine if endogenous 4-HNE is present in myelinated axons after permanent focal cerebral ischaemia.

5.3 MATERIALS AND METHODS

5.3.1 Intracerebral injection of 4-hydroxynonenal, ethanol and artificial cerebrospinal fluid in rats

Sprague Dawley rats were anaesthetised and placed in a stereotaxic frame. An incision was made in the scalp and the skull exposed. A craniotomy was made using a dental drill and using a Hamilton syringe 0.5µl of 64mM 4-HNE (n=6), vehicle (ethanol n=5)

or artificial cerebral spinal fluid (aCSF) (n=3) was injected into the subcortical white matter (Figure 5.1) at stereotaxic co-ordinates (A/P = -0.26mm from Bregma, L/M = 2mm and D/V = 3mm). 4-HNE, ethanol or aCSF were injected at a rate of 0.1μl per minute and the needle left for 10 minutes before removal to allow diffusion of the injectate from the needle tip. Animals were allowed to survive for 24 hours and then transcardially perfused with 4% paraformaldehyde. Brains were removed and processed for paraffin embedding and 5μm sections cut for histology and immunohistochemistry.

5.3.1.2 Volumetric analysis of lesion

Serial sections were cut throughout the lesion. Every tenth section was stained with H & E and the area of pallor within the sections was determined using an imager analyser (Imaging Research, Canada). All sections were measured and normalised to a cyrostat non-fixed rat brain to correct for shrinkage that may have occurred during the fixation and paraffin embedding process. The area of damage in mm^2 was plotted against the distance between sections and the area under the curve was used to calculate the volume of damage in mm^3. Statistical analysis was performed using a one way ANOVA and post tested using Student's *t* test and corrected with Bonferroni for multiple comparisons.

5.3.1.3 Immunohistochemistry

Immunohistochemistry was performed (see 2.7.1) using DAB as the chromogen. Adjacent sections were processed for β-APP to assess axonal injury, a polyclonal antibody raised against 4-HNE which detects 4-HNE-Michael adducts and the polyclonal antibody SBAbS2 to determine if there was any evidence of calpain-mediated spectrin breakdown products. For information of primary antibodies see Table 2.1.

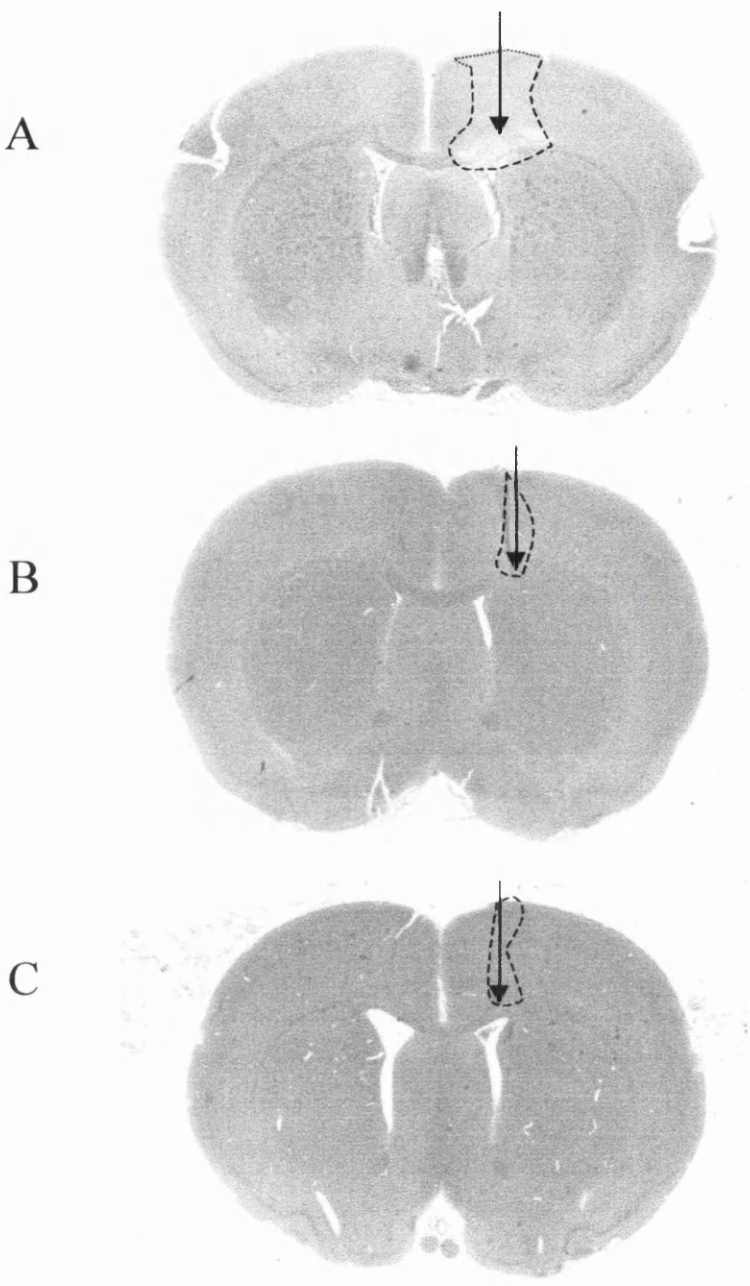

Figure 5.1 Digitised image of haematoxylin and eosin stained sections showing histological damage

Digitised images of representative sections at the coronal plane showing areas of histological damage in rats injected with: A) 4-HNE; B) ethanol and C) aCSF. The arrows in each section indicate the injection site and the dotted lines delineate the areas of pallor, defining the extent of histological damage measured using the image analyser. Serial sections throughout the extent of the lesion were measured and the volume of the histological lesion calculated.

5.3.1.4 Quantitative analysis of neuronal perikarya damage and axonal injury

Using a previously described method (Yam et al., 1999) the extent of neuronal perikaryal damage in grey matter and axonal injury in subcortical white matter was determined in all three treated groups. Neuronal damage was assessed in haematoxylin and eosin stained sections and axonal injury was assessed in adjacent β-APP stained sections. Neuronal damage was defined by the presence of pyknotic eosinophilic perikarya and axonal damage was defined by the presence of β-APP positive axonal bulbs or swellings in white matter. The areas of grey and white matter damage were quantified by placing a $1mm^2$ grid on a transparency over the diagrams and counting the number of grid points that fell within the lesion area (Figure 5.2).

5.3.2 Effect of 4-hydroxynonenal on oligodendrocyte cultures

Oligodendrocyte cultures were prepared from Sprague Dawley neonates (0-3 days old) and enzymatically dissociated and mixed glia cells plated for 10-12 days (see 2.7.1). Thereafter cultured flasks were shaken overnight in an orbital shaker and filtered to obtain pure oligodendrocyte cultures (see 2.7.2). Mature oligodendrocytes were identified *in vitro* using galactocerebroside immunofluorescent labelling (Figure 2.5). After seven days in culture, cells were exposed to 1, 10 or 50μM 4-HNE and incubated for either 1, 2 or 4 hours (see 2.7.6). Concentrations of 4-HNE are within the range known to induce damage in cells exposed to $FeSO_4$ and other insults that induce membrane lipid peroxidation. (Esterbauer et al., 1991; Mark et al., 1997). Oligodendrocyte cell death was determined by trypan blue exclusion (see 2.7.5) and morphological changes detected by immunohistochemistry (see 2.1.7) using a monoclonal antibody to the cytoskeletal protein spectrin (Table 2.1).

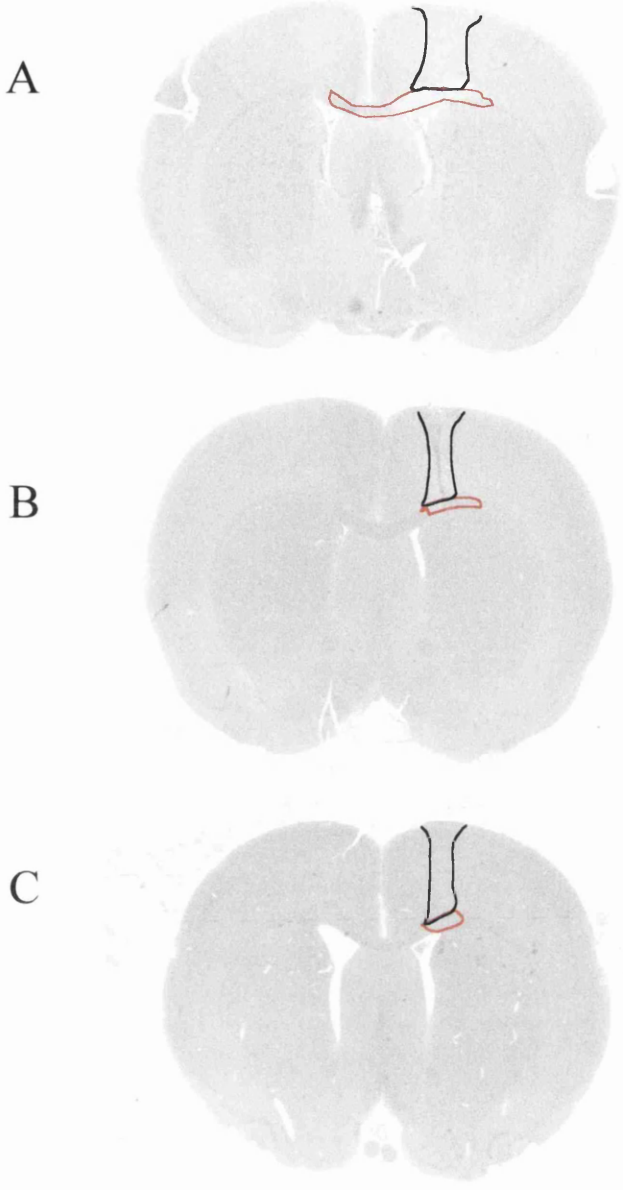

Figure 5.2 Mapping of grey and white matter damage onto digitised images of haematoxylin and eosin stained sections from 4-hydroxynonenal, ethanol and artificial cerebrospinal treated animals

Digitised images of representative sections at the coronal plane of histological damage in rats injected with A) 4-HNE, B) ethanol and C) aCSF. The area of neuronal damage is outlined in red and axonal injury is outlined black. Perikaryal damage was determined by their characteristic necrotic appearance while axonal injury was determined by the presence of β-APP bulbs and swellings.

5.3.3 Permanent focal cerebral ischaemia

Male Sprague Dawley rats (Harlan Olac, UK) weighing between 270-320g were housed together before surgery and individually housed afterwards in a cage with soft bedding, food and water throughout the 24 hour recovery period. Animals were anaesthetised with 5% halothane and 70% nitrous oxide/30% oxygen in a perspex box (n = 6). Rats were then intubated with a 16G catheter and mechanically ventilated with 1.5% halothane and 70% nitrous/30% oxygen. Focal cerebral ischaemia was induced by the intraluminal thread method (Longa et al., 1989). A neck medial incision was made and the left common carotid artery exposed. The pterygopalatine branch of the internal carotid was ligated with a 6.0 silk suture. The external carotid was electrocoagulated distally and an aneurysm clip placed on the common and internal artery while an artertiotomy was made in the external carotid and a 6.0 nylon monofilament suture advanced to the clip on the internal carotid. The clip was removed and the monofilament suture was advanced up for approximately 22mm or until some resistance was felt to block the origin of the middle cerebral artery. After 2 hours the animals recovered with the thread still in place. The muscle and skin of the neck incision were sutured and 0.5mls of atropine and 2mls of sterile saline given subcutaneously. Animals were allowed to recover for a period of 22 hours and during this period monitored for any gross behavioural changes. Animals were then re-anaesthetised, with 5% halothane 70% nitrous/30% oxygen in a perspex box and then perfused transcardially with 0.9% saline and 4% paraformaldehyde. Rats were decapitated, heads post-fixed for 24 hours in 4% paraformaldehyde, brains removed and post-fixed for a further 48 hours before being processed through a series of dehydrating and clearing agents and then paraffin embedded (see 2.4.2). 5μm microtome sections were collected onto poly-L-lysine slides for histology and immunohistochemistry.

All surgical procedures and tissue processing for these experiments were performed by Dr.V.Valeriani . Immunohistochemistry experiments was performed by E. McCracken.

5.4 RESULTS

5.4.1 Intracerebral injection of 4-hydroxynonenal, ethanol or artificial cerebrospinal fluid

5.4.1.1 Histology

In haematoxylin and eosin stained sections extensive tissue damage was observed extending rostrocaudally and medialolaterally away from the injection site in 4-HNE treated animals. There was evidence of tissue damage in both grey and white matter of the 4-HNE treated animals (Figures 5.3A & D). In the core of the lesion there was cellular and axonal loss within the subcortical white matter. In the adjacent grey matter, damaged neuronal perikarya appeared shrunken and eosinophilic. In contrast, in the vehicle, ethanol- and aCSF-treated animals the majority of neurons appeared morphologically unchanged (Figures 5.3B & E and Figures 5.3C & F) although, there was some evidence of damaged perikarya around the needle tract. There appeared to be some axonal damage in the subcortical white matter but this was restricted to the injection site in both ethanol and aCSF treated groups. Intracerebral injection of 4-HNE caused a significantly larger lesion compared to either ethanol or aCSF treated groups $p<0.01$ (Figure 5.4).

5.4.1.2 Axonal pathology

In the 4-HNE treated animals there was intense β-APP immunoreactivity across the subcortical white matter adjacent to the injection site. β-APP immunoreactive axons were also prominent within the genu of the corpus callosum and in the subcortical white matter of the contralateral hemisphere (Figure 5.5A). Medial to the injection site there was intense β-APP immunoreactivity in the subcortical white matter but in the adjacent grey matter neuronal perikarya appeared normal (Figure 5.5B). Ethanol treated animals did exhibit some β-APP immunopositive axons but this was confined to a region around the site of injection. A similar pattern of immunoreactivity was observed in the aCSF treated group (Figure 5.5C).

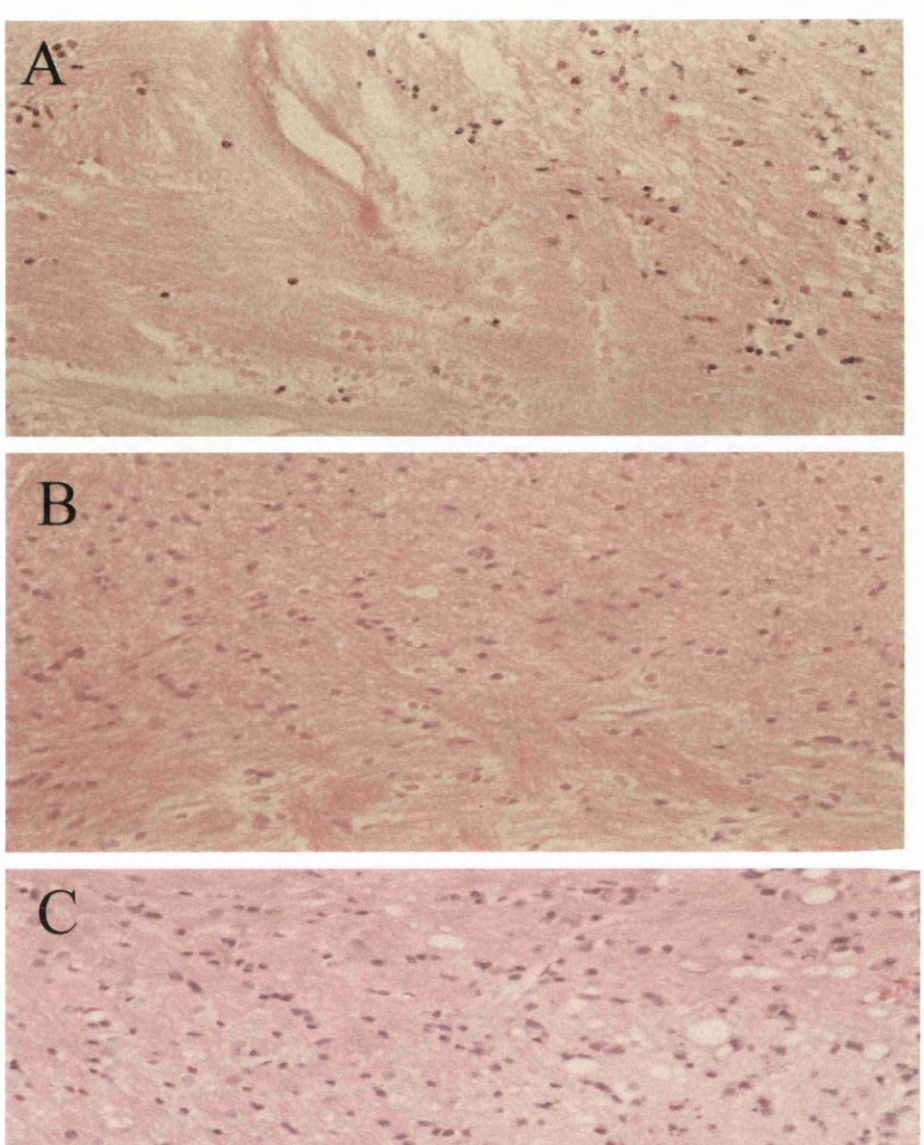

Figure 5.3A Morphological changes in white matter following intracerebral injection of 4-hydroxynonenal, ethanol or artificial cerebrospinal fluid at high magnification

Haematoxylin and eosin histology in A) 4-HNE, B) ethanol and C) aCSF. There was extensive axonal damage observed in the subcortical white matter in the 4-HNE treated groups compared to the ethanol and aCSF treated groups. X400 Magnification.

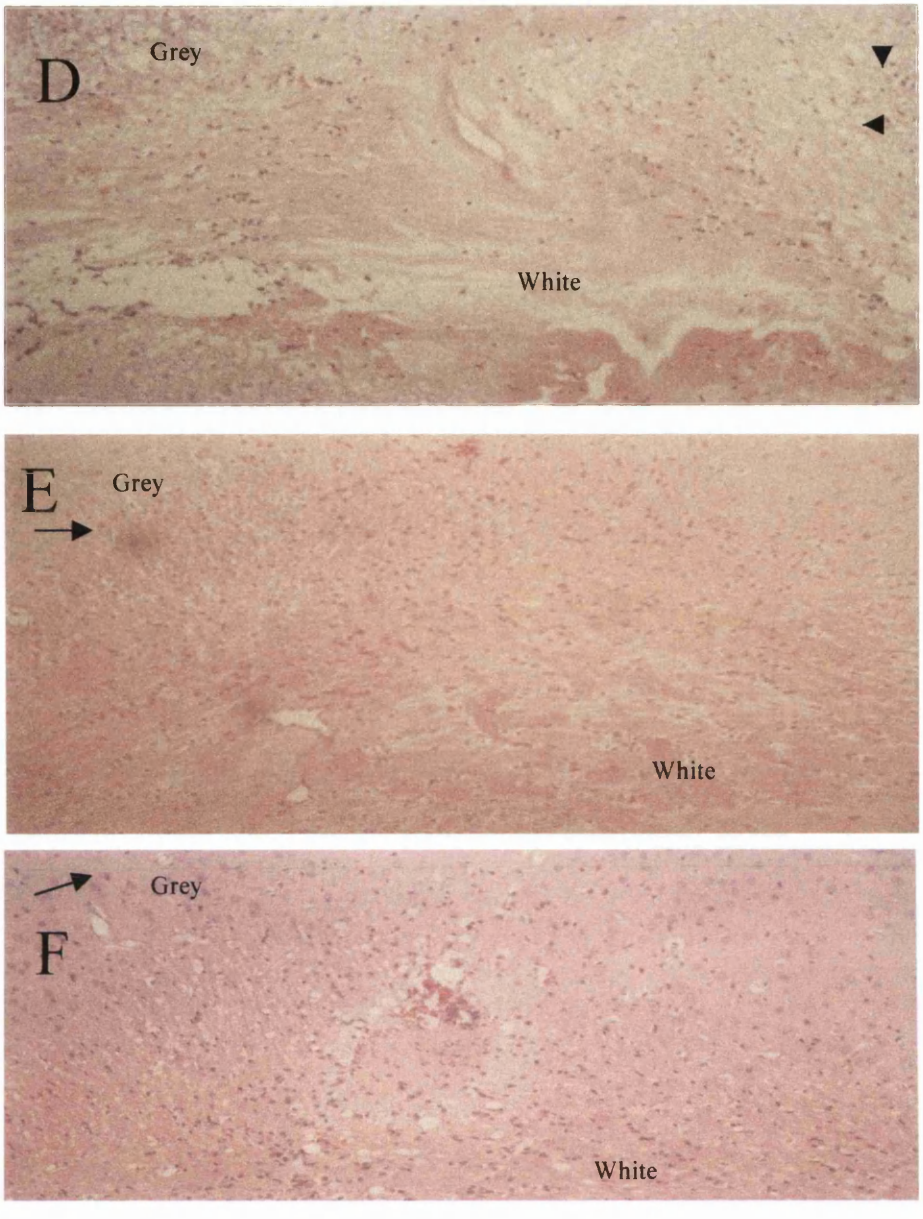

Figure 5.3B Morphological changes in grey and white matter following intracerebral injection of 4-hydroxynonenal, ethanol or artificial cerebrospinal fluid at low magnification

Haematoxylin and eosin histology in D) 4-HNE, E) ethanol and F) aCSF. In the vehicle, treated group, the majority of neurons and axons appeared normal (arrows heads) with the exception of a few damaged neurons and axons around the needle tract. This type of pathology was also indicative in the aCSF treated group. In the 4-HNE treated animals there was shrinkage of neuronal perikarya (arrows) with extensive cellular and axonal loss within the subcortical white matter. X200 Magnification.

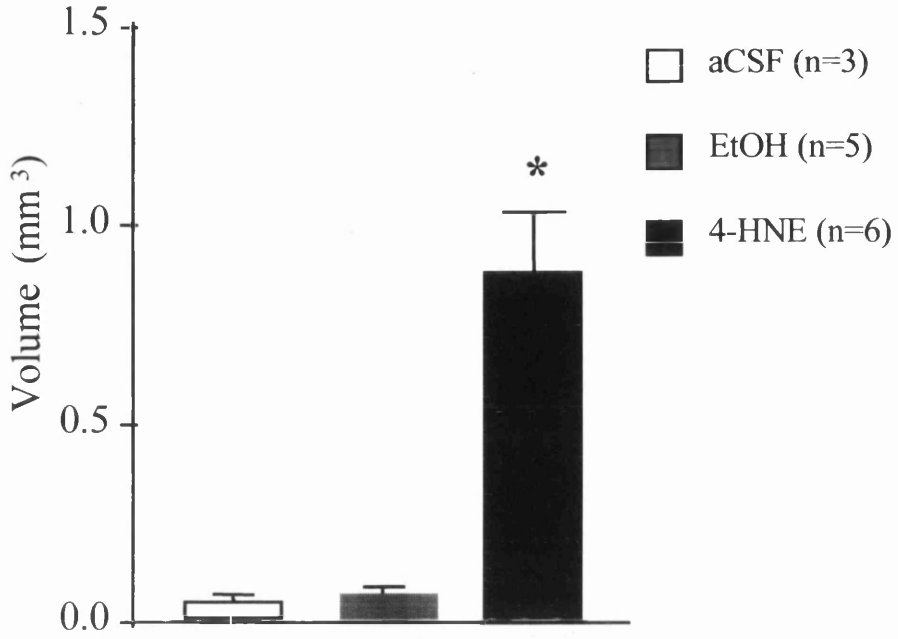

Figure 5.4 4-hydroxynonenal induces brain damage (lesion volume)

There was a significant increase in lesion volume of the 4-HNE (n = 6) treated group compared to ethanol (n = 5) or CSF (n = 3) treated groups. There was no difference in lesion size between ethanol or CSF treated animals. Statistical analysis was performed using one way ANOVA and post tested with Student's *t* test and corrected for Bonferroni. Data expressed as ± SEM * $p < 0.01$.

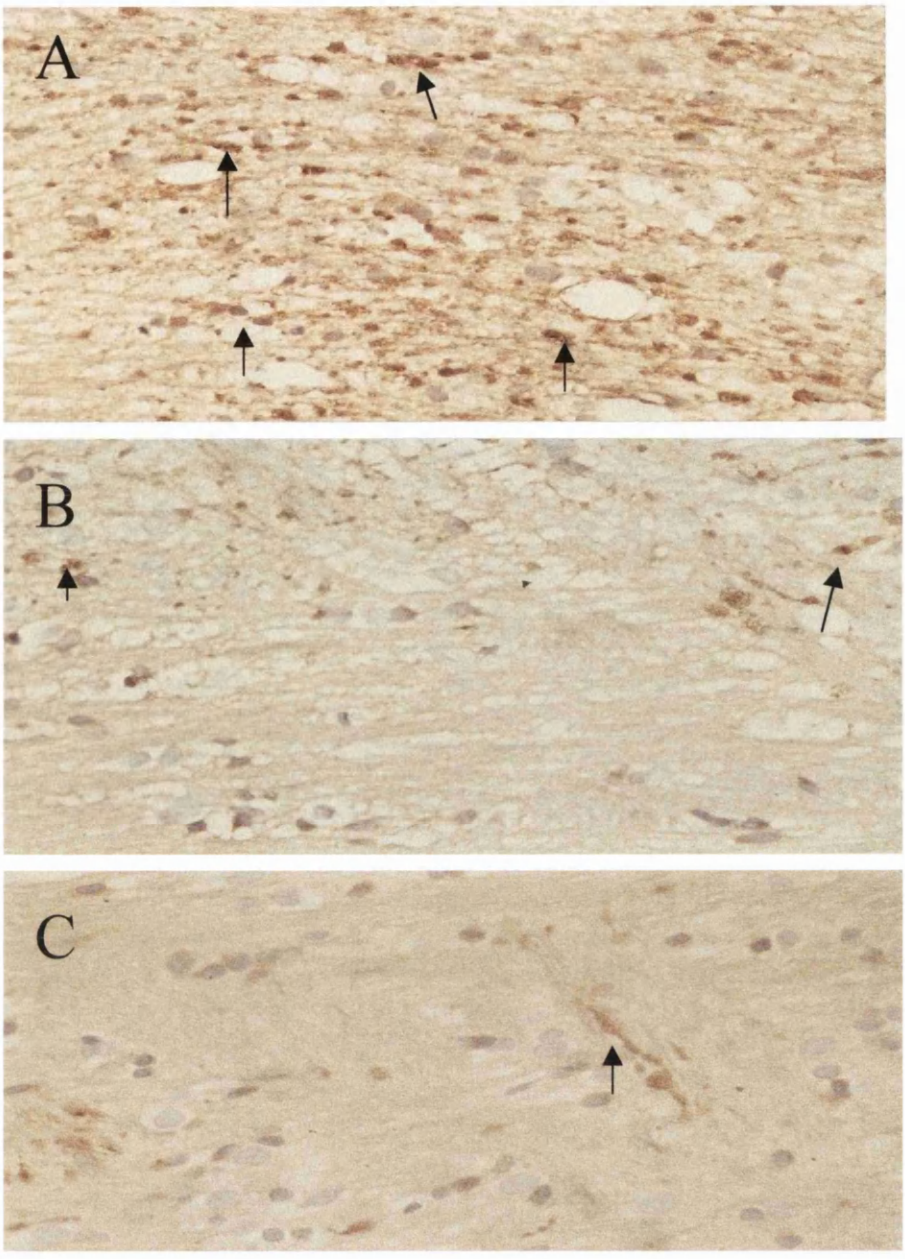

Figure 5.5 β-amyloid precursor protein immunohistochemical staining in the subcortical white matter following intracerebral injection of 4-hydroxynonenal, ethanol or artificial cerebrospinal fluid

β-APP immunostaining in A) 4-HNE, B) ethanol and C) aCSF treated animals. In the 4-HNE treated animals there was intense β-APP accumulation around the injection site. These β-APP immunopositive bulbs and swellings were still evident in the subcortical white matter of the contralateral hemisphere. In contrast, in the control groups B) and C) there were relatively few β-APP immunoreactive axons and these were restricted to the injection site. Arrows indicate β-APP immunopositive axons. X400 Magnification.

5.4.1.3 Quantitative analysis of neuronal perikaryal damage and axonal injury

The extent of neuronal perikaryal damage in grey matter was significantly greater in the 4-HNE treated animals compared to the relatively small amount of damage observed in the ethanol and aCSF treated animals. Quantitative analysis demonstrated an approximately 75% increase in the amount of neuronal perikaryal damage in the 4-HNE treated group (Figure 5.6A). The amount of axonal injury in the subcortical white matter was approximately 85% greater in the 4-HNE treated group than in either of the ethanol or aCSF treated groups (Figure 5.6B). β-APP immunostained sections counterstained with haematoxylin from the 4-HNE treated group revealed that in an area away from the injection site where the neuronal perikarya appeared normal there was evidence of β-APP immunopositive axons in the underlying white matter (Figure 5.7). Thus the data suggests that components of white matter could be more vulnerable to 4-HNE than neuronal cell bodies.

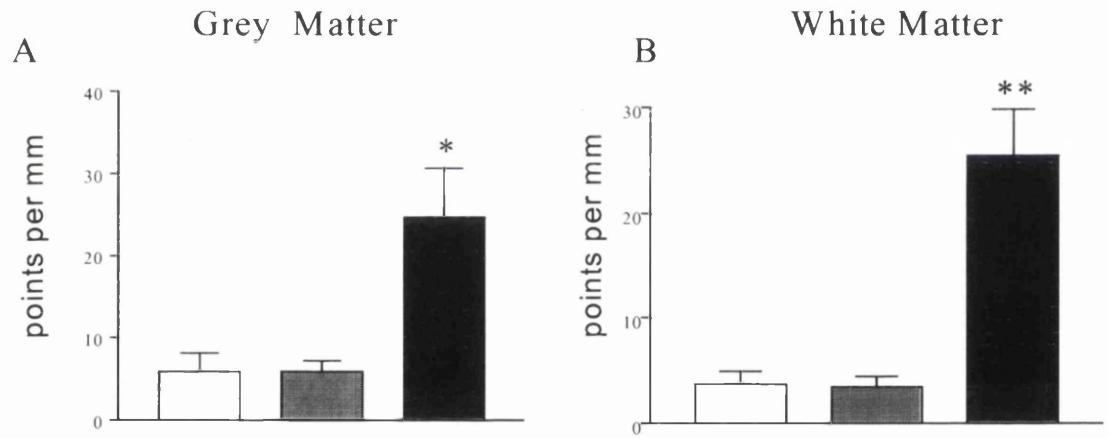

Figure 5.6 Extent of grey and white matter damage following intracerebral injection of 4-hydroxynonenal, ethanol and artificial cerebrospinal fluid

The number of grid points counted per mm^2 in the 3 treated groups in A) grey matter and B) white matter. The data in A) 4-HNE demonstrated a significantly larger increase in the extent of neuronal damage compared to ethanol or aCSF treated group. In B) the amount of β-APP immunoreactive axons following intracerebral injection of 4-HNE also demonstrated a significant increase in axonal damage compared to the ethanol or aCSF treated group. There is no difference in the area of neuronal or axonal damage between either the ethanol or aCSF treated groups. Data are mean + SEM, one way ANOVA post-tested with Student's *t* test and corrected with Bonferroni.

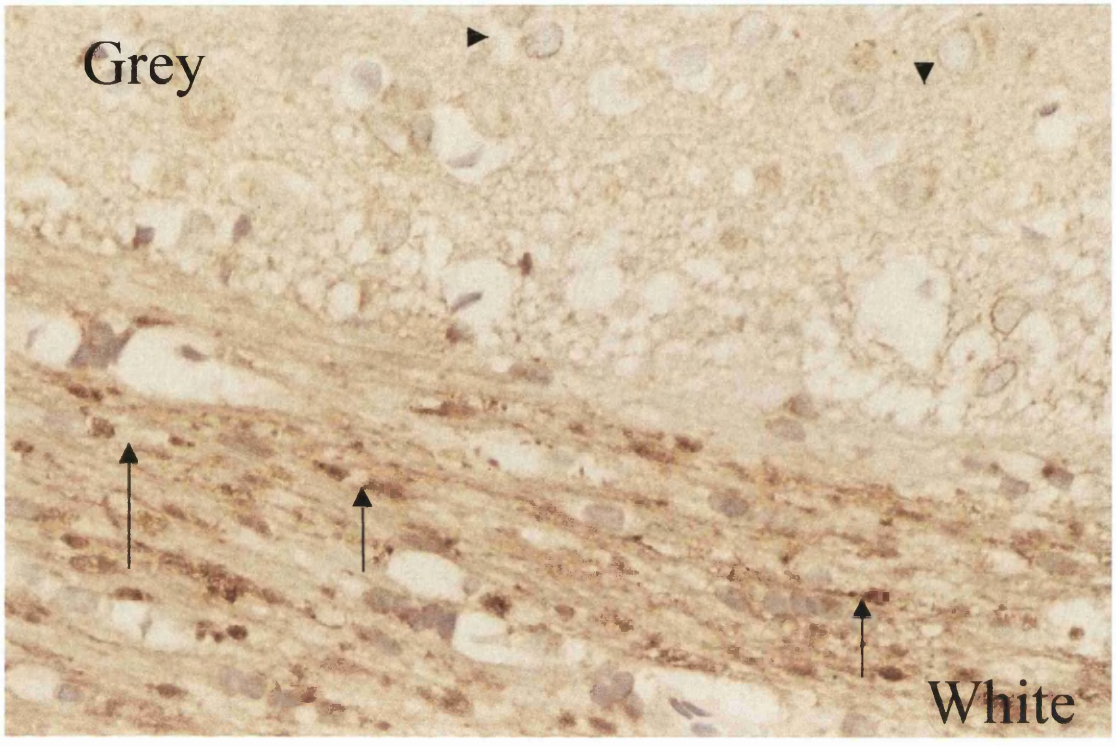

Figure 5.7 β-Amyloid precursor protein immunoreactivity following intracerebral injection of 4-hydroxynonenal

The scanned photograph shows a β-APP immunostained section from an 4-HNE treated animal. β-APP immunopositive axons in the subcortical white matter were prominent in 4-HNE treated animals (arrows) whereas in the adjacent grey matter the neuronal perikarya appeared normal (arrow heads). X400 Magnification.

5.4.1.4 Immunohistochemistry

4-HNE immunoreactivity was present in damaged neurons around the needle tract in all three treated groups. In contrast, in the subcortical white matter 4-HNE immunoreactivity was restricted to the site of injection in the 4-HNE and ethanol treated animals (Figure 5.8A and Figure 5.8B) but was absent from the subcortical white matter in the aCSF treated animals. However there was greater intensity of 4-HNE immunoreactivity in the 4-HNE treated group in contrast to the ethanol-treated group (Figure 5.8C).

Calpain-mediated spectrin breakdown products detected by the polyclonal antibody SBAbS2, detected pathological changes in the cortex in all three treated groups. SBAbS2 immunopositive neuronal perikarya were present in the cortex of the 4-HNE treated group (Figure 5.9A). However, in the ethanol and aCSF treated groups there was no evidence of immunopositive neuronal perikarya but there was an irregular rough appearance in the neuropil around the needle tract in these two groups. There was no evidence of calpain-mediated spectrin breakdown products within the subcortical white matter in any of the three treated groups (Figure 5.9B and Figure 5.9C).

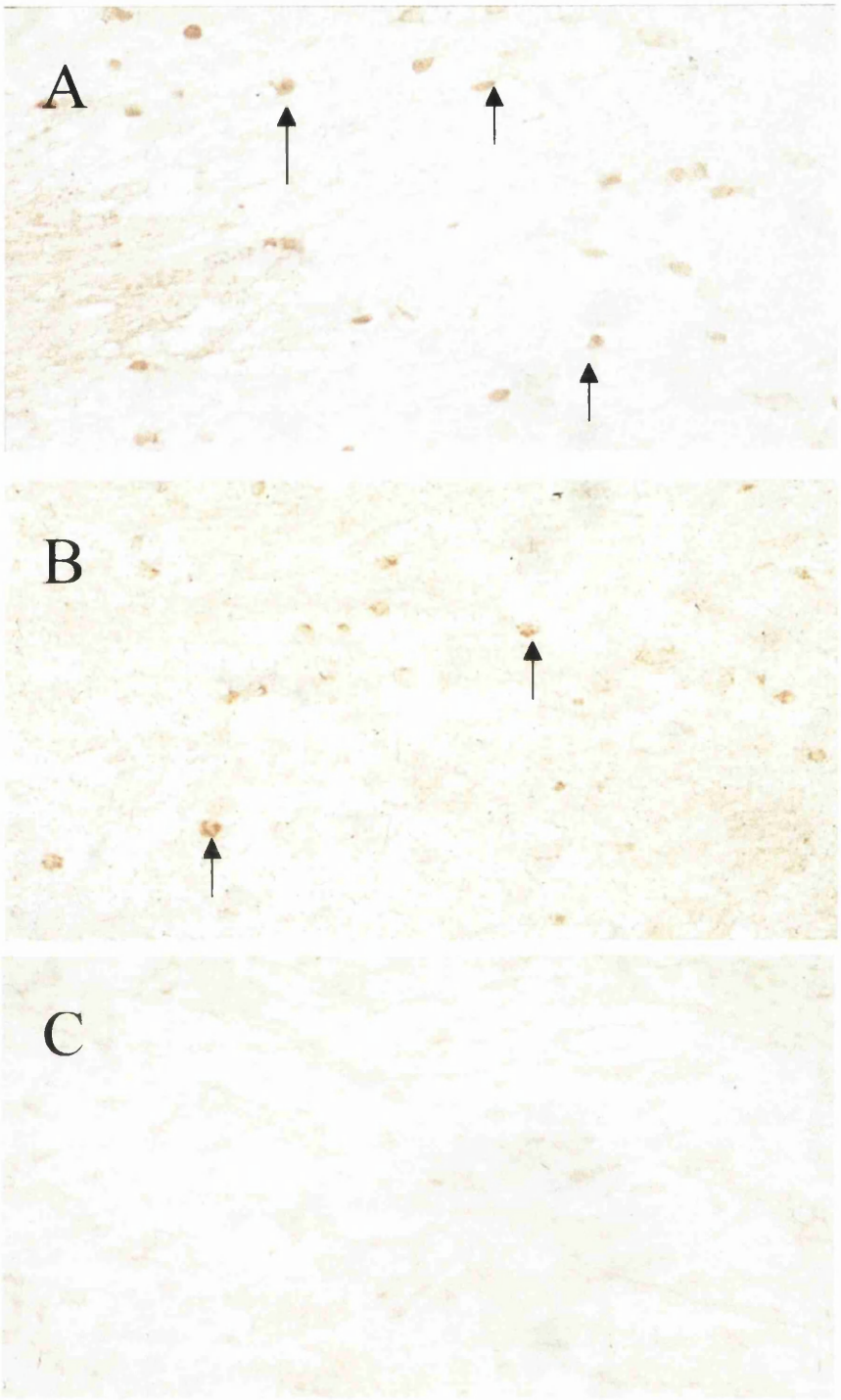

Figure 5.8 4-HNE-Michael adducts immunostaining following intracerebral injection of 4-hydroxynonenal, ethanol or artificial cerebrospinal fluid

4-HNE immunostaining in A) 4-HNE, B) ethanol and C) 4-HNE treated animals. There were 4-HNE-Michael adducts present within the subcortical white matter in the 4-HNE and ethanol treated groups (arrows). There was no evidence of 4-HNE immunoreactivity in the aCSF treated group. X400 Magnification.

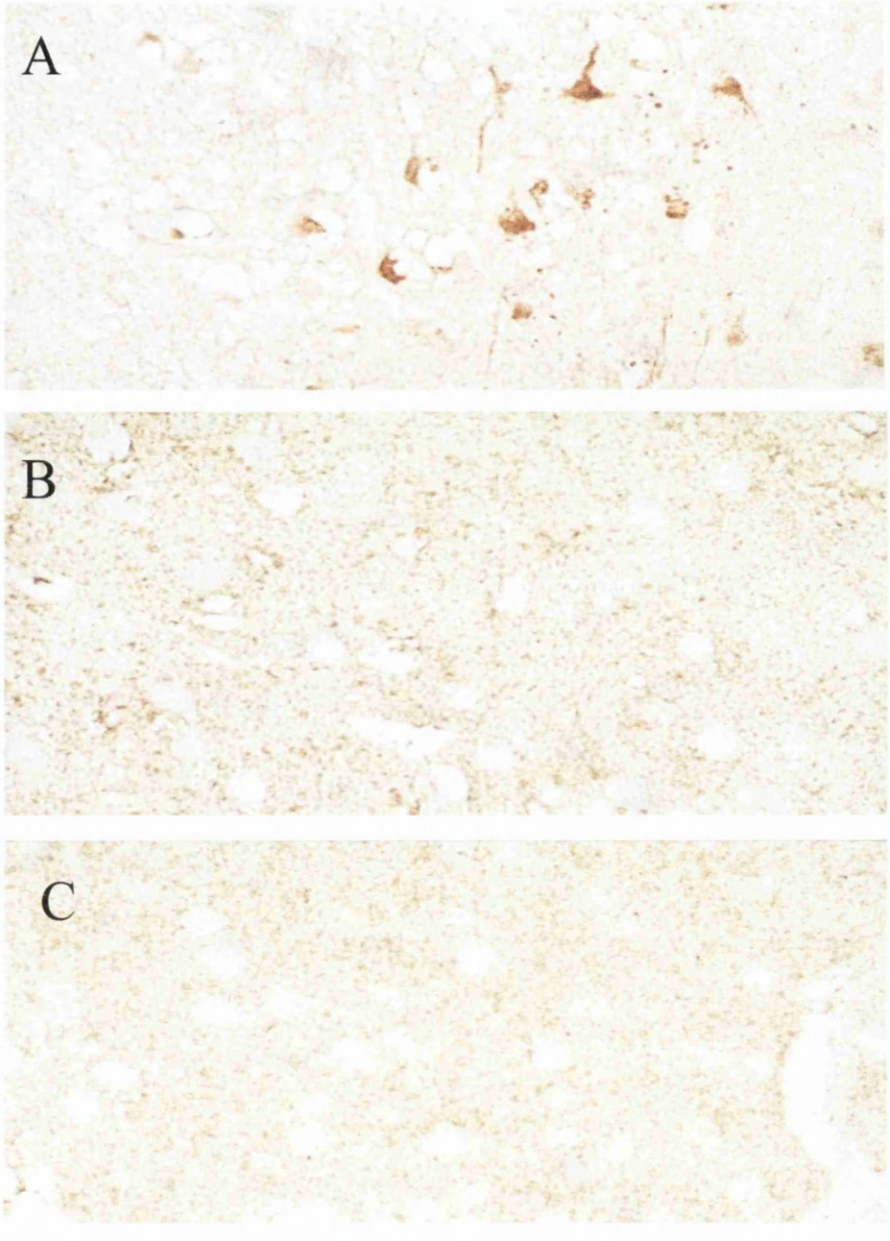

Figure 5.9 Calpain-mediated spectrin breakdown products immunostaining following intracerebral injection of 4-hydroxynonenal, ethanol or artificial cereberospinal fluid

The polyclonal antibody SBAbS2, detected calpain-mediated spectrin breakdown products in A) 4-HNE, B) ethanol and C) aCSF treated animals. In the ethanol- and aCSF-treated animals immunoreactivity had an irregular rough appearance around the injection site in the cortex. However, in the 4-HNE treated group neuronal perikarya in the cortex was immunopositive for calpain-mediated spectrin breakdown products positive. X400 Magnification

5.4.2 Effect of 4-hydroxynonenal in oligodendrocyte cultures

Exogenous 4-HNE induced both time and concentration dependent oligodendrocyte death in culture *in vitro*. There was microscopic evidence of oligodendrocyte cell death detected by trypan blue uptake within 1 hour at the lowest concentration, 1μM 4-HNE. However after 4 hours incubation with the highest concentration, 50μM 4-HNE had killed all the oligodendrocytes in culture (Figure 5.10 and Figure 5.11). At this same time point concentration dependent changes in oligodendrocyte morphology were observed detected by the cytoskeletal protein, spectrin. In the vehicle, 0.2% ethanol and 1μM 4-HNE treated cells, perikarya were preserved and oligodendrocyte processes showing spectrin immunoreactivity were evident. However, treatment with 10 or 50μM 4-HNE caused fragmentation of processes and cell shrinkage (Figure 5.12).

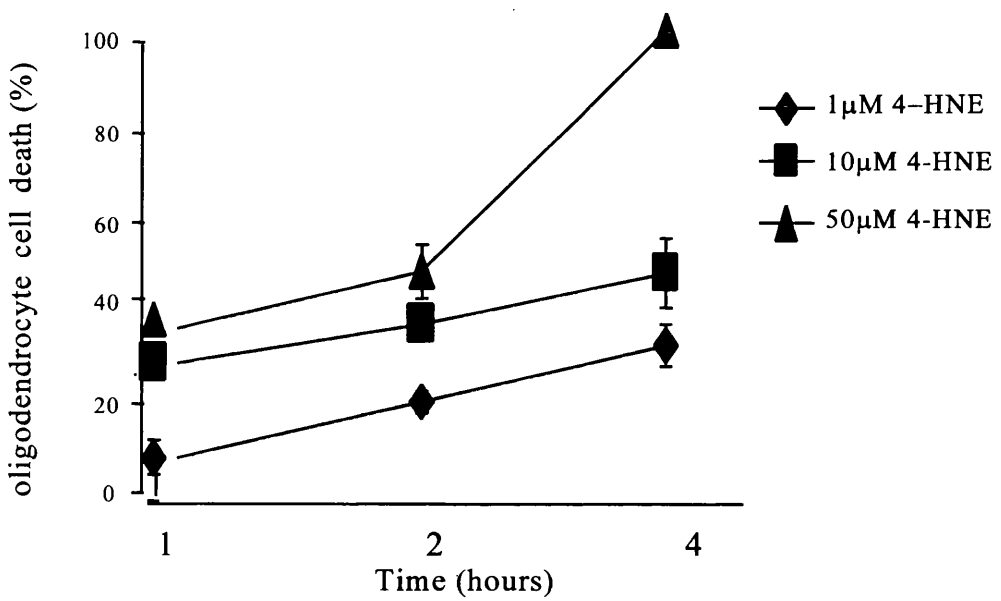

Figure 5.10 Exogenous 4-hydroxynonenal increased oligodendrocyte cell death in a time dependent manner

The percentage of oligodendrocyte cell death was increased at 1, 2 and 4 hours. There was 100% cell death after 4 hours at the highest concentration of 4-HNE.

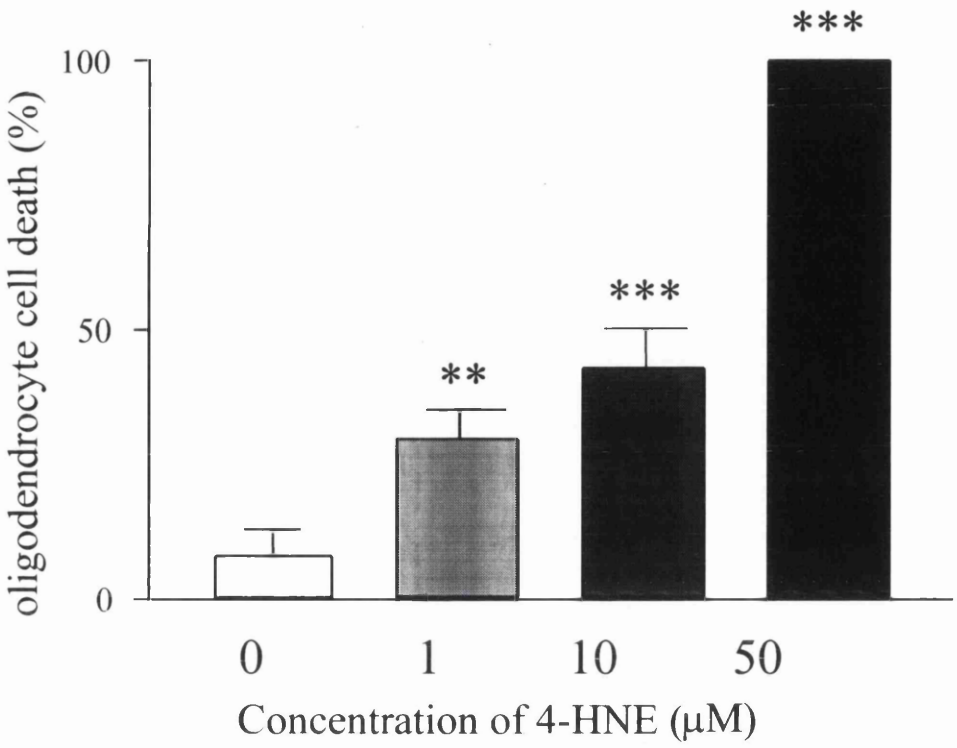

Figure 5.11 Exogenous 4-hydroxynonenal increased oligodendrocyte cell death in a concentration dependent manner

Percentage of oligodendrocyte cell death is increased in a concnetration dependent manner. There was a significant increase produced in percentage cell death after 1 and 10μM 4-HNE incubation. The highest concentration 50μM 4-HNE produced 100% oligodendrocyte cell death after 4 hours incubation. Data are mean + SEM, one way ANOVA post-tested with Student's *t* test and corrected with Bonferroni. *** p>0.001, ** p>00.1

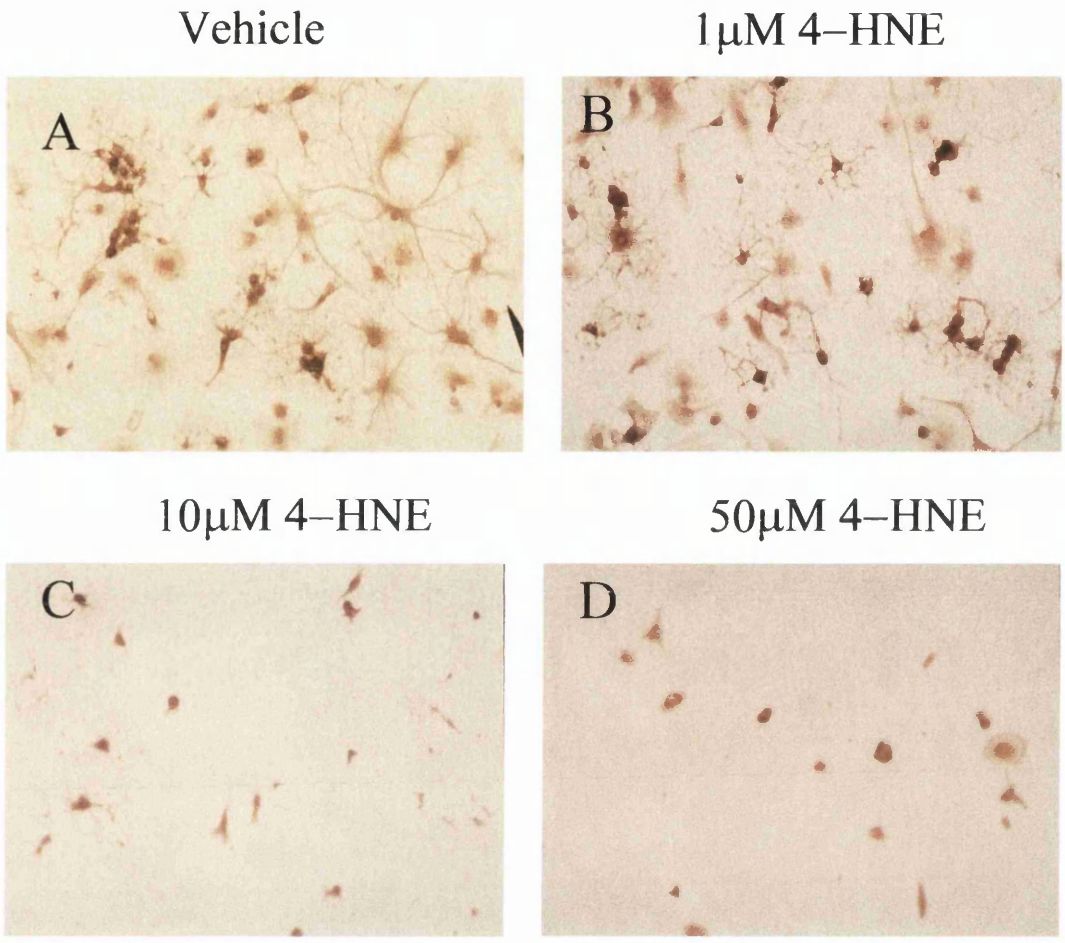

Figure 5.12 Morphological changes observed in oligodendrocyte cultures

The antibody to cytoskeletal protein spectrin detected morphological changes in oligodendrocyte cultures incubated with A) 0.2% ethanol, B) 1μM 4-HNE, C) 10μM 4-HNE and D) 50μM 4-HNE over a period of 4 hours. X200 Magnification.

5.4.3 Immunohistochemistry following permanent focal cerebral ischaemia

Neuronal pathology following 24 hours of cerebral ischaemia was demonstrated using haematoxylin and eosin staining. The ischaemic damage was confined to the hemisphere where the artery had been occluded. The amount and distribution of axonal damage reflected by the accumulation of β-APP was widespread within the ischaemic lesion. Neuronal and axonal damage demonstrated characteristic patterns of pathology observed after permanent focal cerebral ischaemia in the rat. 4-HNE-Micheal adducts were evident in neuronal perikarya, axons and glial cells within the infarcted region. The distribution of 4-HNE immunopositive axons (Figure 5.13B) in the ischaemic hemisphere was identical to that of β-APP accumulation in axons observed in adjacent sections (Figure 5.13A). 4-HNE immunoreactive neurons marked a defined boundary between ischaemic and normal tissue in the cortex (Figure 5.13C). There was no 4-HNE-Michael adducts or β-APP immunoreactivity present in the contralateral hemisphere.

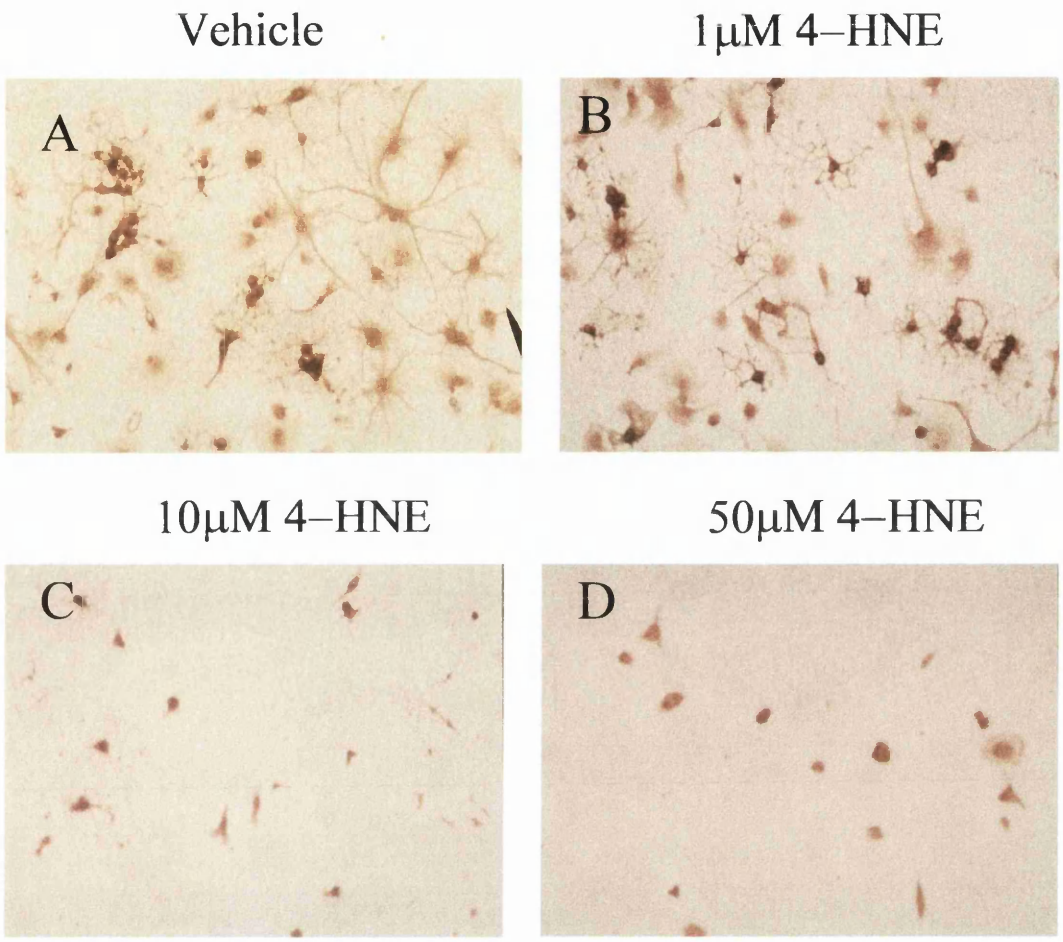

Figure 5.12 Morphological changes observed in oligodendrocyte cultures

The antibody to cytoskeletal protein spectrin detected morphological changes in oligodendrocyte cultures incubated with A) 0.2% ethanol, B) 1μM 4-HNE, C) 10μM 4-HNE and D) 50μM 4-HNE over a period of 4 hours. X200 Magnification.

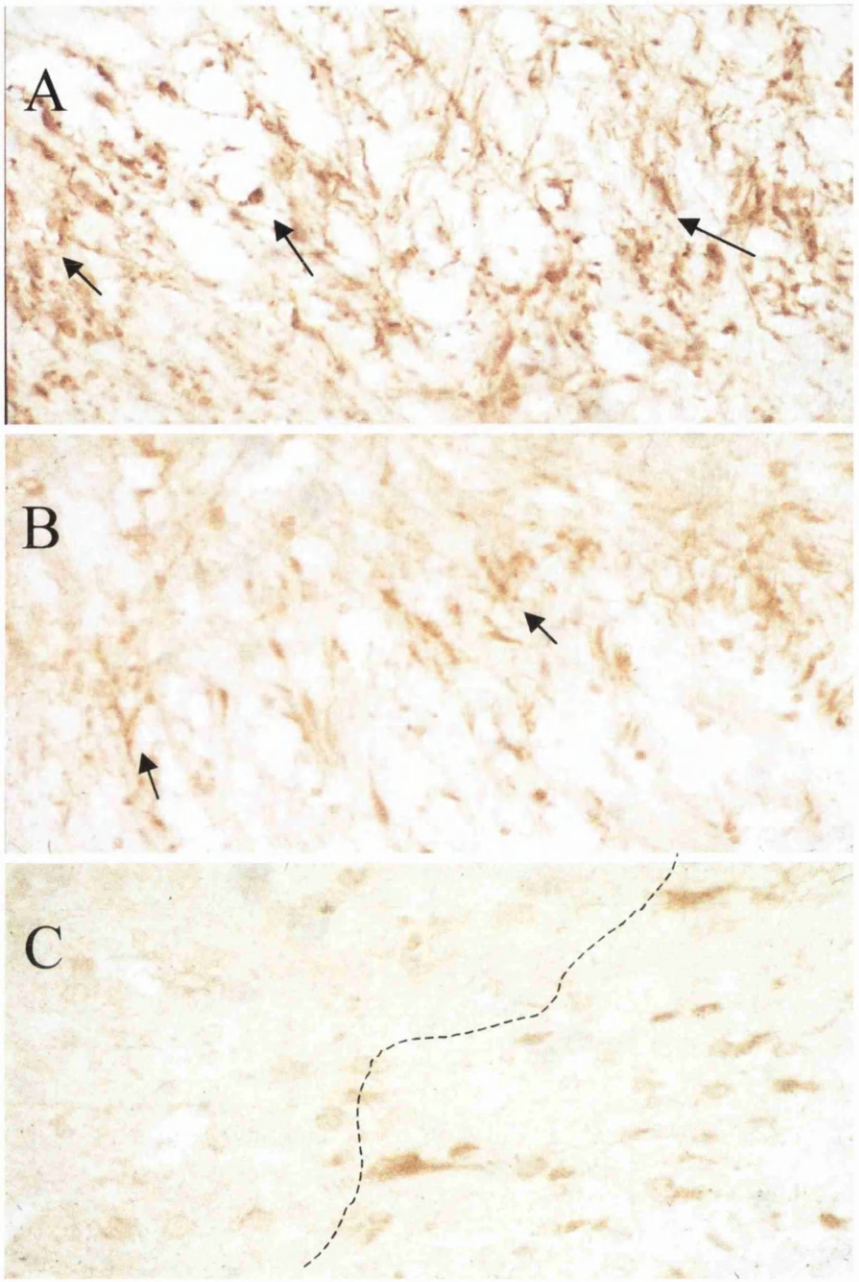

Figure 5.13 Immunostaining of 4-HNE-Michael adducts and β-APP accumulation following 24 hours permanent focal cerebral ischaemia

A) β-APP accumulation in axons within the ischaemic lesion B) 4-HNE-Michael adducts immunoreactivity in myelinated axons and C) cerebral cortex. 4-HNE-Micheal adducts paralleled the pattern of β-APP accumulation in axons. In the cerebral cortex 4-HNE immunopositive neurons marked a clear boundary (dotted line) tissue showing evidence of ischaemic damage and that with a normal appearance. X400 Magnification.

5.5 DISCUSSION

Intracerebral injection of 4-HNE caused extensive cellular and axonal damage within the subcortical white matter in vivo. A previous study induced neuronal perikaryal damage following injection of a 10 fold higher concentration of 4-HNE into the basal forebrain (Bruce-Keller et al,. 1998). However, in the present study, a 10 fold lower concentration of 4-HNE injected into the subcortical white matter caused damage to both neuronal perikaryal and myelinated axons. Axonal damage, detected by the β-APP accumulation, was observed transversing medially and laterally along the subcortical white matter away from the injection site. Within the core of the lesion, β-APP accumulation was intense across the depth of the subcortical white matter and immunopositive swellings and bulbs were also evident in the subcortical white matter in the contralateral hemisphere to the injection site. In contrast, in the ethanol- or aCSF-treated animals there were relatively minor pathological changes within axons and these were restricted to an area immediate to the injection site. Shrunken neuronal perikarya, detected by conventional histology, in the adjacent grey matter were present in all animals from the 4-HNE ethanol and aCSF treated groups. However, neuronal damage extended further away from the injection site in the 4-HNE treated group whereas it was confined to a small region around the needle tract in the ethanol and aCSF treated groups. It has been suggested that 4-HNE causes damage to neuronal perikarya by binding to microtubules, microtubule associated proteins and neurofilaments (Montine et al., 1996a; Mattson et al., 1997; Neely et al., 1999). In axons these proteins are essential for both structural stability and transportation mechanisms. Therefore, in axons 4-HNE induced injury may also be mediated by damage to these cytoskeletal proteins. Conformational changes in β-tubulin located in synaptosomes were induced by exposure to 4-HNE (Subramaniam et al., 1997) and β-tubulin is an essential component of microtubules which are responsible for axonal transport. Thus, conformational changes in axonal β-tubulin by 4-HNE may cause cessation of axonal transport which is reflected by the accumulation of β-APP. In patients who died after a head injury there was accumulation of β-APP in axons, however there was no change in the protein levels of β-tubulin compared to control patients (see Chapter III). Although, at present it is not known if 4-HNE levels are increased in the human brain after head injury, it might be speculated that 4-HNE induced damage of β-tubulin is involved in the process of axonal damage.

Following intracerebral injection of 4-HNE preserved neuronal perikarya were present in grey matter overlying the subcortical white matter in which there was β-APP immunoreactive axons. This suggests that pathological changes in the myelinated axons are independent of neuronal cell body damage. The extent of white matter pathology in the 4-HNE treated animals compared to controls could be due to the exogenously administered 4-HNE initiating a process of reactive changes within axons. 4-HNE itself, could initiate lipid peroxidation and the large quantity of lipids within myelinated axons could increase their susceptibility to this self propagating process. This process could account for the spread of axonal pathology observed away from the initial injection site.

4-HNE-Michael adducts were detected in neuronal and glial cells but not in axons following intracerebral injection of 4-HNE and this immunostaining was restricted to a small area around the injection site. In the ethanol treated group a similar pattern of immunostaining was observed to that seen in the 4-HNE treated group. In contrast, in the aCSF treated animals there was no 4-HNE immunostaining in the subcortical white matter and only a few 4-HNE immunopositive neuronal perikarya were observed adjacent to the needle tract in the cortex. β-APP accumulation within myelinated axons was observed distant from the injection site although there were no 4-HNE-Michael adducts present in the same region. However, this does not necessarily mean that the toxic properties of 4-HNE were not involved in the production of axonal pathology. Exogenous 4-HNE may initiate secondary mechanisms of damage and these are discussed further below. 4-HNE can form either Michael or pyrolle adducts and the antibodies used in the present study detect only the former one. A comparative study in Alzheimer's disease brain tissue demonstrated that antibodies against 4-HNE Michael or pyrolle adducts have distinct patterns of immunoreactivity (Montine et al., 1998). In the present study, the presence of pyrolle adducts was not determined and it is possible that these also exist after intracerebral injection of 4-HNE. This may explain the disparity between the extent of 4-HNE-Michael adducts immunoreactivity and that of axonal pathology.

Secondary pathologic mechanisms may be induced by exogenously injected 4-HNE initiating elevation of intracellular Ca^{2+} and subsequent activation of calpains. 4-HNE inhibits the $Na^{+}K^{+}$-ATPase transporter by either reducing ATP, via mitochondrial

dysfunction (Keller et al, 1997; Picklo et al., 1999), or by directly binding to the ionic transporter (Siems et al., 1996; Mark et al., 1997). Inhibition of the Na^+K^+ATPase transporter could cause disturbances of Ca^{2+} homeostasis and increases of intracellular Ca^{2+} levels. Calpain-mediated spectrin breakdown products were present in grey matter adjacent to the injection site in all the 4-HNE- ethanol- and aCSF-treated groups. This immunoreactivity appeared as a diffuse staining localised mainly in the neuropil. However, calpain-mediated spectrin breakdown products were present in neuronal cells only in the 4-HNE treated group but not in controls. There was no evidence of calpain-mediated spectrin breakdown products within myelinated axons in any of the treated groups. Calpain immunopositive oligodendrocyte-like cells were present in the 4-HNE treated group but these cells were also present in the ethanol and aCSF treated group. Therefore, these findings do not support a role for calpain-mediated damage as a secondary pathogenic mechanism in white matter after intracerebral injection of 4-HNE.

Histological and immunohistochemical analysis of the tissue following 4-HNE injection readily detected pathological changes in neurons and axons. However, these methods did not reveal marked changes in oligodendrocytes, which may have indicated a direct toxic effect of 4-HNE on these cells. In addition, damage to white matter oligodendrocytes could be secondary to changes in their microenvironment resulting from damage to adjacent axons or astrocytes. Oligodendrocyte vulnerability secondary to changes in the microenvironment has been proposed to be predominately due to alterations in astrocytic function. 4-HNE crosslinks to the GLT 1 glutamate uptake transporter (Springer et al., 1997; Keller et al., 1997; Blanc et al., 1998) and inhibition of this transporter could render adjacent cells vulnerable to excitotoxicity. Li et al., 1999 have demonstrated in a model of spinal cord injury and *in vitro* anoxia that there was an efflux in glutamate from axonal cylinders and possibly oligodendrocytes. The rise in extracellular glutamate probably occurs as a result of membrane depolarisation and reversal of the Na^+-dependent glutamate transporter. Therefore, excess glutamate into restricted spaces could damage axons and oligodendrocytes. Oligodendrocytes are extremely vulnerable to glutamate toxicity via AMPA (α-amino-3-hydroxy-5-methyl-4-isoxate propionic acid) or kainate receptors (McDonald et al., 1998). Cell culture was used in the present study to provide an isolated situation to assess whether 4-HNE had a direct effect on oligodendrocytes rather than secondary induced mechanisms involving

axons and other glial cells. Exogenous 4-HNE was also toxic to oligodendrocytes in culture *in vitro*. Oligodendrocyte cell death was both time and concentration dependent with maximum cell death following 4 hours exposure to the highest concentration, 50μM 4-HNE. At the lowest concentration there was evidence of oligodendrocyte cell death after 1 hour exposure to 1μM 4-HNE. The percentage of oligodendrocyte cell death after treatment with 10 or 50μM 4-HNE also increased with incubation time.

Morphological alterations of these cells were detected by changes in immunohistochemistry of the cytoskeletal protein, spectrin. After treatment with either vehicle (0.2% ethanol) or 1μM 4-HNE, oligodendrocyte perikarya were preserved and processes emanating from the cell body were clearly evident. After exposure to 10 or 50μM 4-HNE, oligodendrocyte cell bodies were shrunken and their processes were fragmented. This study demonstrates that 4-HNE has a direct toxic effect on oligodendrocytes. Taken together the *in vivo* and *in vitro* data indicate that exogenously administered 4-HNE is toxic to both axons and oligodendrocytes. However, if this toxin by-product is to be implicated as a pathogenic factor in acute brain injury, it is necessary to demonstrate that the levels of endogenous 4-HNE are elevated in response to acute brain injury.

To address this issue the presence or absence of 4-HNE-Michael adducts were determined in an experimental model of acute brain injury, permanent focal cerebral ischaemia in the rat. Conventional histology revealed pyknotic neurons and morphological characteristics of ischaemic brain damage in the cortex and striatum of the cerebral hemisphere where the middle cerebral artery had been occluded. Endogenous 4-HNE detected by immunohistochemistry was present in neurons, axons and glia cells within the area of ischaemic damage. 4-HNE-Michael adducts were present in necrotic neurons particularly at the boundary between ischaemic and normal tissue in the cerebral cortex. There was widespread axonal injury within the ischaemic striatum detected by β-APP accumulation. 4-HNE-Michael adducts revealed immunostaining within ischaemic axons and the staining pattern paralleled the pattern of axonal β-APP accumulation. 4-HNE modified proteins were demonstrated in experimental traumatic brain injury (Zhang et al., 1999), a model of transient cerebral ischaemia in rats (Urabe et al., 1998) and global ischaemia in apolipoprotein E (apoE)

knockout mice. In this latter model, intraventricular infusion of apoE reduced both ischaemic neuronal and 4-HNE immunoreactivity (Horsburgh et al,. unpublished data). ApoE has been proposed as an antioxidant (Miyata and Smith 1996). This data suggests that there is an interaction between endogenous 4-HNE and oxidative stress. Oxidative stress and 4-HNE have been implicated as a major factor involved in the pathogenesis of the chronic neurodegenerative condition, Alzheimer's disease (Montine et al.,1997a; Montine et al., 1997b; Lovell et al., 1997; see review Mattson and Pedersen 1998). Therefore, 4-HNE toxicity may play a role in both acute and chronic degenerative conditions.

In summary, exogenous 4-HNE was toxic to both axons and neurons *in vivo* and to oligodendrocytes in culture *in vitro*. In addition, endogenous levels of 4-HNE were increased in axons, neurons and glia after acute brain injury induced by ischaemia. Therefore, the results suggest that 4-HNE induced damage may constitute a common pathologic mechanism in both grey and white matter following acute brain injury.

CHAPTERVI
GENERAL DISCUSSION

6.1 GENERAL DISCUSSION

6.1.1 Pathogenic mechanisms in white matter

The data produced within this thesis provide substantial evidence to support the hypothesis that myelinated axons and oligodendrocytes, components of white matter, are susceptible to multiple pathogenic mechanisms following acute brain injury. These include calpain-mediated breakdown of the cytoskeleton, oxidative stress and lipid peroxidation.

In human head injury there was degradation of axonal cytoskeletal proteins and evidence of calpain activation in the corpus callosum, a white matter commissure, where axonal damage is frequently observed following head injury (Adams et al., 1989; McKenzie et al., 1996). Although, there is evidence suggesting a role for calpain-mediated damage in experimental models of traumatic brain injury (TBI) the results from this study demonstrate that calpain-mediated proteolysis has a direct role in producing axonal damage in the clinical condition. Axonal damage was present in patients with the characteristic pathology of diffuse axonal injury (DAI) or ischaemia. This suggets that blunt head injury could prompt different pathogenic mechanisms that are involved in axonal damage.

Axonal injury was produced following systemic injection of the mitochondrial inhibitor, 3-nitropropionic acid in the rat. There was a concentration dependent increase in the amount and distribution of axonal pathology. The correlation between β-APP accumulation and calpain-mediated spectrin breakdown products in head-injured patients was not present in this experimental animal model. Calpain-mediated proteolysis only detected cytoskeletal changes in oligodendrocyte-like cells within the subcortical white matter. Increased Mn-SOD immunoreactivity within the striatum supports a role for oxidative stress mediating axonal injury. However, this experimental model of oxidative stress could increase the amount of calpain activation via increased intracellular calcium (Dykens 1994; Desphande et al., 1997; Silver and Ercinska 1990). Calpain activation stimulates production of free radicals through irreversible conversion of xanthine dehydrogenase to xanthine oxidase (Fridovich 1970; McCord 1985;

Sussman and Bulky 1990). This suggests that at least two pathogenic mechanisms could be working alone or in alliance mediating damage in axons and oligodendrocytes.

Intracerebral injection of the lipid peroxidation cytotoxic by-product, 4-HNE into the subcortical white matter of rats produced damage in myelinated axons. The distribution of axonal pathology did not appear to be associated with endogenous 4-HNE or calpain-mediated damage. Thus, suggesting that exogenous 4-HNE could be inducing secondary pathogenic mechanisms other than lipid peroxidation or calpains that are responsible for axonal damage observed away from the injection site. Cytoskeletal protein changes and cell death were observed in cultured oligodendrocytes after administration of exogenous 4-HNE. To investigate if 4-HNE induced oligodendrocyte cell death was coupled to calpain activation, an experimental paradigm could be devised which would determine the protein levels of calpain-mediated spectrin breakdown products in oligodendrocyte cultures by means of Western blotting. Endogenous 4-HNE modifed proteins were present within damaged axons and glia cells after permanent cerebral ischaemia in the rat. The results in these studies demonstrate that axons and oligodendrocytes are vulnerable to the pathogenic mechanisms calpains, oxidative stress and lipid peroxidation.

In the past white matter damage was thought to be secondary to neuronal necrosis after cerebral ischaemia (Marcoux et al., 1982). Axonal and oligodendrocyte damage was observed within 1 hour following cerebral ischaemia preceding neuronal necrosis (Yam et al.,1998b; Pantoni et al., 1996). DAI is a primary pathological occurrence observed after head injury. It was once perceived that DAI occurred as a result of the initial traumatic injury (Povlishock and Christman 1995; Gennarelli 1997). However, it is now recognised that many axons undergo secondary delayed damage. (Graham and Gennarelli 1997; Maxwell et al., 1997). However, the data from this thesis highlights the vulnerability of axons and oligodendrocytes to secondary pathogenic mechanisms that could be triggered after acute brain injury. The axonal cytoarchitecture provides a pathway for transportation of protein organelles along the axon. Damage to these cytoskeletal proteins could result in disruption of the unique structural arrangement and cessation of axonal transport. Although this thesis has focused on white matter injury it is important not to forget the rest of the neuron. Perikaryal damage along side a

protected axon could still lead to brain dysfunction as the cell body is the source of protein synthesis.

The experimental animal model of oxidative stress used in this thesis demonstrated neuronal perikaryal damage within the striatum. The amount and distribution of neuronal damage was not present in any of the 3-NPA concentrations before accumulation of β-APP or SNAP-25 was observed. Although this model does not distinguish between neurons and axons it does suggest that axonal injury could be independent of neuronal damage. To decipher whether axons themselves were vulnerable to this toxin, 3-NPA could be injected into the subcortical white matter and the extent of axonal damage measured by the same endpoints as was used in Chapter V. Following intracerebral injection, damaged perikarya were observed in the adjacent grey matter next to the injection site. The amount of neuronal damage was greater in the 4-HNE-treated compared to the control groups. This data demonstrates that both neurons and axons are vulnerable to pathogenic mediators, whether these are primary or secondary mechanisms, it does provide a link between grey and white matter damage.

6.1.2 Common pathological mechanisms in grey and white matter

There is compelling evidence supporting a role for calpain-mediated damage in grey matter in experimental animal models of stroke and TBI. The breakdown of cytoskeletal proteins and increased calpain-mediated spectrin breakdown products in grey matter have been demonstrated in models of traumatic (Posmantur et al., 1994; Kampfl et al., 1996; Saatman et al., 1996; Fitzpatrick et al., 1997) and ischaemic (Inzuka et al, 1990; Hong et al., 1994; Roberts-Lewis et al.,1994; Bartus et al., 1995; Pettigrew et al., 1996) brain injury. However, in the literature there is not as much evidence for cytoskeletal breakdown with concomitant increase in calpain-mediated proteolysis in white matter after traumatic (Saatman et al., 1996a; Fitzpatrick et al., 1997) or ischaemic (Dewar and Dawson 1996) brain injury compared to grey matter. Damage to neuronal perikarya and axons after acute brain injury are likely to contribute to behavioural dysfunction after acute brain injury. Calpain inhibitors have been reported as potential therapeutic agents for treatment of acute brain injury. In models of experimental TBI administration of calpain inhibitors attenuated cytoskeletal breakdown and calpain-mediated spectrin breakdown products (Saatman et al., 1996b;

Posmantur et al., 1997). The amount of ischaemic damage can be reduced by a calpain inhibitor (Takagaki et al., 1997) even when administration is delayed for up to six hours after induction of ischaemia (Markgraf et al., 1998). Banik et al., (1997b) demonstrated protection of the myelinated fibre tracts after spinal cord injury. Combination therapy, where a calpain I inhibitor and methylprednisolone, (an anti–inflammatory and free radical inhibitor), prevented neurofilament breakdown in the spinal cord (Banik et al., 1998). Therefore, suggesting that calpain inhibition could prove successful in protecting the neuronal perikarya and the axonal cytoskeleton after acute brain injury.

The axonal cytoskeleton is vulnerable to oxidative stress detected by the accumulation of the axonal transport proteins β-APP and SNAP-25 following systemic injection of 3-NPA. Oxidative stress has been implicated as a major pathogenic factor in neuronal perikaryal damage (see reviews Flamm et al., 1978; Chan 1994; Doopenberg et al., 1998; Murphy et al., 1999; Love 1999). Thus representing another common mechanism between grey and white matter damage. The introduction of transgenic mice has led to a great deal of research investigating the role of endogenous antioxidants. The size of infarction was increased in Mn-SOD knockout mice (Murakami et al., 1998) while Cu/Zn SOD knockout mice demonstrated enhanced neuronal perikaryal and axonal damage (Reaume et al,. 1996) compared to their wildtypes, further supporting a role for oxidative stress as a pathogenic link between grey and white matter. Transgenic mice can also be used to investigate the role of neuroprotection. Mice overexpressing the cytosolic Cu/Zn SOD enzyme demonstrated a reduction in infarct volume in models of reperfusion and experimental TBI (Kinouchi et al., 1991; Yang et al., 1994; Mikawa et al, 1996) but not following permanent ischaemia (Chan 1993). Therefore accumulation of free radicals, which occurs after acute brain injury and the relative paucity of endogenous antioxidants in the brain (Coyle and Puttfarcken 1993) could contribute to the neuronal and axonal damage. The failure of overexpressed Cu/Zn SOD mice to protect against neuronal damage following permanent cerebral ischaemia suggests that different mechanisms could be involved depending on the type of insult. Although these animal studies look encouraging, antioxidants are hydrophilic and cannot cross the blood brain barrier (BBB). In a previous study, addition of vitamin E failed to protect against global ischaemia (Clemens and Panetta 1994). However, the addition of a lipophilic triphyenlphosphonium cation, allowed the compound to cross the BBB and

increase the half life of the enzyme. Entry of this compound into the mitochondria induced an 80 fold increase in the pool of antioxidants available (Smith et al., 1999). The lipophilic polyethylene glycol conjugated to SOD increased functional outcome in head-injured patients (Muizellar et al., 1993). Increase SOD activity leads to elevated tissue levels of hydrogen peroxide. If there is not a compensatory increase in catalase or glutathione peroxidase (GPx) then hydrogen peroxide will be converted to the potent hydroxyl radical which can initiate a continuous cascade of oxidative stress.

Tirilazad mesylate, a 21 aminosteroid compound is member of the antioxidant family, the Lazeroids. Tirilazad is lipid soluble and inhibits lipid peroxidation (Braughler et al., 1989b). However, at concentrations administrated during a phase II clinical trial the drug appeared to be unsafe (Marshall and Marshall 1995). A lipid peroxidation inhibitor pyrrolopyrindine U101033E, penetrates the BBB restoring function in the electron transport chain, energy coupling and ion homeostasis after trauma (Xiong et al., 1997) and reduced infarct volume after cerebral ischaemia (Oostveen et al., 1998). This type of therapeutic agent could also be beneficial following acute brain injury as it prevents pathogenic mediators that have been shown to induce neuronal perikarya and axonal damage. Combinational therapy of a Lazaroid and pyrrolopyrimdine reduced total infarct volume by over 50% (Schmid-Elsasser et al., 1999). This result also suggests that more than one mechanism could be involved in the pathogenesis of brain injury as the results in this thesis have demonstrated.

The spin trap agent, PBN (α-phenyl-tert-butyl-nitrone) reacts with free radicals resulting in the formation of the stable nitroxide radical adducts. PBN has been previously demonstrated to reduce neuronal damage following permanent cerebral ischaemia (Cao and Phillis 1994). Increased immunoreactivity of the cytoskeletal protein tau was present in oligodendrocytes after human head injury and stroke (Irving 1996). PBN administration reduced these tau positive oligodendrocytes after permanent ischaemia in the rat at the same concentration that reduced neuronal damage (Irving et al., 1997). In contrast, administration of the NMDA antagonist and the AMPA antagonist, NBQX (2,3-dihydroxy-6-nitro7-sulfamylbenzo(f)quinoxaline) at concentrations known to be neuroprotective failed to reduce the number of tau positive

oligodendrocytes. The interaction of glutamate as a secondary mechanism will be discussed below.

Ebselen (2-phenyl-1-2-benzioselenazol-3-2H(ene)) acts as a glutathione peroxidase (GPx) mimic reducing hydrogen peroxide to water; detoxifying lipid hydroperoxides; preventing arachadonic acid metabolism and inducing anti-inflammatory responses (Schewe 1995). Ebselen administration reduced total infarct volume in animal models of transient (Dawson et al., 1995) and permanent cerebral ischaemia (Takasgo et al., 1997). Phase III clinical trials showed efficacy and safety of the drug (Yamaguchi et al., 1998). This type of therapeutic agent could be beneficial in the treatment of acute brain injury as it scavanges elements of oxidative stress, lipid peroxidation and inflammation.

The data produced in this thesis demonstrated that there is a differential response between axons and oligodendrocytes to different pathogenic mechanisms. The literature also demonstrates that neuronal damage following acute brain injury can be reduced by a number of therapeutic agents targeting different pathologic mediators. The pathophysiology of acute brain injury is probably more multifaceted than previously thought. The main theme of this thesis has concentrated on white matter damage induced by non-receptor mediated mechanisms. However, the excitotoxin glutamate cannot be eliminated when discussing pathogenic factors in acute brain injury. Glutamate excitotoxicity is an important trigger in the pathogenesis of neuronal perikaryal death (Rothman and Olney 1986; Choi 1988). Although myelinated axons and oligodendrocytes do not possess NMDA receptors, AMPA and kainate receptors are located on oligodendrocytes (Patneau et al.,1994; Gallo and Russell 1995). Recently, it has been demonstrated that AMPA or kaniate receptor activation could mediate damage in axons after ischaemia and anoxia (Agrawal and Fehlings 1997; Li et al., 1999). The importance of glutamate induced toxicity is not just receptor activation but the biochemical cascade that it could initiate. Glutamate can induce oxidative stress in oligodendrocytes by depleting the glutamate-cysteine exchanger (Oka et al., 1993) or through mitochondrial inhibition (Lafon-Cazal et al., 1993; Dugan et al., 1993). Glutamate can also directly damage oligodendrocytes by binding to AMPA or kainate receptors (McDonald et al.,1998a 1998b). Oxidative stress can also increase extracellular glutamate through the lipid peroxidation aldeyhde, 4-HNE which binds to the GLT 1 transporter on astrocytes (Springer et al., 1997; Keller et al.,1997; Blanc et

al.,1998). Calcium also works in an interactive process with glutamate. Firstly, through membrane depolarisation induces rapid Ca^{2+} influx and glutamate neurotransmitter release and from terminal synapses. Secondly, continuous activation of the NMDA receptor allows leakage of Ca^{2+} into the cell (see review Kristian et al., 1998). This evidence demonstrates the importance of glutamate and its ability to either directly cause white matter damage or through induction of secondary mechanisms that have been shown to cause axonal damage.

In summary, the hypothesised biochemical cascade between metabolic dysfunction, oxidative stress, lipid peroxidation, calcium and glutamate could all contribute to damage in neuronal perikaryal, myelinated axons and glial cells (Figure 6.1). The brain is a complex organ that has multiple neuronal-axonal; neuronal-glia; axonal-glia and glia-glia interactions that may all depend on each other. The complex interaction between one and more of the above pathogenic mediators could account for the varied susceptibility of cellular and axonal damage observed after acute brain injury. The mechanistic pathway could depend on whether the injury is traumatic or ischaemic, primary or secondary and whether the damage is diffuse or focal, emphasising the complexity of the pathophysiology that occurs after acute brain injury. The type of damage and the pathway to that damage also depends on the surrounding microenvironment.

The hypothesis of secondary damage is a complex phenomenon. However, it could provide multiple targets for therapeutic intervention. In the past, clinical intervention was targeted towards salvaging the neuronal perikarya via a single mechanism. However, these therapeutic agents did not prove successful in clinical trials of acute brain injury (Dyker and Lees 1998). It could be speculated that these drugs did not work, as they did not protect axonal damage. Therefore, it is important to protect the whole neuron and not a specific component. Neuronal perikaryal produces cellular information, axons provide the circuitry pathway for this information and synapses allow information to be transmitted from one neuron to another. Therefore because of the combined complexity of brain anatomy and pathogenic mediators, discerning the molecular mechanism involved requires further investigation to gain a comprehensive understanding of the pathophysiology that occurs following acute brain injury.

Figure 6.1 Biochemical cascade of primary and secondary mechanisms after acute brain injury

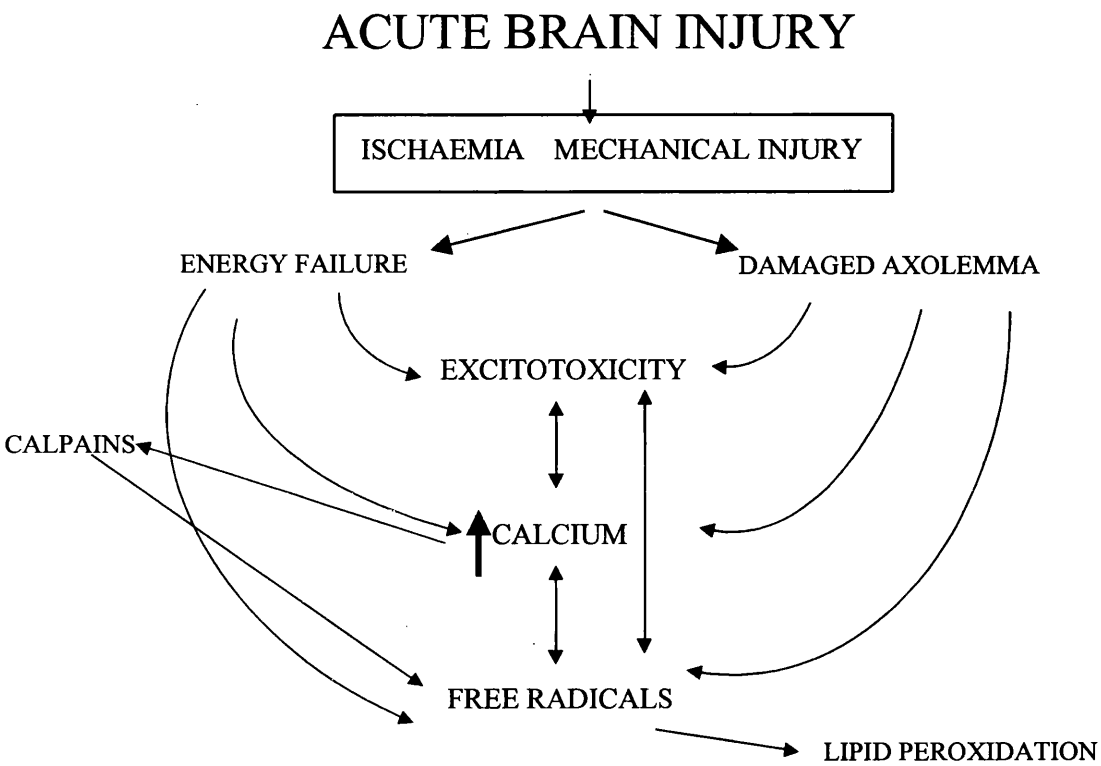

CHAPTER VII
REFERENCES

7. REFERENCES

Adams. J.H., Mitchell, D.E., Graham, D.I. & Doyle, D. (1977). Diffuse brain damage of immediate impact type. *Brain.* 100, 489-502.

Adams, J.H., Graham, D.I., Scott, G., Parker, S.L. & Doyle, D. (1980). Brain damage in fatal non-missile head injury. *Journal of Clinical Pathology.* 33, 1132-1145.

Adams, J.H., Graham, D.I., Murray, L.S., & Scott, G. (1982). Diffuse axonal injury due to non-missile head-injury in humans: an analysis of 45 cases. *Annals of Neurology.* 12, 557-563.

Adams, J.H., Doyle, D., Ford, I., Gennarelli, T.A., Graham, D.I., & McLellan, D.R. (1989). Diffuse axonal injury in head injury: definition, diagnosis and grading. *Histopathology.* 15, 49-59.

Adams, J. H. & Graham, D.I. (1989). An introduction to neuropathology. Trauma. 118-136. Churchill Livingstone.

Agrawal, S.K. & Fehlings, M.G. (1997). Role of NMDA and non-NMDA ionotropic receptors in traumatic spinal cord injury. *Journal of Neuroscience.* 17, 1055-1063.

Alexi, T., Hughes, P.E., Faull, R.L. & Williams, C.E. (1998). 3-Nitropropionic acid's lethal triplet:cooperative pathways of neurodegeneration. *Neuroreport.* 9, R57-R64.

Alston, T.A., Mela, T. & Bright, H.F. (1977). 3-nitropropionate, the toxic succinate of Indiogofera, is a suicide inactivator of succinate dehydrogenase. *Proceedings of the National Acadamy of Science. USA* 74, 3767-3771.

Bamford, J., Sandercock, P., Dennis, M., Warlow, C., Jones, L., McPherson, K., Vessey, M., Fowler, G., Molyneux, A., Hughes, T., Burn, J. & Wade, D.A. (1988). A prospective study of acute cerebrovascular disease in the community; the Oxfordshire community stroke project 1981-1986. 1. Methodology, demography, and incident of

cases of first ever stroke. Journal of Neurology, Neurosurgery and Psychiatry. 51: 1373-1780.

Banik, N.L., Matzelle, D.C., Gantt-Wilford. D, G., Osborne, A. and Hogan, E.L. (1997a). Increased calpain content and progressive degradation of neurofilament protein in spinal cord injury. *Brain Research.* 752, 301-306.

Banik, N.L., Matzelle, D., Terry, E. and Hogan, E.L. (1997b). A new mechanism of methylprednisolone and other corticosteriods action demonstrated *in vitro*: inhibition of a proteinase (calpain) prevents myelin and cytoskeletal protein degradation. *Brain Research.* 748, 205-210.

Banik, N.L., Sheilds, D.C., Ray, S., Davis, B., Matzelle, D., Wilford, G. & Hogan, E.L. (1998). Role of calpain in spinal cord injury: effects of calpain and free radical inhibitors. *Annals of New York Acadamy of Science.* 844, 131-7.

Bartus, R.T., Dean, R.L., Reginald, D.L., Cavanaugh, K., Eveleth, D., Carriero, D.L., & Lynch, G. (1995). Time-related neuronal changes following middle cerebral artery occlusion: Implications for therapeutic intervention and the role of calpain. *Journal Cerebral Blood Flow and Metabolism.* 15, 969-979.

Bartus, R.T., Dean, R.L., Mennerick, S., Eveleth, D. & Lynch, G. (1998). Temporal ordering of pathogenic events following transient global ischaemia. *Brain Research.* 790, 1-13.

Barres. B.A. & Raff, M.C. (1993). Proliferation of oligodendrocyte precursor cells depends on electrical activity in axons. *Nature.* 361, 258-260.

Bast, A., Haenen, G.R. & Doelman, C.J. (1991). Oxidants and antioxidants: state of the art. *American Journal of Medicine.* 3C. 2S-3S.

Beal, M.F., Brouillet, E., Jenkins, B.G., Ferrante, R.J., Kowall, N.W., Miller, J. M., Storey, E., Srivastava, R., Rosen,B.R. & Hyman, B.T. (1993). Neurochemical and

histological characterisation of striatal excitotoxic lesions produced by the mitochondrial toxin 3-nitropropionic acid. *Journal of Neuroscience.* 13, 4181-4191.

Beal, F.M., Ferrante, R.J., Henshaw, R., Matthews, R.T., Chan, P.H., Kowall, N.W., Epstein, C.J., & Schulx, J.B. (1995). 3-Nitropropionic acid neurotoxicity is attenuated in copper/zinc superoxide dismutase transgenic mice. *Journal of Neurochemistry.* 65, 919-922.

Beal, MF. (1998). Mitochondrial dsyfunction in neurodegenerative diseases. *Biochimica et Biophysica Acta.* 1366, 211-223.

Beckman, J.S., Beckman, T.W., Chen, J., Marshall, B.A & Freeman, B.A. (1990). Apparent hydroxyl radical production by peroxynitrite: implications for endothelial injury from nitric oxide and superoxide. *Proceedings of the National Acadamy of Sciences USA.* 87, 1620-1624.

Beckman, J.S. & Crow, J.P. (1993). Pathological implications of nitric oxide, superoxide, and peroxynitrite formation. *Biochemical Society Transactions.* 21, 330-334.

Beckman, J.S. (1994). Peroxynitrite versus hydroxyl radical: the role of nitric oxide in superoxide-dependent cerebral injury. *Annals of New York Acadamy of Sciences.* 738, 69-75.

Beckman, J.S. & Koppenol. W.H. (1996). Nitric oxide, superoxide, and peroxynitrite: the good the bad and the ugly. *American Journal of Physiology.* 271, C1424-C1437.

Binder, L.I., Frankfurter, A. & Rebhun, L.I. (1985). The distribution of tau in the mammalian central nervous system. *The Journal of Cell Biology.* 101. 1371-1378.

Binienda, Z. & Kim, C.S. (1997). Increase in levels of total free fatty acids in rat brain regions following 3-nitropropionic acid. *Neuroscience Letters.* 230, 199-201.

Binienda, Z., Simmons, C., Hussain, S., Slikker, W.Jr. & Ali, S.F. (1998). Effect of acute exposure to 3-nitropropionic acid on activities of endogenous antioxidants in the rat brain. *Neuroscience letters*. 251, 173-176.

Blanc, E.M., Keller, J.N., Fernandez, S. & Mattson, M.P. (1998). 4-Hydroxynonenal, a lipid peroxidation product, impairs glutamate transport in cortical astrocytes. *Glia.* 22, 149-160.

Blumbergs, P.C., Scott, G., Manavis, J., Wainwright, H., Simpson, D.A., & McLean, A.J. (1994). Staining of amyloid precusor protein to study axonal damage in mild head injury. *Lancet.* 344, 1055-1056.

Blumbergs, P.C., Scott, G., Manavis, J., Wainwright, H., Simpson, D.A., & McLean, A.J. (1995). Topography of axonal injury as defined by amyloid precusor protein and the sector scoring method in mild and severe closed head injury. *Journal of Neurotrauma.* 12, 565-572.

Borlongan, C.V., Koutouzis, T.K., Randall, T.S., Freeman, T.B., Cahill, D.W. & Sanberg, P.R. (1995). Systemic 3-nitropropionic acid: Behavioural deficits and striatal damage in adult rats. *Brain Research Bulletin.* 36, 549-556.

Bralet, J., Schraber, L. & Bouvier. C. (1992). Effect of acidosis and anoxia on iron delocalisation from brain homogenates. *Biochemical Pharmacology.* 43, 979-83.

Braughler, J.M. & Hall, D.E. (1989a). Central Nervous System Trauma and Stroke I: Biochemical considerations for oxygen radical formation and lipid peroxidation. *Free Radical Biology and Medicine.* 6, 289-301.

Braughler, J.M. & Hall, E. (1989b). Central Nervous System Trauma and Stroke I: Biochemical considerations for oxygen radical formation and lipid peroxidation. *Free Radical Biology and Medicine.* 6, 303-313.

Brouillet, E., Jenkins, B.G., Hyman, B.T., Ferrante, R.J., Kowall, N.W., Srivastava, R., Roy, D.S., Rosen, B.R. & Beal, M.F. (1993). Age-dependent vulnerability of the

striatum to the mitochondrial toxin 3-nitropropionic acid. *Journal of Neurochemsitry.* 60, 356-359.

Brouillet, E., Guyot, M-C., Mittoux, V., Altairac, S., Conde, F., Palfi, S. & Hantraye, P. (1998). Partial inhibition of brain succinate dehydrogenase by 3-nitropropionic acid is sufficient to initiate striatal degeneration in rat. *Journal of Neurochemistry.* 70, 794-805.

Bruce-Keller, A.J., Li, Y-J., Lovell. M.A., Kraemer, P.J., Gray, D.S., Brown, R.R., Marksberry, W.R. & Mattson, M.P. (1998). 4-hydroxynonenal, a product lipid peroxidation, damages cholinergic neurons and impairs visuospatial memory in rats. *Journal of Neuropathology and Experimental Neurology.* 57, 257-267.

Bullock , R., Butcher, S., Chen, M.H., Teasdale, G.M & McCulloch, J. (1991). Extracellular glutamate concentrations correlates with the extent of blood flow reduction after subdural haematoma. *Journal of Neurosurgery.* 72, 794-802.

Bunge, M.P., Bunge, R.P. & Pappas, G.D. (1962). Electron microscope demonstrations of connections between glia and myelin sheaths in the developing mammalian central nervous system. *Journal of Cell Biology.* 12, 448-453.

Bunge, R.P. (1968). Glial cells and the central myelin sheath. *Physiological Reviews.* 48, 197-251.

Cajal, S.R. (1913). Sobre un neuro proceder de impregnacion de la neuroglia del hombre y animales. *Trab. Lab. Invest. Biol. Univ. Madr.* 11, 219-237.

Cajal, S.R. (1916). El proceder del cro-sublimado para la coloracon de la neuroglia. *Trab. Lab. Invest. Biol. Univ. Madr.* 14, 155-162.

Cao, X. & Phillips, J.W. (1994). α-Phenyl-tert-butyl-nitrone reduces cortical infarct and edema in rats subjected to to focal ischaemia. *Brain Research.* 644, 267-272.

Castro, G.D., Stamato, C.J. & Castro, J.A. (1994). Tryosine attack by free radicals derived from catalytic decomposition of carbon tetrachloride. *Free Radical Biology and Medicine.* 16, 69-701.

Chan, P.H., Kamii, H., Yang, G., Epstein, C.J., Carslon, E. & Reola, L. (1993). Brain infarction is not reduced in SOD-1 transgenic mice after a permanent focal cerebral ischaemia. *Neuroreport.* 5, 293-296.

Chan, P.K. (1994). Oxygen radicals in focal cerebral ischaemia. *Brain Pathology.* 4, 59-65.

Choi, D.W. (1987). Ionic dependence of glutamate neurotoxicity. *Journal of Neuroscience.* 7, 369-379.

Choi, D.W., (1988). Calcium-mediated neurotoxicity:relationship to specific channel types and role in ischaemic damage. *Trends in Neurosciences.*11: 465-469.

Christman, C.W., Grady, M.S., Walker, S.A., Hollway, K.L. & Povlishock, J.T. (1994). Ultrastructural studies of diffuse axonal injury in humans. *Journal of Neurotrauma.* 11: 173-187.

Cino, M & Del Maestro, R.F. (1989). Generation of hydrogen peroxide by brain mitochondria: the effect of reoxygenation following postdecapitation ischemia. *Archives of Biochemistry and Biophysics.* 269-623-638.

Clemens, J.A. & Paretta, J.A. (1994). Neuroprotection by antioxidants in models of global and focal ischaemia. *Annals of the New York Acadamy of Sciences.* 738. 250-256.

Coles, C.J., Edmondson, D.E. & Singer, T.P. (1979). Inactivation if succinate dehydrogenase by 3-nitropropionate. *The Journal of Biological Chemistry.* 254, 5161-5167.

Comporti, M. (1985). Biology of disease lipid peroxidation and cellular damage in toxic liver injury. *Laboratory Investigation.* 53: 599-623.

Comporti, M. (1989). Three models of free radical induced cell injury. *Chemical and Biological Interactions* 72, 1-56.

Compston, A. (1993). Non-infective inflammatory, demyelinating and paraneoplastic disease of the nervous system. In: Walton, J (Ed), Brain's Diseases of the Nervous System.Oxford Univ. Press. 351-358.

Crow, J.P. & Beckman, J.S. (1996). The importance of superoxide in nitric oxide-dependent toxicity: evidence for peroxynitrite-mediated injury. *Advances in Experimental Medicine and Biology..* 387, 147-161.

Coyle, J.T. & Puttfarcken, P. (1993). Oxidative stress, glutamate, and neurodegenerative disorders. *Science.* 262, 689-695.

Darely-Usmar, V.M., Hogg, N., Leary, V.J., Wilson, M.T. & Moncada. S. (1992). The simultaneous generation of superoxide and nitric oxide can initiate lipid peroxidation in human low density lipoprotein. *Free Radical Research.* 17, 9-20.

Dawson, D.A., Graham, D.I., McCulloch, J. & Macrae. I.M. (1993). Evolution of ischaemic damage in a new model of focal cerebral ischaemia in the rat. *Journal of Cerebral Blood Flow and Metabolism.* 13, S1 S461.

Dawson, D.A., Masayasu, H., Graham, D.I. & Macrae., I.M. (1995). The neuroprotective efficacy of ebselen (a glutathione peroxidase mimic) in brain ischaemia damage induced by transient focal cerebral ischaemia in the rat. *Neuroscience letters.* 185, 65-69.

Del Rio-Hortega, P. (1921). La glia de escasa radiaciones (oligodendroglia). *Buletin de la real sociedad esponla de historia natural.* 21, 63.

Del Rio-Hortega, P. (1928). Tercera aportacion al concocimienta mortologica et interpratacion functional de la oligodendroglia. *Mem. Real. Soc. Espan Hist.* 14, 5.

Demple. B. & Amabile-Cueras, C.F. (1991). Redox redux: the control of oxidative stress responses. *Cell.* 87, 837-839.

Desphande, S.B., Fukuda, A. & Nishino, H. (1997). 3-Nitropropionic acid increases the intracellualr Ca^{2+} in cultured astrocytes by reverse operation of the Na^{+}-Ca^{2+} exchanger. *Experimetnal Neurology.* 145, 38-45.

Dewar, D & Dawson, D. (1996). Changes of cytoskeletal protein immunostaining in myelinated fibre tract after focal cerebral ischaemia in the rat. *Acta Neuropathologica.* 116, 1-7.

Dewar, D. & Dawson, D.A. (1995). Tau-protein is altered by focal cerebral-ischaemia in the rat brain - an immunohistochemical and immunoblotting study. *Brain Research.*684, 70-78.

Dewar, D., & Graham, D.I. (1996). Depletion of choline acetyltransferase activity but preservation of M1 and M2 muscarinic receptor binding sites in temporal cortex following head injury: a preliminary human post-mortem study. *Journal Neurotrauma.* 13, 181-187.

Dietrich, D.W., Kraydieh, S., Prado, R & Stagliano, N.E. (1998). White matter alterations following thromboembolic stroke: a β-amyloid precusor protein immunocytochemical study in rats. Acta Neuropathologica. 95: 524-531.

Dixon, C.E., Clifton, G.L., Lighthall, J.W., Yaghmai, A.A. & Hayes, R.L. (1991). A controlled cortical impact model of traumatic brain injury. *Journal of Neuroscience Methods.* 39, 253-262.

Dugan, L.L., Sevisi, S.L.,Canzoniero, L.M., Handran, S.D., Rothman, S.M., Goldberg, M.P. & Choi, D.W. (1995). Mitochondria production of reactive oxygen species in cortical neurons following exposure to N-methyl-D-asparate. *Journal of Neuroscience.* 15, 6377-6388.

Dykens, J.A. (1994). Isolated and cerebellar mitochondria produce free radicals when exposed to elevated Ca^{2+} and Na^{+}: implications for neurodegeneration. *Journal of Neurochemistry.* 63, 584-91.

Doopenberg, E.M., Rice, M.R., Di, X., Young, H.F., Woodward, J.J. & Bullock, R. (1998). Increased in free radical production due to subdural haematoma in the rat: Effect of increased oxygen fraction. *Journal of Neurotrauma.* 15, 337-347.

Dyker, A.G. & Lees, K.R. (1998). Duration of neuroprotective treatment for ischaemic stroke. *Stroke.* 29, 535-542.

Espinosa de los Monteros, A., Zhang, M. & de Vellis, J. (1993). O2A progenitor cells transplanted into neonatal rat brain develop into oligodendrocytes but not astrocytes. *Proceedings of the National Acadamy of Science. USA.* 90, 50-54.

Esterbauer, H., Schaur, R.J. & Zollner, H. (1991). Chemistry and biochemistry of 4-hydroxynonenal, malonaldehyde and related aldehydes. *Free Radical Biology and Medicine.* 11, 81-128.

Fern, R., Ransom, B.R. and Waxman, S.G. (1994). Ca^{2+}-mediated injury in anoxic white matter: autoprotective mechanisms and therapeutic strategies. (Kriegistein, J. Oberpricher-Schwenk, H. eds). *Pharmacology of cerebral ischaemia.* 31-54.

Fern , R., Ransom, B.R., Waxman, B.R. (1995). Voltage-gated calcium channels in the CNS white matter: role in anoxic injury. *Journal of Neurophysiology.* 74, 369-377.

Fineman, I., Hovda, D.A., Smith, M., Yoshino, Y, & Becker, D.P. (1993) Concussive brain injury is associated with a prolonged accumulation of calcium: a ^{45}Ca autoradiographic study. *Brain Research.* 624: 94-102.

Flamm, E.S., Demopoulos, H.B., Seligman, M.L., Poser, R.G. & Ransohoff. J. (1978). Free radicals in cerebral ischaemia. *Stroke.* 9, 445- 447.

Forbes, J.F. (1993). Cost of Stroke. *Scottish Medical Journal.* 38, S4-5.

Fukuyama, N., Takizawa, S., Ishida, H., Hoshiai, K., Shinohara Y. & Nakazawa, H. (1998). Peroxynitrite formation in focal cerebral ischemia-reperfusion in rats occurs predominately in the peri-infarct region. *Journal of Cerebral Blood Flow and Metabolism.* 18, 123-129.

Fitzpatirck, M.O., Maxwell, W., McCracken, E., Graham, D.I & Dewar, D. (1997). Cytoskeletal disruption in white matter underlying acute subdural haematoma. *Journal of Cerebral Blood Flow and Metabolism.* Suppl 1 17: S415.

Friguet, B., Stadtman, E.R. & Szweda, L.I. (1994). Modification of glucose-6-phosphate dehydrogenase by 4-hydroxy-2-nonenal. *Journal of biological Chemistry.* 269, 21639-21643.

Fridovoch, I. (1970). Quantitative aspects of the production of superoxide anion radical by milk xanthine oxidase. *Journal of Biological Chemistry.* 245, 4053-4057.

Fullerton, H.J., Ditelberg, J.S., Chen, S.F., Sarco, D.P., Epstein, C.J. & Ferriero, D.M. (1998). Copper/Zinc superoxide dismutase transgenic brain accumulates hydrogen peroxide after perinatal ischemia. *Annals of Neurology.* 44, 357-64.

Fu, T-Y., He, F-S., Zhang, S-L. & Zhang, J-S. (1995). Lipid peroxidation in rats intoxicated with 3-nitropionic acid. *Toxicon.* 33, 327-3331.

Gallo, V. & Russell, J.T. (1995). Excitatory amino acid receptors in glia: different subtypes for distinct functions? *Journal of Neuroscience Research.* 42, 1-8.

Geddes, J.W., Pang, Z., Tekirian, T. & Siman, R.G. (1994). Alterations in the neuronal cytoskeleton following *in vivo* administration of a metabolic inhibitor 3-nitropropionic acid. *Neurobiology and Aging.* S25

Geddes, J.W., Pang, Z. & Wiley, D.H. (1996). Hippocampal damage and cytoskeletal disruption resulting from impaired energy metabolism. Implications for Alzheimer disease. *Molecular Chemistry Neuropathology.* 28, 65-74.

Gennarelli, T.A., Thibault, L.E., Adams, J.H., Graham, D.I., Thompson, C.J. & Marcinncin, R.P. (1982). Diffuse axonal injury and traumatic coma in primate. *Annals of Neurology.* 12, 564-574.

Gennarelli, T.A., Thibault, L.E., Tipperman, R (1989). Axonal injury in the optic nerve: a model of simulating diffuse axonal injury in man. *Journal of Neurosurgery.* 71, 244-253.

Gennarelli, T.A. (1997). The pathobiology of traumatic brain injury. *The Neuroscientist.* 3, 73-81.

Genazzani, A.A., Empsom, R.M. & Galione, A. (1996). Unique inactivation properties of NAADP-senstive Ca2+ release. *Journal of Biological Chemistry.* 271, 11599-11602.

Gentleman, S.M., Nash M.J., Sweeting, G C.J., Graham, D.I., and Roberts, G.W. (1993). β-Amyloid precursor protein (β-APP) as a marker for axonal injury after head injury. *Neuroscience Letters.* 160, 139-144.

Gentleman, S.M., Roberts, G.W., Gennarelli, T.A., Maxwell, W.L., Adams, J.H., Kerr, S. and Graham, D.I. (1995). Axonal Injury: A universal consequence of fatal closed head injury? *Acta Neuropathologica.* 89: 537-543.

Goldman, J.E. (1992). Regulation of oligodendrocyte differentiation. *Trends in Neurosciences.* 15, 359-362.

Goldstein, M.E., Sternberger, N.H. & Sternberger, L.A., (1987). Phosphorylation protects neurofilaments against proteolysis. *Journal of Neuroimmunology.* 14, 149-160.

Goodman, S.R. & Zagon, I.S (1986). The neural cell spectrin skeleton: a review, invited review. *American Journal of Physiology Society.* C347-C360.

Goodman, Y., Bruce, A.J., Cheng, B. & Mattson, M.P. (1996). Estrogens attenuate and corticosterone exacerbates exitotoxicity, oxidative injury and amyloid β-peptide toxicity in hippocampal neurons. *Journal of Neurochemistry.* 66, 1836-1844.

Goss, J. R., Taffe, K.M., Kochanek, P.M. & DeKosky, S.T. (1997). The antioxidant enzymes glutathione peroxidase and catalase increase following traumatic brain injury in the rat. *Experimental Neurology.* 146, 291-294.

Grady, M.S., McLaughlin, M.R., Christman, C.W., Valadaka, A.B., Finger, C.L., & Povlishock, J.T., (1993). The use of antibodies against neurofilament subunits for the detection of diffuse axonal injury in humans. *Journal of Neuropathology and Experimental Neurology.* 52, 143-152.

Graham, D.I., Adams, H.J. & Doyle, D. (1978). Ischaemic brain damage in fatal non-missile head injuries. *Journal of the Neurological Sciences.* 39, 213-234.

Graham, D.I., Ford, I., Adams, J.H., Doyle, D., Teasdale, G.M., Lawrence, A.E. & McLellan, D.R. (1989). Ischaemic damage is still common in fatal non-missile head-injury. *Journal of Neurology, Neurosurgery and Psychiatry.* 52, 346-350.

Graham, D.I., Adams, J.M., Nicoll, J.A.R., Maxwell, W.L. & Gennarelli, T.A. (1995). The nature, distribution and causes of traumatic brain injury. *Brain Pathology.* 5, 397-401.

Graham, D.I., Gentleman, S.M., Lynch, A., & Roberts, G.W. (1995). Distribution of β-amyloid protein in the brain following severe head injury. *Neuropathology and Applied Neurobiology.* 21, 27-34.

Graham, D.I. (1996). Blunt head injury: prospects for improved outcome. *Neuropathology and Applied Neurobiology.* 22, 505-509.

Graham, D.I. & Gennarelli, T.A. (1997). Trauma. Greenfields Neuropathology 6th edition. London, Arnold. pp 197-262.

Grcevic, N. (1982). Topography and pathogenic mechanisms of lesions in inner cerebral trauma. *Rad jug Akad Znan Umj Od Med Nauke.* 18, 265-331.

Greene, J.G., Sheu, S-S., Gross, R.A. & Greenamyres, J.T. (1998). 3-Nitropropionic acid exacerbates N-mehyl-D-aspartate toxicity in striatal culture by multiple mechanisms. *Neuroscience.* 84, 503-510.

Guroff, G. (1964). A neutral calcium-activated protaese from the soluble fraction of rat brain. *Journal of Biological Chemistry.* 239, 149-155.

Hall, E.D. (1993). Cerebral ischaemia, free radicals and antioxidant protection. *Biochemical Society transactions.* 21, 334-339.

Halliwell, B. (1992). Reactive oxygen species and the central nervous system. *Journal of Neurochemistry.* 59, 1609-1623.

Halliwell, B. and Gutteridge, J.M.C. (1986). Oxygen free radicals and iron in relation to biology and medicine: Some problems and concepts. *Archives of Biochemistry and Biophysics.* 246, 501-514.

Hamakubo, T., Kannagi, R., Murachi, T. & Matus, A. (1986). Distribution of calpains 1 and 2 in the rat brain. *Journal of Neuroscience.* 6, 3103-3111.

Hansen, A.J. (1985). Effect of anoxia on ion distribution in the brain. *Physiology Reviews.* 65, 101-148.

Hausladen, A. & Fridovich, I. (1994). Superoxide and peroxynitrite inactivate acontinases, but nitric oxide does not. *Journal of Biological Chemistry.* 269, 29405-29408.

Hildebrand, C. & Waxman, S.G. (1984). Postantal differentiation of rat optic nerve fibers: electron microscopic observations on the development of nodes of Ranvier and axoglia relations. *Journal of Comparative Neurology.* 224, 25-37.

Holtzclaw, L.A., Gallo, V. & Russell, J.T. (1995). AMPA receptors shape Ca^{2+} responses in cortical oligodendrocyte progenitors and CG-4 cells. *Journal of Neuroscience Research.* 42. 125-130.

Hong, S-C., Lanzino, G., Goto, Y., Kong, S.K., Schotter, F., Kassel, N.F & Lee, S.K. (1994). Calcium-activated proteolysis in rat neocortex induced by transient focal ischaemia. *Brain Research.* 661, 43-50.

Horsburgh, K., McCulloch, J., Nislen, M., McCracken, E., Large, C., Roses, A.D. & Nicoll, J. Intraventricular infusion of apolipoprotein E amerliorates acute neuronal damage after global cerebral ischaemia in mice. *In submission to Nature Medicine*

Hovda, D.A., Lee, S.M., Smith, M.L., Von-Stuck, V., Bergsneider, M., Kelly, D., Shalmon, E., Martin, N., Caron, M., Mazziotta, J.,. Phelps, M. & Becker, D.P. (1995). The neurochemical and metabolic cascade following brain injury: Moving from animal models to man. *Journal of Neurotrauma.* 12, 903-906.

Huie, R.E. & Padmaja, S. (1993). The reaction of NO with superoxide. *Free Radical Research and Communications.* 18, 195-199.

Ingraham, C.A. & McCarthy, K.D. (1989). Plasticity of process-bearing glial cell cultures from neonatal rat cerebral cortical tissue. *Journal of Neuroscience.* 9, 63-69.

Inuzuka, I., Tamura, A., Sato, S. Kirino, T., Yanagisawa, K., Toyoshima, I. & Miyatake, T. (1990). Changes in the concentrations of cerebral proteins following occlusion of the middle cerebral artery in rats. *Stroke.* 21, 917-922.

Irving, E.A., Nicoll, J., Graham, D.I. & Dewar, D. (1996b). Increased tau immunoreactivity following human stroke and head injury. *Neuroscience Letters.* 213, 189-192.

Irving, E.A., Yatsushiro, K., McCulloch, J. & D. Dewar. (1997). Rapid alteration of tau in oligodendrocytes after focal ischaemic injury in the rat: Involvement of free radicals. *Journal of Cerebral Blood Flood and Metabolism.* 17, 612-622.

Jafari, S.S., Maxwell, W.L., Neilson, M & Graham, D.I. (1997). Axonal cytoskeletal changes after non-disruptive axonal injury. *Journal of Neurocytology.* 26, 207-221.

Jain, A., Martensson, J., Stole, E., Auld, P.A. & Meister, A. (1991). Glutathione deficiency leads to mitochondrial damage in brain. *Proceedings of the National Acadamy Sciences. USA.* 88, 1913-1917.

Jendroska, K., Hoffman, O.M. & Patt. S. (1997). Amyloid beta peptide and precursor protein (APP) in mild and severe brain ischaemia. *Annals of New York Acadamy of Sciences USA.* 826, 401-405.

Juurlink, B.H. (1997). Repsonse of glial cells to ischaemia: Roles of reactive oxygen species and glutathione. *Neuroscience and Biobehavioural Reviews.* 21, 151-166.

Juurlink, BH., Thornburne, S.K. & Hertz, L. (1998). Peroxide-scavenging deficit underlies oligodendrocytes susceptibility to oxidative stress. *Glia.* 22, 371-378.

Kampfl, A., Posmantur, R., Nixon, R., Grynspan, F., Zhao, X., Lui, S.J., Newcomb, J.K., Clifton, G.L., & Hayes, R.L. (1996). μ-Calpain activation and calpain-mediated cytoskeletal proteolysis following traumatic brain injury. *Journal of Neurochemistry.* 67, 1575-1583.

Kandel, E.R. & Schwartz, J.H. (1985). Nerves cells and behavior. *Principles of Neural Science.* Second Edition. Elservier.

Karlbuber, G.M., Bauer, H.C. & Eckl, P.M. (1997). Cytotoxic and genotoxic effects of 4-hydroxynonenal in cerebral endothethial cells. *Mutation Research.* 381, 209-216.

Keller, J.N., Mark, R.J., Bruce, A.J., Blanc, E., Rothstein, J.D., Uchida, K., Waeg, G. & Mattson, M.P. (1997). 4-Hydroxynonenal, an aldehydic prouduct of membrane lipid peoxidation, impairs glutamate transport and mitochondrial function in synaptosomes. *Neuroscience.* 80, 685-696.

Keller, J.N., Kindy, M.S., Holtsberg, F.W., St Clair, D.K., Yen, H.C., Germeyer, A., Steiner, S.M., Bruce-Keller, A.J., Hutchins, J.B. & Mattson, M.P. (1998). Mitochondrial manganese superoxide dismutase prevents neural apoptosis and reduces ischaemic brain injury: suppression of peroxynitrite production, lipid peroxidation, and mitochondrial dysfunction. *Journal of Neuroscience.* 15, 687-97.

Kim, Y.S. & Kim, S.U. (1991). Oligodendroglia cell death induced by oxygen radicals and its protection by catalase. *Journal of Neuroscience Research.* 29, 100-106.

Kinouchi, H., Epstein, C.J., Mizui, T., Carlson, E. Chen, S.F. & Chan, P.H. (1991). Attenuation of focal cerebral ischemic injury in transgenic mice overexpressing Cu/Zn SOD. *Proceedings of the Acadamy of Science. USA.* 88, 11158-11162.

Kinter, M & Roberts, R.J. (1996). Glutathione consumption and glutathione peroxidase inactivation in fibroblast cell lines by 4-hydroxynon-2-nenal. *Free Radical Biology and Medicine.* 21, 457-462.

Kishimoto, A., Mikawa, K., Hashimoto, K., Yasuda, I., Tanaka, S., Tominaga, M., Kuroda,T., & Nishizuka, Y. (1989). Limited proteolysis of protein kinase C subspecies by calcium dependent neutral protease (calpain). *Journal of Biological Chemistry.* 264, 4088-4092.

Koo, E.H., Sisodia, S.S., Archer, D.R., Martin, L.J., Weidmann, A., Beyeuther, K., Fischer, P., Masters, C.L., & Price, D.L. (1990) Precursor of amyloid protein in Alzheimer disease undergoes fast anterograde axonal transport. *Proceedings of the National Acadamy of Science USA.* 87, 1561-1565.

Kristian, T. & Siesjo,B. (1998). Calcium in ischaemic cell death. *Stroke.* 29, 705-718.

Kumura, E., Graf, R., Dohmen, C., Rosner, G. & Heiss, W.D. (1999). Breakdown of calcium homeostasis in relation to tissue depolarisation: comparison between gray and white matter ischemia. *Journal of Cerebral Blood Flow and Metabolism.* 19, 788-793.

Kumura, E., Yoshimine, T., Kubo, S., Tanaka, S., Hayakawa, T., Shiga, T. & Kosaka, H. (1995). Effects of superoxide dismutase on nitric oxide production during reperfusion after focal cerebral ischaemia in rats. *Neuroscience Letters.* 200, 137-140.

Kuroiwa, T., Nagaoka, T., Ueki, M., Yamada, I., Miyasaka, N. & Akimoto, H. (1998). Different apparent diffusion coefficient: water content correlations of gray and white matter during early ischaemia. *Stroke.* 29, 859-65.

Laemmli, U.K. (1970). Cleavage of structural proteins during the assembly of the head of bacteriophage T4. *Nature.* 227, 680-685.

Lafon-Cazal, M., Pietri, S., Culcasi, M. & Bocaert, J. (1993). NMDA-dependent production and neurotoxicity. *Nature.* 364, 535-537.

Le Blanc, A.C., Kovacs, D.M., Chen, H.Y., Villare, F., Tyskocinski, M. Autilio-Gambetti, L & Gambetti, P. (1992). Role of amyloid precursor protein (APP): study with antisense transfection of human neurobalstoma cells. *Journal of Neuroscience Research.* 31, 635-645.

Leppanen, L.L. & Stys, P.K. (1997). Ion transport and membrane potential in CNS myelinated axons. II: Effects of metabolic inhibition. *Journal of Neurophysiololgy.* 78, 2095-2107.

Levi, G., Gallo, V. & Giotti, M.T. (1986). Bipotential precursors of putative fibrous astrocytes and oligodendrocytes in rat cerebeller cultures express distinct surface features and "neuron-like" gamm-aminobutyric acid transport. *Proceedings of the National Acadcamy of Science, USA.* 83, 1504-1508.

Levison, S.W., Chuang, C., Abranson, B.J., Goldman, J.E. (1993). The migrational patterns and developmental fates of glial precursors in the rat subventricular zone and temporally regulated. *Development.* 119, 611-622.

Levison, S.W. & Golman,, J.E. (1993). Both oligodendrocyte and astrocytes develop from progenitors in the subventricular zone of postnatal rat forebrain. *Neuron.* 2, 201-212.

Li, S., Mealing, G.A.R., Morely, P. & Stys, P.K. (1989). Novel injury mechanism in anoxia and trauma of spinal cord white matter: glutamate release via reverse Na^+-dependent glutamate transport. *Journal of Neuroscience.* 19, 1-9.

Li, Z., & Banik, N.L. (1995). The localisation of mcalpain in myelin: immunocytochemical evidence in different areas of rat brain and nerves. *Brain Research.* 697, 112-121.

Linder, S & Rinder, L. (1966). Experimental studies in head injury. II. Pressure propagation in "percussion concussion". *Biophysik.* 3, 174-180.

Liu, X.H., Kato, H., Araki, T., Itoyama, Y., Kato, K. & Kogure, K. (1994). An immunohistochemical observation of manganese superoxide dismutase in rat substantia nigra after occlusion of middle cerebral artery. *Neuroscience Letters.* 173, 103-106.

Lomnitski, L., Chapman, S., Hochman, A., Kohen, R., Shohami, E., Chen, Y., Trembovler, V. & Michaelson, D.M. (1999). Antioxidant mechanisms in apolipoprotein E deficient mice prior to and following closed head injury. *Biochimca et Biophysica Acta.* 1453, 359-368.

Longa, E.Z., Weinstein, P.R., Carlson, S. & Cummins, R. (1989). Reversible middle cerebral artery occlusion without craniectomy in rats. *Stroke.* 20, 84-91.

Lowry, O.H., Rosebrough, N.J., Farr, A.L., & Randall, R.J. (1951). Protein measurement with the Folin phenol reagent. *Journal of Biololgy Chemistry.* 193, 265-275.

Love, S. (1999). Symposium: Oxidative stress in Neurological Disease. *Brain Pathology.* 9, 119-131.

Lovell, M.A., Ehmann, W.D., Mattson, M.P. & Marksberry, W.R. (1997). Elevated 4-hydroxynonenal in ventricular fluid in Alzheimer's disease. *Neurobiology of Aging*. 18, 457-461.

Lovinger, D.M. (1993). Excitotoxicity and alcohol-related brain damage. *Alcoholism Clinical and experimental Research.* 17, 19-27.

Ludolph, A.C., He, F., Spencer, P.S., Hammerstad, J. & Sabri, M. (1991). 3-Nitropropionic acid exogenous animal neurotoxin and possible human striatal toxin. *Candian Journal of Neuroscience Science.* 18, 492-498.

Ludwin, S.K. (1984). Proliferation of mature oligodendrocytes after trauma to the central nervous system. *Nature.* 308, 274-275.

Ludwin, S.K. (1997). The pathobiology of the oligodendrocyte. *Journal of Neuropathology Experimental Neurology.* 56, 111-124.

Lunn, K.F., Baas, P.W. & Duncan, I.D. (1997). Microtubule organisation and stability in the oligodendrocyte. *Journal of Neuroscience.* 17, 4921-4932.

MacMillan-Crow, L.A. & Thompson, J.A. (1999). Tyrosine modifications and inactivation of active site of manganese superoxide dismutase mutant (Y34F) by peroxynitrite. *Archives of Biochemistry and Biophysics*. 366, 82-88.

Macrae, I.M. (1992). New models of focal cerebral ischaemia. *British Journal of Pharmacology.* 34, 302-308.

Macrae, I.M., Robinson, M.J. Graham, D.I. Reid, J.L. & McCulloch. (1993). Endothelian 1 induced reduction in cerebral blood flow: dose dependency, time course, and neuropathological consequences. *Journal of Cerebral Blood Flow and Metabolism.* 13, 276-284.

Malinski, T., Bailey, F., Zhang, ZG. & Chopp, M. (1993). Nitric oxide measured by a porphyrinic microsensor in rat brain after transient middle cerebral ischaemia. *Journal of Cerebral Blood Flow and Metabolism.* 13, 355-358.

Marcoux, F.W., Morawetz, R.B., Crowell, R.M., DeGirolami, U. & Halsey, J.H. (1982). Differential regional vulnerability in transient focal cerebral ischaemia. *Stroke.* 13, 339-347.

Mark. R.J., Lovell, M.A., Marksberry, W.R., Uchida, K. & Mattson. M.P. (1997). A role for 4-hydroxynonenal, an aldehydic product of lipid peroxidation, in disruption of ion homeostasis and neuronal death induced by amyloid β-peptide. *Journal of Neurochemistry.* 86, 255-264.

Marksberry, W.R. (1997). Oxidative stress hypothesis in Alzheimer's disease. *Free Radical Biology and Medicine.* 23, 134- 147.

Marksberry, W.R. & Lovell, M.A. (1998). Four-hydroxynonenal, a product of lipid peroxidation, is increased in the brain in Alzheimer's disease. *Neurobiolology of Aging.* 19, 33-36.

Marshall, L.F. & Marshall, S.B.(1995). Pitfalls and advances for the international tirilazad trial in moderate and severe head injury. *Journal of Neurotrauma.* 12, 929-932.

Martinez, M.C., Bosh-Morell, F., Raya, A., Roma, J., Aldasoro, M., Vila, J., Lluch, S. & Romero, F.J. (1994). 4-Hydroxynonenal, a lipid peroxidation product, induces relaxation of human cerebral arteries. *Journal of Cerebral Blood Flow and Metabolism.* 14, 693-696.

Masliah, E., Cole, G., Shimohama, S., Hansen, L., DeTeresa., Terry, R.D., & Saitoh,T. (1990). Differential involvement of protein kinase C isozymes in Alzheimer's disease. *Journal of Neuroscience.* 10, 2113-2124.

Mattson, M.P., Lovell, M.A., Furikawa, K. & Markesbery, W.R. (1995). Neurotrophic factors attenuate glutamate-induced accumulation of peroxides, elevation of intracellular enzyme activities in hippocampal neurons. *Journal of Neurochemistry.* 65, 1740-51.

Mattson, M.P., Weiming, F., Weag, G. & Uchida, K. (1997). 4-Hydroxynonenal, a lipid peroxidation, inhibits dephosphorylation of the microtubule-associated protein tau. *NeuroReport.* 8, 2275-2281.

Mattson, M.P. (1998). Modification of ion homeostasis by lipid peroxidation : roles in neuronal degeneration and adaptive plasticity. *Trends in Neurosciences.* 20, 53-57.

Mattson, M.P. & Pedersen, W.A. (1998). Effects of amyloid precursor protein derivatives and oxidative stress on basal forebrain cholinergic systems in Alzheimer's disease. *International Journal of Developmental Neuroscience.* 16, 737-753.

Markgraf C.G., Velayo N.L., Johnson M.P., McCarty, D.R., Medhi S., Koehl J.R., Chmielewski, P.A., & Linnik M.D. (1998) Six-hour window of opportunity for calpain inhibition in focal cerebral ischemia in rats. *Stroke.* 29, 152-158.

Maxwell, W.L., Irvine, A., Graham, D.I., Adams, J.H. & Gennarelli, T.A. (1991). Focal axonal injury: the early axonal response to stretch. *Journal of Neurocytology.* 20, 157-164.

Maxwell, W.L., Watt, C., Graham, D.I. & Gennarelli, T.A. (1993). Ultrastructural evidence of axonal shearing as a result of lateral acceleration of the head in non-human primates. *Acta Neuropatholollgica.* 86, 136-144.

Maxwell, W.L., McCreath, B.J., Graham, D.I., & Gennarelli, T.A. (1995). Cytochemical evidence for redistribution of membrane pump calcium-ATPase and ecto-Ca-ATPase activity, and calcium influx in myelinated nerve fibres of the optic nerve after stretch injury. *Journal of Neurocytology.* 24, 925-942.

Maxwell, W.L., Povlishock, J.T, & Gaham, D.I. (1997). A mechanistic analysis of non-disruptive axonal injury: A review. *Journal of Neurotrauma.* 14, 419-439.

McCarthy, K. D & De Vellis, J. (1980). Preparation of separate astroglia and oligodendroglia cell cultures from rat cerebral tissue. *Journal of Cell Biology.* 85, 890-902.

McCord, J. (1985). Oxygen derived free radicals in postischaemic tissue injury. *New England Journal of Medicine.* 312, 159-163.

McIntosh, T.K. (1994). Neurochemical sequelae of traumatic brain injury: therapeutic implications. *Cerebrovascular and Brain Metabolism Reviews.* 6, 109-162.

McLaurin, J.A. & Yang, V.W. (1995). Oligodendroglia and myelin. *Neurological Clinics.* 13, 23-49.

McDonald, J.W., Althomsons, S.P., Hyrc, K.L., Choi, D.W. & Goldberg, M.P. (1998). Oligodendrocytes from forebrain are highly vulnerable to AMPA/kainate receptor-mediated excitoxicity. *Nature Medicine.* 4, 291-295.

McKenzie, K.J., McLellan, D.R., Gentleman, S.M., Maxwell, W.L., Gennarelli, T.A. & Graham, D.I. (1996). Is β-APP a marker of axonal damage in short-surviving head injury? *Acta Neuropathologica.* 92, 608-613.

McLellan, D.R. Adams, J.H., Graham, D.I., Kerr. A.E. & Teasdale, G.M. (1986). The structural basis of the vegetative state and prolonged coma after non-missile head injury. In Papo I, Cohadon F. Massaotti M. eds. Le Coma Traumatique. Pavoda: Liviana Editrice. 165-185.

Mikawa, S., Kinouchi, H., Kamii, H., Gobbel, G.T., Chen, C.F., Carlson, E., Epstein, C.J. & Chan, P.H. (1996). Attenuation of acute and chronic damage following TBI in copper, zinc superoxide dismutase transgenic mice. *Journal Neurosurgery.* 85, 885-891.

Miller, R.H., Ffrench-Constant, C. & Raff, M.C. (1989). The macroglia cells of the rat optic nerve. *Annuals Reviews Neuroscience.* 12, 517-534.

Miller, J.D., Bullock, R., Graham, D.I. Chen, M.H. & Teasdale, G.M. (1990). Ischaemic brain damage in a model of acute subdural haematoma. *Journal of Neurology, Neurosurgery and Psychiatry.* 1978. 41. 122-127.

Miller, P.J. & Zaborszky, L. (1997). 3-Nitropropionic acid neurotoxicity: Visualisation by silver staining and implications for use as an animal model of Huntington's disease. *Experimental Neurology.* 146.212-229.

Mitchison, T. & Kirschner, M. (1984). Dynamic instability of microtubule growth. *Nature.* 312, 237-242.

Mitya, N. & Smith, J.D. (1996). Apolipoprotein E allele specific antioxidant activity and effects on cytotoxicity by oxidative insults and beta amyloid peptides. *Nature Genetics.* 14, 55-61.

Moncada, S., Palmer, R.M. & Higgs, E.A. (1991). Nitric oxide: physiology, pathophysiology, and pharmacology. *Pharmacology Reviews.* 43, 109-142.

Montine, T.J., Amaranath, V., Martin, M.E., Strittmatter, W.J. & Graham, D.G. (1996a). E-4-hydroxy-2-nonenal is cytotoxic and cross-links cytoskeletal proteins in P19 neuroglia cultures. *American Journal of Pathology.* 148, 89-93.

Montine, T.J., Huang, D.Y., Valentine, W.M., Amarnath, V., Saunders, A., Weisgraber, K.H., Graham, D.G., Strittmatteer, W.J. (1996b). Crosslinking of apolopoprotein E by products of lipid peroxidation. *Journal of Neuropathology and Experimental Neurology.*55, 202-210.

Montine, K.S., Kim, P.J., Olson, S.J., Marksberry, W.R. & Montine, T.J. (1997a). 4-Hydroxynonenal-2-nonenal pyrrole adducts in human neurodegerenative disease. *Journal of Neuropathology and Experimental Neurology.* 56, 866-871.

Montine, K.S., Oslon, S.J., Amarnath, V., Whetsell, W.O., Graham, D.G. & Montine, T.J. (1997b). Immunohistochenical detection of 4-hydroxy-2-nonenal adducts in Alzheimer's Disease is associated with inheritance of APOE4. *American Journal of Pathology.* 150, 437-444.

Montine, K.S., Reich, E., Neely, M.R., Disell, K.R., Olson, S.J., Markesbery, W.R. & Montine, T.J. (1998). Distribution of reducible 4-hydroxynonenal adduct immunoreactivity in Alzheimer Disease is associated with APOE Genotype. *Journal of Neuropathology and Experimental Neurology.* 57, 415-425.

Muizellar, J.P., Marmarou, A., Young, H.F., Choi, S.C, Wolf, A., Schneider, R.L. & Kontos, H.A. (1993). Improving outcome of severe head injury with the oxygen radical scavenger polyethene glycol-conjugate SOD: a phase II trial. *Journal of Neurosurgery.* 78, 375-382.

Murakami, K., Kondo, T., Kawase, M., Li, Y., Sato, S., Chen, S. & Chan, P.H. (1998). Mitochondrial susceptibility to oxidative stress exacerbates cerebral infarction that follows permanent focal cerebral ischaemia in mutant mice with manganese superoxide dismutase deficiency. *Journal of Neuroscience.* 18, 205-213.

Murphy, A.N., Fiskum, G. & Beal, M.F. (1999). Mitochondria in neurodegeneration: Bioenergetic function in cell life and death. *Journal of Cerebral Blood Flow and Metabolism.* 19, 231-245.

Neely, M.D., Sidell, K.R., Graham, D.G. & Montine, T.J. (1999). The lipid peroxidation product 4-hydroxynonenal inhibits neurite outgrowth, disrupts neuronal microtubules, and modifies cellular tubulin. *Journal of Neurochemistry.* 72, 2323-2333.

Newcomb. J.K., Kampfl, A., Posmantur, R.M., Zhao, X.R., Pike, B.R., Lui S.J., Clifton, G.L. & Hayes, R.L. (1997). Immunohistochemical study of calpain-mediated breakdown products to alpha-spectrin following controlled cortical impact injury in the rat. *Journal of Neurotrauma.* 14, 369-383.

Newcomb, J.K., Kampfl, A., Posmantur, R.M. Zhao, X.R., Pike, B.R., Lui, S.J., Clifton, G.L. & Hayes, R.L. (1997). Immunohistochemical study of calpain-mediated breakdown products to alpha-spectrin following controlled cortical impact injury in the rat. *Journal of Neurotrauma.* 14, 369-383.

Nicholl, D.G. (1985). A role for the mitochondrion in the protection of cells against calcium overload. *Brain Research.* 63, 97-106.

Nishino, H., Fujimoto, I., Shimanto, Y., Hida., H., Kumazaki, M. & Fukuda, A. (1996). 3-Nitropropionic acid produces striatum selective lesions accompanied by iNOS expression. *Journal of. Chemical Neuroanatomy.* 10, 209-212.

Nixon, R.A., & Siag, R.K. (1991). Neurofilament phosphorylation: a new look at regulation and function. *Trends in Neurosciences.* 14, 501-506.

Oghami, T., Kitamoto, T., Tateisha, J. (1992) Alzheimer's amyloid precursor protein accumulates within axonal swellings in human brain lesions. *Neuroscience Letters.* 136, 75-78.

Oka, A., Belliveau, M.J., Rosenberg, P.A. & Volpe, J.J. (1993). Vulnerability of oligodendroglia to glutamate: Pharmacology, mechanisms and prevention. *Journal of Neuroscience.* 13, 1441-1453.

Okonkwo, D.O., Pettus, E.H., Moroi, J. & Povishock, J.T. (1998). Alteration of the neurofilament sidearm and its relation to neurofilament compaction occurring with axonal injury. *Brain Research.* 784, 1-6.

Oostveen, J.A., Dunn, E., Carter, D.B. & Hall, E.D. (1998). Neuroprotective efficacy and mechanisms of novel pyrrolpyrimidine lipid peroxidation inhibitors in the gerbil forebrain ischaemia model. *Journal of Cerebral Blood Flow and Metabolism.* 18, 539-547.

Osborne, K.A., Shigeno, T., Balarsky, A-M., Ford, I., McCulloch, J., Teasdale, G.M. & Graham, D.I. (1987). Quantitative assessment of early brain damage in a rat model of

focal cerebral ischaemia. *Journal of Neurology, Neurosurgery, and Psychiatry.* 50, 402-410.

Pang, Z. & Geddes, J. W. (1997). Mechanisms of cell death induced by the mitochondrial toxin 3-nitropropionic: acute excitotoxic necrosis and delayed apoptosis. *Journal of Neuroscience.* 17, 3064-3073.

Pant, H.C. (1988). Dephosphorylation of neurofilament proteins enhances their susceptibility to degradation by calpain. *Biochemistry Journal.* 256, 665-668.

Pantneau, D.K., Wright, P.W., Winters, C., Mayer, M.C. & Gallo, V. (1994). Glial cells of the oligodendrocyte lineage express both kaniate-AMPA-preferring subtypes of glutamate receptors. *Neuron.* 12, 357-371.

Pantoni, L., Garcia, J.H. & Gutierrex, J.A. (1996). Cerebral white matter is highly vulnerable to ischaemia. *Stroke.* 27, 1641-1647.

Pantoni, L. & Garcia, J.H. (1997). Pathogenesis of leukoaraiosis. A review. *Stroke.* 28, 652-659.

Park, C.K. & Hall, E.D. (1994). Dose-response analysis of the effect of 21-aminosteriod tirilazad (U-74006F) upon neurological outcome and ischemic brain damage in permanent focal ischemia. *Brain Research.* 645. 157-163.

Patel, R.P., McAndrew, J. Sellak, H., White, R. C., Hanjoong, J., Freeman, B.A. & Darely-Usmar, V.M. (1999). Biological aspects of reactive species. *Biochimica et Biophysica Acta.* 1411, 385-400.

Peeless. S.J., Rewcastle, A.B (1967). Shear injuries of the brain. *Candian Medical Association Journal.* 96, 577-582.

Perlmutter, L.S., Gall. C., Baundry, M. & Lynch. G. (1990). Distribution of calcium-activated protease calpain in the rat brain. *Journal Comparative Neurology.* 296, 269-276.

Pettus, E.H., Christman, C.W., Giebel, M.L., & Povlishock, J.T. (1994). Traumatically induced altered membrane permeability: its relationship to traumatically induced reactive axonal change. *Journal of Neurotrauma.* 11, 507-522.

Pettus, E.H & Povlishock, J.T. (1996). Characterisation of a distinct set of intra-axonal ultrastructual changes associated with traumatically induced alteration in axolemma permeability. *Brain Research.*772, 1-11.

Pettigrew, C.L., Holtz, M.L., Craddock, S.D., Minger, S.L., Hall, N. & Geddes, J.W. (1996). Microtubular proteolysis in focal cerebral ischemia. *Journal of Cerebral Blood Flow and Metabolism.* 16, 1189-1202.

Piantadosi, C.A. & Zhang, J. (1996). Mitochondrial generation of reactive brain ischaemic in the rat. *Stroke.* 27, 327-31

Picklo, J. M., Amatnath, V., Mcintyre, J.O., Graham, D.G. & Montine, T.J. (1999). 4-hydroxy-2(E)-nonenal inhibits CNS mitochondrial respiration at multiple sites. *Journal of Neurochemistry.* 72, 1617-1624.

Pinteaux, E., Perraut, & Tholey, G. (1998). Distribution of mitochondrial manganese superoxide dismuatse among rat glial cells in culture. *Glia.* 22, 408-414.

Posmantur, R., Hayes, R.L., Dixon, C.E., & Taft, W.C. (1994). Neurofilament 68 and neurofilament 200 protein levels decrease after traumatic brain injury. *Journal of Neurotrauma.* 11, 533-545.

Posmantur, R., Kampfl, A., Simans, R., Lui, J., Zhao, X., Clifton, G.L., & Hayes, R.L. (1997) A calpain inhibitor attenuates cortical cytoskeletal protein loss after experimental traumatic brain injury in the rat. *Neuroscience.* 77, 875-888.

Povlishock, J.T., Astruc, J. & Erb, D.E. (1992). Axonal response to traumatic brain injury: reactive axonal change, deafferenation, and neuroplasticity. *Journal of Neurotrauma.* Suppl 19 S189-200.

Povlishock, J.T. (1993). Pathobiology of traumatically induced axonal injury in animals and man. *Annals of Emergency Medicine.* 22, 980-986.

Povlishock , J.T., Hayes, R.L., Michel, , M,Y. & McIntosh, T.K. (1994). Workshop on animals models of traumatic brain injury. *Journal of Neurotrauma.* 11, 723-731.

Povlishock, J.T., & Christman, C.W. (1995). The pathobiology of traumatically induced axonal injury in animals and humans: A review of current thoughts. *Journal of Neurotrauma.* 12, 555-565.

Povlishock, J.T., Marmarou, A., McIntosh, T., Trojanowski, J.Q., & Moroi, J. (1997). Impact acceleration injury in the rat: evidence for focal axolemmal change and related neurofilament sidearm alteration. *Journal of Neuropathology and Experimental Neurology.* 56, 347-359.

Pryor. W.A & Porter, N.A. (1990). Suggested mechanisms for the production of 4-hydroxy-2-nonenal from the autooxidation of polyunsaturated fatty acids. *Free Radical Biology and Medicine.* 8, 541-543.

Pulsinelli, W.A., Brierley, J.B. & Plum, F. (1982). Temporal profile of neuronal damage in a model of transient froebrain ischaemia. *Annals of Neurology.* 11, 491-498.

Qi, Y., Jamindar, T.M & Dawson, G. (1995). Hypoxia alters iron homeostasis and induces ferritin synthesis in oligodendrocytes. 64, 2458-2464.

Raddi, R., Beckman, J.S., Bush, K.M. & Freeman, B.A. (1991). Peroxynitrite-induced membrane lipid peroxidation: the cytotoxic potential of superoxide and nitric oxide. *Archives of Biochemistry and Biophysics.* 288, 481-487.

Raichle, M.E. (1983). The pathophysiology of brain ischaemia. *Annals of Neurology.* 13, 2-10.

Ransom, B.R., Stys, P.K. & Waxman, S.G. (1990). The pathophysiology of anoxic injury in central nervous system white matter. *Stroke.* 21, SIII-52-SIII-57.

Ransom, B.R. & Philbin, D.M. (1992). Anoxia-induced extracellular ionic changes in CNS white matter: the role of glial cells. *Candian Journal of Physiology and Pharmacology*. 70, S181-189.

Raff, M.C. (1989). Glial cell diversification in the rat optic nerve. *Science*. 243, 1450-1455.

Reaume, A.G., Elliot, J.L., Hoffman, E.K., Kowall, N.W., Ferrante, R.J., Siwek, D.F., Wilcox, H.M., Flood, D.G., Brown, R.H., Scott, R.W. & Sinder, W.D. (1996). Motor neurons in Cu-Zn superoxide dismutase-deficient mice develop normally but exhibit enhanced cell death after axonal injury. *Nature Genetics*. 13, 43-47.

Rehncrona, S., Hauge, H.N. & Siesjo, B.K. (1989). Enhancement of iron-catalysed free radical formation by acidosis in brain homogenates: difference in effect by lactic acid and CO_2. *Journal of Cerebral Blood Flow and Metabolsim*. 9, 65-70.

Riepe, M.W., Hori, N., Ludolph, A.C. & Carpenter, D.O. (1995). Failure of neuronal ion exchange, not potentiated excitation, causes excitotoxcity after inhibition of oxidative stress. *Neuroscience*. 64, 91-97.

Robertson, W. (1899). On a new method of obtaining a black reaction in certain tissue-elements of the CNS (platinum method) *Scottish Medical Surgery Journal*. 4, 23.

Roberts-Lewis, J.M., Savage, M.J., Marcy, V.R., Pinsker, L.R., & Siman, R. (1994). Immunolocalisation of calpain 1-mediated spectrin degradation to vulnerable neurons in the ischemic gerbil brain. *Journal of Neuroscience*. 14, 3934-3944.

Rosenbaum, D.M., Kalberg, J. & Kessler, J.A. (1994). Superoxide dismutase ameliorates neuronal death from hypoxia in culture. *Stroke*. 25, 857-863.

Rothman, S.M. & Olney, J.W. (1978). Excitotoxicity and the NMDA receptor. *Trends in Neurosciences*. 10, 299-302.

Rothman, S.M. & Olney, J.W. (1986). Glutamate and the pathophysiology of hypoxic-ischemic brain damage. *Annals of Neurology.* 19, 105-111.

Rubbo, H., Radi, R., Trujillo, M., Telleri, R., Kalyanaraman, B., Barnes, M., Kirk, M. & Freeman, B.A. (1994). Nitric oxide regulation of superoxide and peroxynitrite-dependent lipid peroxidation derivatives. *Journal of Biological. Chemistry.* 269, 26066-26075.

Rubin, R & Faber, J.L. (1984). Mechanism of the killing cultured hepatocytes by hydrogen peroxide. *Archives of Biochemistry and Biophysics.* 22, 450-459.

Saatman, K.E., Bozyczko-Coyne, D., Marcy, V., Siman, R., and McIntosh, T.K. (1996a). Prolonged calpain-mediated spectrin breakdown occurs regionally following experimental brain injury in the rat. *Journal of Neuropathology and Experimental Neurology.* 55, 850-860.

Saatman, K.E., Murai, H., Bartus, R.T., Smith, D.H., Hayward, N.J. Perri B.R. & McIntosh, T.K. (1996b). Calpain inhibitor AK925 attenuates motor and cognitive deficits following experimental brain injury in the rat. *Proceedings of the National Acadamy of Sciences of U.S.A.* 93, 3428-3444.

Salzer, J.L. (1997). Clustering of sodium channels at the node of Ranvier: close encounters of the axon-glia kind. *Neuron.* 18, 843-846.

Schewe, T. (1985). Molecular actions of Ebselen – an anti-inflammatory antioxidant. *General Pharmacology.* 26, 1153-1169.

Schimd-Elsaesser, R., Hungerhuber, E., Zausinger, S., Baethmenn, A. & Reulen, H-J. (1999). Neuroprotective efficacy of combinational therapy with two different antioxidants in rats subjected to transient focal ischaemia. *Brain Research.* 816, 471-479.

Schlapfer, W.W. (1987). Neurofilaments: structure, metabolism and implications in disease. *Journal of Neuropathology and Experimental Neurology.* 46, 117-129.

Schraufstatter, I.U., Hinshaw, D.W., Hyslop, P.A., Spragg, R.G. Cochrane, C.G. (1985). Glutathione cycle activity and pyridine nucleotide levels in oxidant-induced injury of cells. *Journal of Clinical Investigation.* 76, 1131-1139.

Schulz, J.B., Henshaw, D.R., MacGarvey, N & Beal, M.F. (1996). Involvement of oxidative stress in 3-nitropropionic acid neurotoxicity. *Neurochemistry International.* 29, 167-171.

Shapira, Y., Yadid, G., Cotev, S, & Shomami, E. (1989) Accumulation of calcium in the brain following head trauma. *Neurological Research.* 11, 169-172.

Sherriff, F.E., Bridges, L.R. & Sivalganatha, S. (1994). Early detection of axonal injury after human head trauma using immunocytochemistry for β-amyloid precusor protein. *Acta. Neuropathologica* 87, 55-62.

Shigematsu, K., McGeer, P.L., Wlaker, D.G., Ishii, T. & McGeer, E.G. (1992). Reactive microglia/macrophages phagocytose amyloid precursor protein produced by neurons following neural damage. *Journal of Neuroscience Research.* 31, 443-453.

Siddiqi, F.A., Darakchiev, B.J., Cohen, S.M., Hariri, R. J. & Fantini, G.A. (1996). Free radicals, antioxidants and reperfusion injury in the CNS. *Ballieres Clinical Anaesthesiology.* 10, 497-509.

Siems, W.G., Hapner, S.J. & Van Kuijk, F.J. (1996). 4-Hydroxynonenal inhibits Na^+K^+-ATPase. *Free Radical Biology and Medicine.* 20, 215-223.

Siesjo, B.K. (1981). Cell damage in the brain: a speculative synthesis. *Journal of Cerebral Blood Flow and Metabolism.* 1, 155-185.

Siesjo, B.K. (1985). Acid-base homeostasis in the brain: physiology, chemistry, and neurochemical pathology. *Progressive Brain pathology.* 63, 121-154.

Siesjo, B.K., Agardth, C-D & Bengtsson, F. (1989). Free radicals and brain damage. *Cerebrovascular and Brain Metabolism Reviews.* 1. 165-211.

Siesjo, B.K. & Bengtsson, F. (1989). Calcium fluxes, calcium antagonists, and calcium-related pathology in brain ischemia, hypoglycemia, and spreading depression: a unifying hypothesis. *Journal of Cerebral of Blood and Metabolism.* 9, 127-140.

Siesjo, B.K. (1992). Pathophysiology and treatment of focal cerebral ischemia. Part 1: Pathophysiology. *Journal of Neurosurgurgy.* 77, 169-184.

Silver, I.A. & Ercinska, M. (1990). Intracellular and extracellular changes (Ca^{2+}) in hypoxia and ischaemia in rat brain. *Journal of General Physiology.* 95, 837-866.

Sims, N.R., Williams, V.K., Zaidan, E. & Powell, J.A. (1998). The anitoxidant defences of brain mitochondria during short term forebrain ischaemia and recirculation in the rat. *Molecular Brain Research.* 60, 141-149.

Smith, C.D., Carson, M., van der Woerd, M., Chen, J., Ischiropoulos, H. & Beckman, J.S. (1992). Crystal structure of peroxynitrite-modifed bovine Cu,Zn superoxide dismutase. *Archives of Biochemistry and Biophysics.* 299, 350-355.

Smith, M-L, Auer, R.N. & Siesjo, B.K. (1984). The density and distribution of ischaemic brain injury in the rat following 2-10 minutes of forebrain ischaemia. *Acta Neuropathica.* 64, 319-3332.

Smith, M.L., Von Hanwehr, R., Siesjo, B.K. (1986). Changes in extra- and intracellular pH in the brain during and following ischaemia in hyperglycemic and in moderately hypogylcemic rats. *Journal Cerebral Blood Metabolism.* 6, 574-583.

Smith, R.A.J., Porteous, C.M., Coulter, C.V. & Murphy, M.P. (1999). Selective targeting of an antioxidant to mitochondria. *European Journal of Biochemistry.* 263, 709-716.

Soehle, M., Heimann, A. Kempski, O. (1998). Postischaemic application of lipid peroxidation inhibitor U-101033E reduces neuronal damage after global cerebral ischaemia in rats. *Stroke.* 1240-1247.

Southam, E., Thomas, P.K., King, R.H., Goss-Sampson, M.A. & Muller, D.P. (1991). Experimental vitamin E deficiency in rats. Morphological and functional evidence of abnormal axonal transport secondary to free radical damage. *Brain.* 114, 915-936.

Springer, J.E., Azbill, R.D., Mark. R.J., Begley, J.G., Waeg, G. & Mattson, M.P. (1997). 4-Hydroxynonenal, a lipid peroxidation, rapidly accumulates following traumatic spinal cord injury and inhibits glutamate uptake. *Journal of Neurochemistry . 68, 2469-2476.*

Stamler, J.S., Singel, D.J. & Loscalzo, J. (1992). Biochemistry of nitric oxide and its redox activated forms. *Science.* 258, 1998-1902.

Sternberger, L.A. & Sternberger, N.H. (1983). Monoclonal antibodies distinguish phosphorylated and non-phosphorylated forms of neurofilaments in situ. *Proceedings of the National Acadamy of Sciences USA.* 80, 6126-6130.

Stys, P.K., Ransom, B.R., Waxman, S.G. & Davis, P.K. (1990). Role of extracellular calcium in anoxic injury of mammalian central white matter. *Proceedings of the National Acadamy of Sciences USA.* 87, 4212-4216.

Stys, P.K. (1998). Anoxic and ischaemic injury of myelinated axons in CNS white matter: from mechanistic concepts to therapeutics. *Journal of Cerebral Blood Flow and Metabolism.* 18, 2-25.

Strich, S.J. (1956). Diffuse degeneration of the cerebral white matter in severe dementia following head injury. *Journal of Neurology, Neurosurgery and Psychiatry.* 19, 163-185.

Subramaniam, R., Roediger, F., Jordan, B., Mattson, M.P., Keller, J.N., Waeg, G. & Butterfield, A.D. (1997). The lipid peroxidation product, 4-hydroxy-2-trans-nonenal,

alters the conformation of cortical synaptosomal membrane proteins. *Journal of Neurochemistry*.69, 1161-1169

Sullivan, H.B., Martinez, J., Becker, D.P., Miller, D.J., Griffith, R. & Wist, A.O. (1976). Fluid-percussion model of mechanical brain injury in the cat. Journal of Neurosurgery.

Sussman, M.S. & Bulkley, G.B. (1990). Oxygen-derived free radicals in reperfusion injury. *Methods Enzyme.* 186. 711-723.

Suzuki, K., Sorimachi, H., Yoshizawa, T., Kimbara, K. & Ishiura, S. (1995). Calpain: novel family members, activation, and physiologic function. *Biology Chemistry Hoppe Seyler.* 376-523-9

Suenaga, T., Ohnishi, K., Nishimura, M., Nakamura, S., Akiguchi, I., Kimura, J. (1994) Bundles of amyloid precursor protein-immunoreactive axons in human cerebrovascular white matter lesions. *Acta Neuropathologica.* (Berl.) 87, 450-455.

Swanson, R.A., Morton, M.T., Tsao-Wu, G., Savalos, R.A., Davidson, C. & Sharp, F.A. (1990). A semiautomated method for measuring brain infarct volume. *Journal of Cerebral Blood Flow and Metabolism.* 10, 290-293.

Szendrei, G.I., Lee, V.M-Y., & Otvos, L Jr. (1993). Recognition of the minimal epitope of monclonal antibody tau-1 depends upon the presence of a phosphate group but not its location. *Journal of Neuroscience Research.* 34, 243-249.

Takagaki, Y., Itoh, Y., Soki, Y., Ukai, Y., Yoshikuni, Y. & Kimura, K. (1997). Inhibition of ischaemia-induced fodrin breakdown by a novel phenylpyrimidine derivative NS-7: an implication for its neuroprotective action in rats with middle cerebral artery occlusion. *Journal of Neurochemistry.* 68, 2507-2517.

Takamatsu, H., Kondo, K., Ikeda, Y. & Umerura, K. (1998). Hydroxyl radical generation after the third hour following ischaemia contributes to brain damage. *European Journal of Pharmacology.* 352, 165-169.

Takasago, T., Peters, E.E., Graham, D.i., Masayasu, H & Macrae, I.M. (1997). Neuroprotective efficacy of ebselen, an antioxidant with anti-inflammatory actions, in a rodent model of permanent middle cerebral artery occlusion. *British Journal of Pharmacology.* 122, 1251-1256.

Tamura, A., Graham, D.I., McCulloch, J. & Teasdale, G.M. (1981). Focal cerebral ischaemia in the rat: Description of technique and early neuropathological consequences following middle cerebral artery occlusion. *Journal of Cerebral Blood Flow and Metabolism.* 1, 53-60.

Tanaka, K., Shirai, T., Nagata, E., Dembo, T. & Fukiichi, Y. (1997). Immunohistochemical detection of nitrotyrosine in postischemic cerebral cortex in gerbil. *Neuroscience Letters.* 235, 85-88.

Tomei, G., Spangnolli, D., Ducati, A., Landi, A., Villani, R., Fumagalli, G., Sala, C. & Gennarelli, T. (1990). Morphology and neurophysiology of focal axonal injury experimetns induced in the guinea pig optic nerve. *Acta Neuropathologica.* 80, 506-513.

Truelove, D., Shuaib, A., Ijaz, S., Ishaqzay, R. & Kalra, J. (1994). Neuronal protection with superoxide dismutase in repetitive forebrian ischemia in gerbils. *Free Radical Biology and Medicine.* 17, 445-450.

Tsai, M.J., Goh, C.C., Wan, Y.L. & Chang, C. (1997). Metabolic alterations produced by 3-nitropropionic acid in rat striata and cultured astrocytes: quantitative *in vitro* ^{1}H nucleear magnetic resonannce spectroscopy and biochemical characteristation. *Neuroscience.* 79, 819-826.

Tsuji, S. & Imahori, K (1981). Studies ion the Ca^{2+}-activated neutral proteinase of rabbit skeletal muscle I. The characterisation of the 80K and the 30K subunits. *Journal of Biochemistry.* 90, 233-40.

Urabe, T., Hattori, N., Yoshikawa, M., Yoshino, H., Uchida, K. Mizuno, Y. (1998). Colocalisation of Bcl-2 and 4-hydroxynonenal modified proteins in microglia cells and

neurons of rat brain following transient focal ischaemia. *Neuroscience letters.* 247, 159-162.

Vaux, D.L., Haecker, G. Strasser, A. (1994). An evolutionary perspective on apoptosis. *Cell.* 76, 777-779.

Virchow, R., (1846). Ueber das granulietre ansehen der wadungen der gehirnvetrikel,. *Allg. Z. Psychitr.* 3, 424-450.

Watson, B.D., Busto, R., Goldberg, W.J., Santiso, M., Yoshida, S., & Ginsberg, M.D. (1984). Lipid peroxidation *in vivo* induced by reversible global ischaemia in rat brain. *Journal of Neurochemistry.* 42, 268-274.

Waxman, S.G., Black, J.A., Ransom, B.R. & Stys, P.K. (1993). Protection of the axonal cytoskeletal in anoxic optic nerve by decreased extracellular calcium. *Brain Research.* 614, 137-145.

Waxman, S.G., Black,. J.A., Ransom, B.R. & Stys, P.K. (1994). Anoxic injury of rat optic nerve: Ultrastructural evidence for coupling between Na^+ influx and Ca^{2+}-mediated injury in myelinated CNS axons. *Brain Research.* 644, 197-204.

Waxman, S.G. (1995). Volatage-gated channels in axons: localisation, function and development. *In the axon: structure, function and pathophysiology.* (Waxman, S.G., Kocsis, J.D., Stys, P.K. eds) New York: Oxford University Press. 218-243.

Wei, E.P. (1994). Superoxide dismutase ameliorates neuronal death from hypoxia in culture. *Stroke.* 25, 862-863.

Wilkinson, A.E., Bridges, L.R. & Sivaloganathan, S. (1999). Correlation of survival time with size of axonal swellings in duffuse axonal injury. *Acta Neuropathologica.* 98, 197-202.

Williams, B.P. & Price, J. (1992). What have tissue culture studies told us about the development of oligodendrocytes. *Bioessays.* 14, 693-698.

Williams, S.B. & Price, J. (1995). Evidence for multiple precursor cell types in the embroynic rat cerebral cortex. *Neuron.* 14, 1181-1188.

Wood, P.M & Bunge, R.P. (1984). The biology of the oligodendrocyte. In Norton, WT (ed) Oligodendroglia, Advances in Neurochemistry NY Plenium Publishing. 5, 1

Wood, P.M. & Bunge, R.P. (1986). Evidence that axons are mitogenic for oligodendrocytes isolated from adult animals. *Nature.* 320, 756-758.

Wuulner, U., Young, A.B., Penney, J.B. & Beal, M.F. (1994). 3-Nitropropionic acid toxicity in the striatum. *Journal of Neurochemistry.* 631, 772-1781.

Xiong, Y., Peterson, P.L., Muizelaar, J.P. & Lee, C.P. (1997). Amelioration of mitochondrial function by a novel antioxidant U-101033E following traumatic brain injury in rats. *Journal of Neurotrauma.* 14, 907-917.

Yaghmai, A. & Povlishock, J. (1992). Traumatically induced reactive change as visualised through the use of monoclonal antibodies targeted to neurofilament subunits. *Journal of Neuropathology and Experimental Neurology.* 51, 158-176.

Yam, P.S., Takasago, T., Dewar, D., Graham, D.I. & McCulloch, J. (1997). Amyloid precursor protein accumulates in white matter at the margin of a focal ischaemic lesion. *Brain Research.* 760, 150-157.

Yam, P.S., Dewar. D and McCulloch, J. (1998). Axonal injury caused by focal cerebral ischaemia in the rat. *Journal of Neurotrauma.* 15, 441-450.

Yam, P.S., Patterson, J., Graham, D.I., Takasago, T., Dewar, D. & McCulloch, J. (1998). Topographical and quantitative assessment of white matter injury following a focal ischaemic lesion in the rat. *Brain Resreach Brain Research Protocol.* 2, 315-322.

Yam, P.S., Dunn, L., Graham, D.I. , Dewar, D. & McCulloch, J. (1999). Quantitative analysis of axonal injury following focal cerebral ischaemia in the cat; The effect of MK-801 administration. *Journal of Cerebral Blood Flow and Metabloism.* 19, S146.

Yamaguchi, T., Sano, K., Takaura, K., Isamu, S., Shinohara, Y., asano, T. & Yasuhara, H. (1998). Ebselen in acute ischaemic stroke: A placebo-controlled, double-blind clinical trial. *Stroke.* 29, 12-17.

Yang, G., Chan, P.H., Chen, J., Carlson, E., Chen, S.F., Weisnten, P., Epstein, C.J. & Kamii, H. (1994). Human copperzine superoxide dismutase transgenic mice are highly resistant to reperfusion injury after cerebral ischaemia. *Stroke* 25, 165-170.

Yonezawa, M., Back, S.A., Gan, X., Rosenberg, P.A. & Volpe, J.J. (1996). Cystine deprivation induces oligodendroglia death: Rescue by free radical scavengers and by a diffusible glial factor. *Journal of Neurochemistry.* 67, 566-573.

Yoshizawa, T., Sorimachi, H., Tomioka, S., Ishiura, S. & Suzuki, K. (1995). A catalytic subunit of calpain possesses full proteolytic activity. *FEBS Letters.* 358, 101-103.

Yue, T-L., Gu, J.L., Lysko, P.G., Cheng, H-Y., Barone, F. & Feurstein, G. (1992). Neuroprotective effects of phenyl-t-butyl-nitrone in gerbil brain ischaemia and in cultured rat cerebellar neurons. *BrainResearch.* 574, 193-197.

Zhang, D., Dhillon, H.S., Mattson, M.P., Yurek, D.M. Prasad, R.M. (1999). Immunohistochemical detection of the lipid peroxidation product 4-hydroxynonenal after experimental brain injury in the rat. *Neuroscience letters.* 272, 57-61.

Zingarelli, B., O'Conner, M., Wong, H., Salzman, A.L., Szabo, C. (1996). Peroxynitrite-mediated DNA strand breakage activates poly-adenosine diphosphateribosyl synthetase and causes cellular energy depletion in macrophages stimulated with bacterial lipopolysaccharide. *Journal of Immunology.* 156, 350-358.

Zimmerman, R.A., Larissa, T., Bilanuik, L.T. & Gennarelli, T.A. (1978). Computerised tomography of shearing injuries of the cerebral white matter. *Radiology.* 127, 393-396.

PUBLICATIONS

McCracken, E., Hunter, A.J., Patel, S., Graham, D.I., & Dewar, D. (1999). Calpain activation and cytoskeletal protein breakdown in the corpus callosum of head-injured patients. *Journal of Neurotrauma.* 16, 749-761.

Horsburgh, K., McCulloch, J., Nislen, M., McCracken, E., Large, C., Roses & Nicoll, J.A.R. (1999). Intraventricular infusion of apolipoprotein E ameliorates acute *neruonal damage after global cerebral ischaemia in mice. In submission to Nature Medicine.*

Murdoch, I., Soriano, M.A., McCracken, E., Graham, D.I., Marchonni, M.A., Dewar, D. & McCulloch, J. (1999). Increase in Glial growth factor-2 after human head injury. *In submission to Journal of Cerebral Blood and Metabolism.*

McCracken, E., Dewar. D & Hunter, A.J. White matter damage following systemic injection of the mitochondrial inhibitor 3-nitropropionic acid. *In Preparation.*

McCracken, E., Valerino, V., Simpson, C., Jover, T., McCulloch, J. & Dewar, D. The lipid peroxidation by-product, 4-hydroxynonenal is toxic to white matter *in vivo and in vitro. In Preparation.*

ABSTRACTS

McCracken, E., Jover, T., McCulloch, J. & Dewar, D. (1999). The lipid peroxidation product, 4-hyxroxynonenal, is toxic to oligodendrocytes in vitro and white matter in vivo. *Journal of Cerebral Blood Flow and Metabolism.* Suppl 1. 19. S553. meeting

Murdoch, I., McCracekn, E., Soriano, M.A. & Dewar, D. (1998). Glial growth factor is increased in grey matter following human head injury. *Neuropathology and Applied Neurobiology. 96th Annual Meeting.*

McCracken, E., Graham, D.I. & Dewar, D. (1998). Cytoskeletal protein breakdown and calpain activation in human corpus callosum following head injury. *Neuropathology and Applied Neurobiology.* 95th Annual Meeting.

McCracken, E., Graham, D.I. & Dewar, D. (1997). Quantitative analysis of cytoskeletal protein breakdown in human corpus callosum following head injury. *27th Annual Meeting, Society for Neuroscience.*

McCracken, E., Graham, D.I. & Dewar, D. (1997). Quantitative analysis of cytoskeletal protein breakodwn inhuman corpus callosum following head injury. *Journal of Neurotrauma,* 14, 787. 15th Annual Neurotrauma Symposium.

APPENDICES

APPENDIX 1

Suppliers of commonly used chemicals

ABC	Vector
Alkaline phosphatase substrate kit	Bio-Rad
Anit-mouse IgG HRP	Promega
Anti-rabbit IgG HRP	Promega
Ammonium persulphate	Sigma
Bovine pancreas DNAse	Sigma
Bovine serum albumin, fraction V	GIBCO
BSA path-o-cyte 4	GIBCO
Collagenase	Sigma
DAB	Vector
DMEM	GIBCO
ECL	Amersham
Gentamycin	GIBCO
Glutamine	GIBCO
Hydrogen peroxide	Sigma
4-hydroxynonenal	Cayman chemicals
4-hydroxynonenal-Michael adducts	Calbiochem
HBSS	GIBCO
3-nitropropionic acid	Sigma
PBS	Oxoid
Protogel	National Diagnostics
Progesterone	Sigma
Putrescine	Sigma
SDS	Bio-rad
Sodium selenite	Sigma
Soya bean trypsin inhibitor	Sigma
Streptavidin-alkaline phosphatase	Amersham
TEMED	Sigma
Thyroxine T4	Sigma
Tris	Sigma
Tri-iodo-thryonine T3	Sigma

APPENDIX 2 Stock solutions

CELL CULUTRE

Sato's media

(0.029µl BSA path-o-cyte4 PBS;1.61mg/ml putrescine/H_2O;

0.4mg/ml thyroxine T4/EtOH; 0.34mg/ml tri-iodo-thryonine T3/etoh ; 0.62mg/ml progesterone/EtOH and 0.387mg/ml sodium selenite/etoh Sato's mix is asecptically filtered (0.22µm).

Soya bean trypsin-DNAse inhibitor

(0.52mg/ml soya bean trypsin inhibitor, 0.04mg/ml bovine pancreas DNAse 3.0mg/ml bovine serum albumin, fraction V)

20% fetal calf serum in DMEM

20% fetal calf serum; Dulbecco's Modified Eagles Medium;
200mM glutamine and 25µg/ml gentamycin

WESTERN BLOTTING

Table A. 1 Composition of SDS-PAGE gels

	12.5% resolving gel	*10% resolving gel*	*8% resolving gel*	
H_20	8.6 ml	13.2 ml	H_20	45.6 ml
1.5M tris	12	12	Prosieve	12.8
Protogel	23	18.4	1.5 M Tris	20
Glycerol 50%	4	4	SDS 10%	0.8
APS 10%	0.32	0.32	APS 10%	0.8
TEMED	0.10	0.10	TEMED	0.04

APPENDIX 3

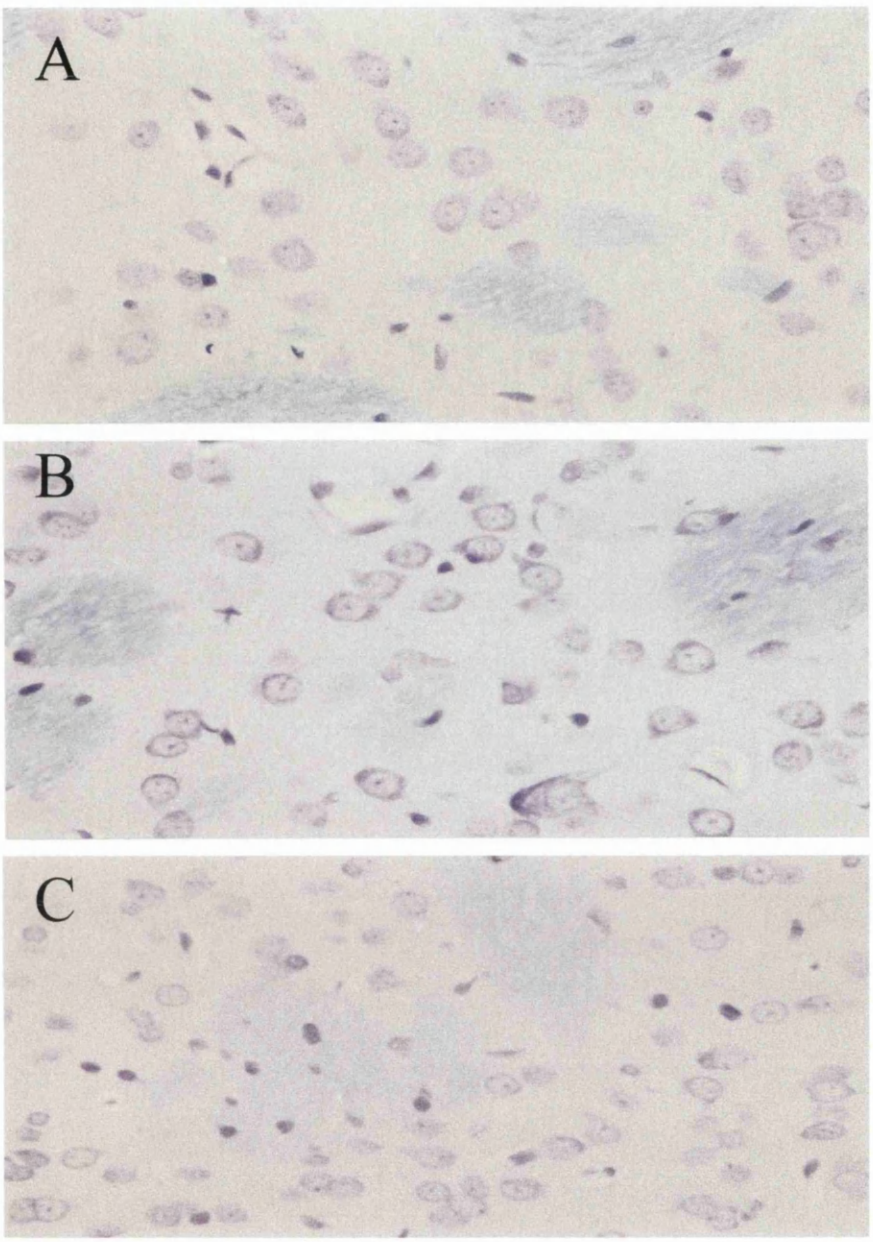

Figure A1 Morphological changes in the striatum following systemic injection of 3-nitropropionic acid

Histological changes in the striatum following systemic injection of A) 10mg/kg B) 15mg/kg and C) 20mg/kg 3-nitropropionic acid.

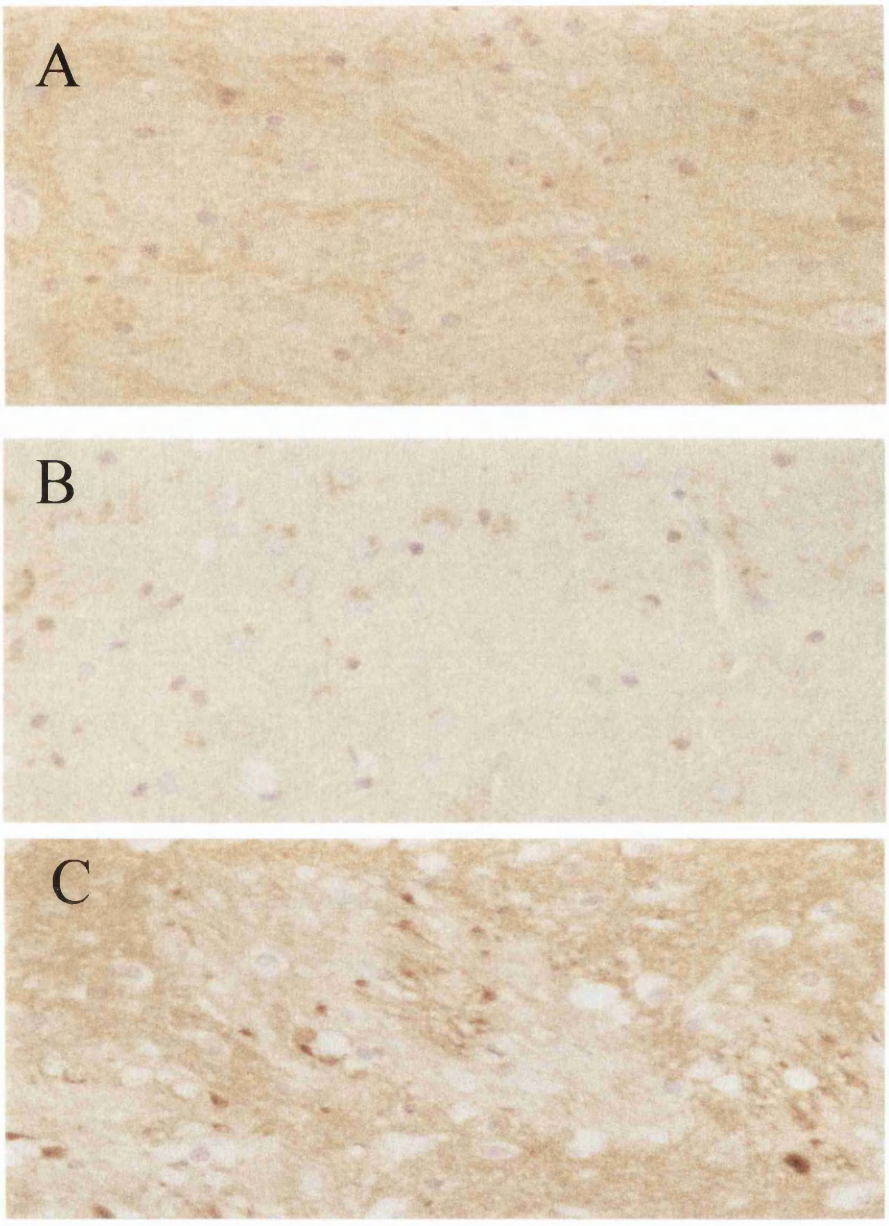

Figure A2 β-Amyloid precursor protein immunostaining within myelinated fibre tracts following systemic injection of 3-nitropropionic acid

β-APP accumulation within the myelinated fibre tracts of the striatum following systemic injection of A) 10mg/kg, B) 15mg/kg and C) 20mg/kg 3-nitropropionic acid.

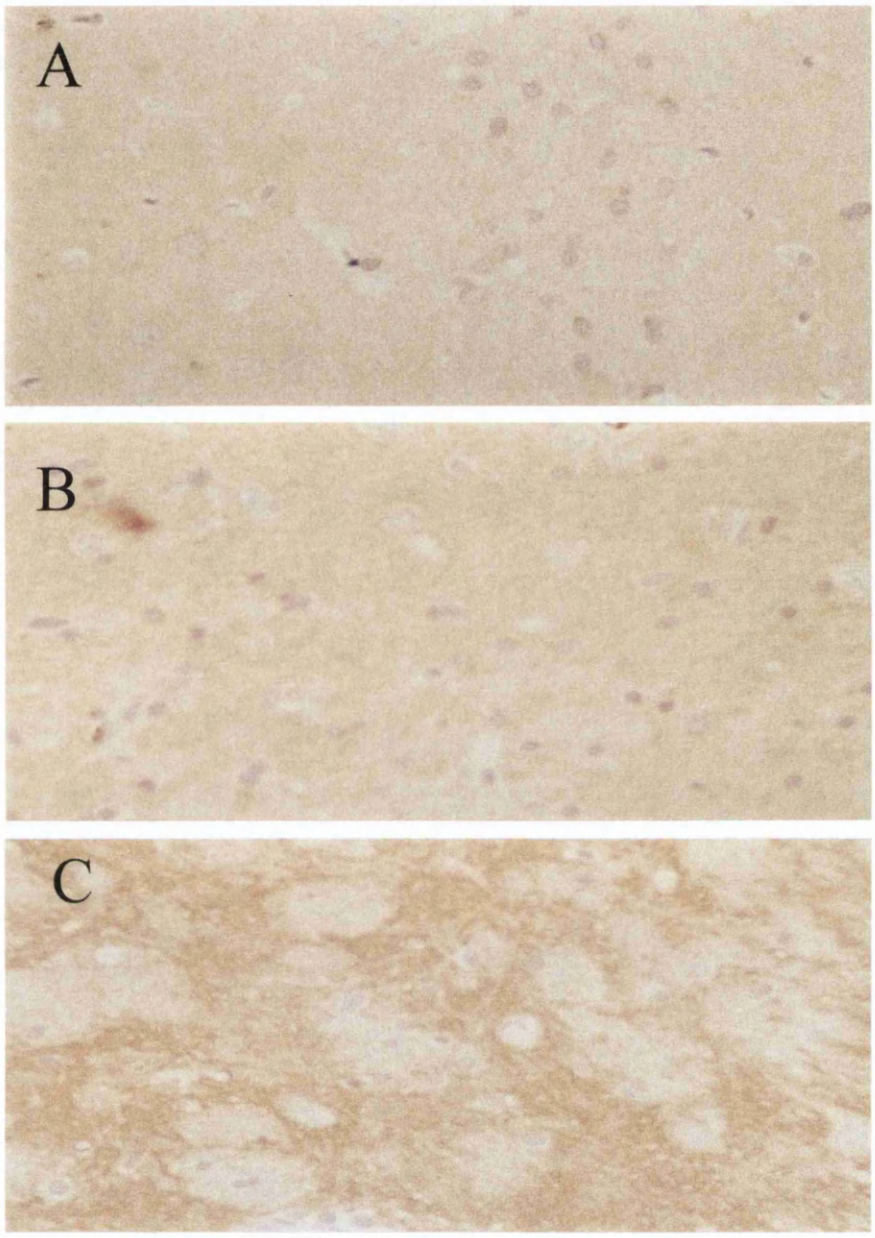

Figure A3 SNAP-25 immunohistochemical staining following systemic injection of 3-nitropropionic acid

SNAP-25 immunoreactivity in the myelinated fibre tracts of the striatum following A) 10mg/kg, B) 15mg/kg and C) 20mg/kg 3-nitropropionic acid.

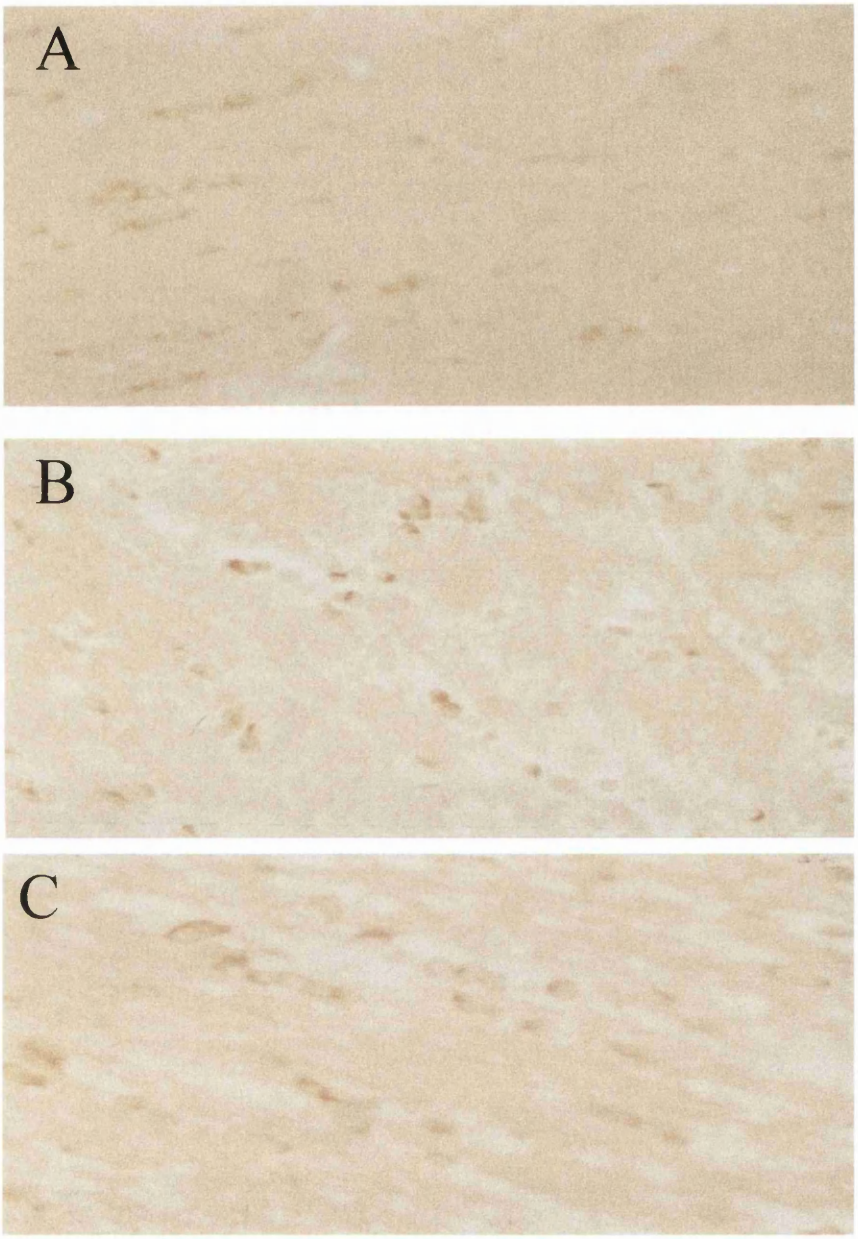

Figure A4 Immunohistochemical staining of calpain-mediated spectrin breakdown products in the subcortical white matter following systemic injection of 3-nitropropionic acid

The number of SBAbS2 immunopositive oligodendrocyte-like cells following increased administration of A)10mg/kg, B) 15mg/kg and C) 20mg/kg 3-NPA

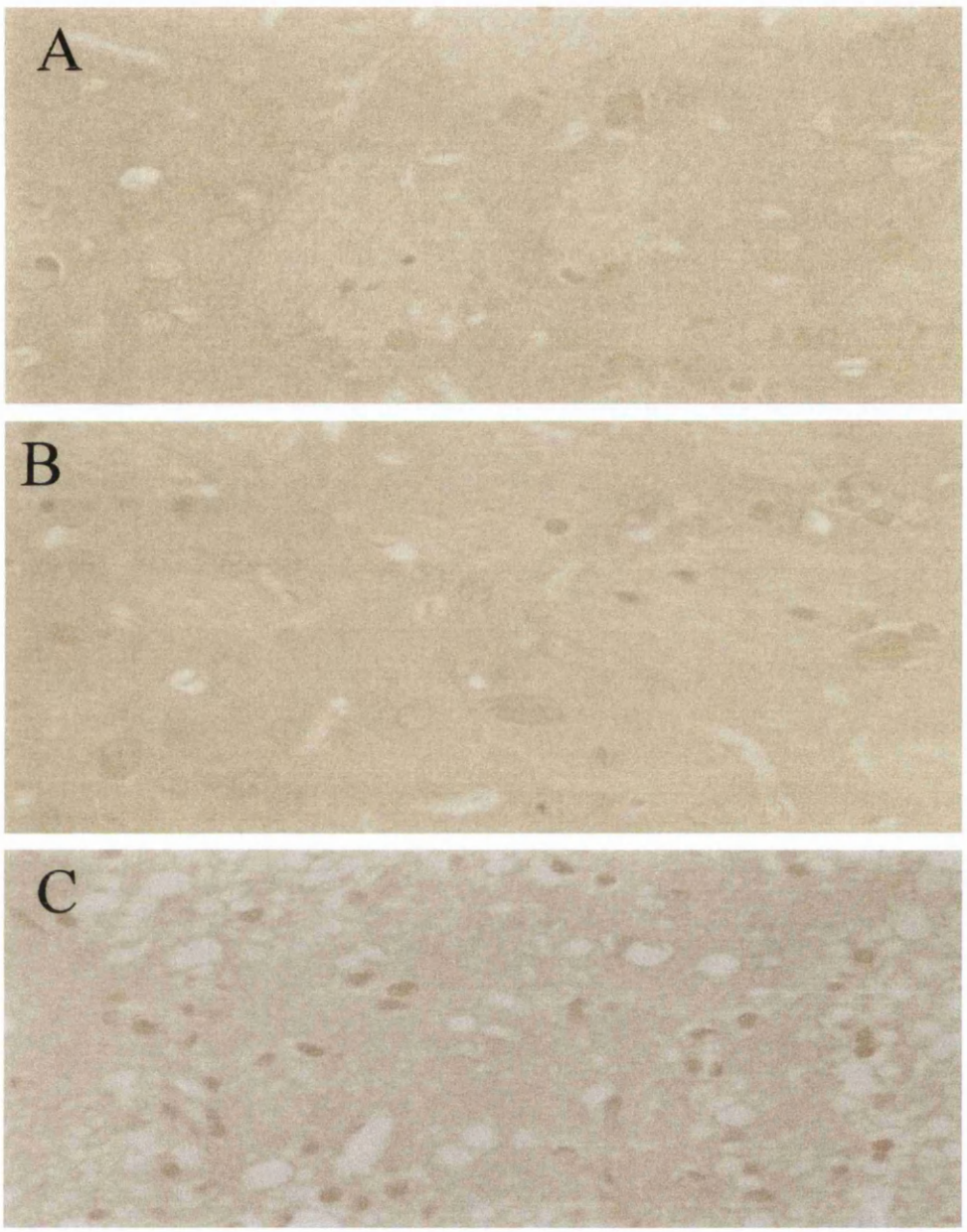

Figure A5 Manganese superoxide dismutase immunohistochemical staining following systemic injection of 3-nitropropionic acid

Increased cellular staining of Mn-SOD in the striatum following systemic injection of A)10mg/kg, B)15mg/kg and C) 20mg/kg 3-nitropropionic acid